



University
of Glasgow

Crawford, Niall Alexander (2016) The biomechanics of tree frog adhesion under challenging conditions. PhD thesis

<http://theses.gla.ac.uk/7102/>

Copyright and moral rights for this thesis are retained by the author

A copy can be downloaded for personal non-commercial research or study, without prior permission or charge

This thesis cannot be reproduced or quoted extensively from without first obtaining permission in writing from the Author

The content must not be changed in any way or sold commercially in any format or medium without the formal permission of the Author

When referring to this work, full bibliographic details including the author, title, awarding institution and date of the thesis must be given.



The Biomechanics of tree frog adhesion under challenging conditions

Niall Alexander Crawford (MRes)

This thesis is submitted for the degree of Doctor of Philosophy

February 2016

Centre for Cell Engineering
College of Medical, Veterinary and Life Sciences

Abstract

Tree frogs have evolved specialised toe pads which allow them to efficiently climb vertical surfaces. The toe pad sticks by using 'wet adhesion' - a combination of forces produced by a thin layer of fluid between the pad and the surface which provide temporary adhesion to allow quick attachment and detachment for climbing. Most studies on tree frogs have been based on their adhesive capabilities on surfaces which are flat, clean and dry (usually glass). However, climbing tree frogs in the wild will come across a variety of surfaces which could affect their adhesive abilities. This PhD investigated whether tree frog adhesion is affected by various 'challenging' surfaces, which reflect conditions that tree frogs may encounter whilst climbing. These include rough surfaces, wet conditions, surfaces with loose particulate and hydrophobic surfaces.

Experiments were predominantly conducted using a force transducer to measure adhesive and frictional forces of single toe pads, as well as whole animal attachment experiments involving a rotating tilting board. The toe pads of tree frogs were shown to possess a self-cleaning mechanism, whereby the pads will remove contaminants (and subsequently recover adhesive forces) through repeated use, thanks to shear movements of the pad and the presence of pad fluid which aids contaminant deposition.

To investigate how torrent frogs (frogs which inhabit waterfalls) can adhere to rough and flooded surfaces, the performance of torrent frogs species *Staurois guttatus* was compared to a tree frog species (*Rhacophorus pardalis*). Torrent frogs could produce higher adhesive forces than tree frogs with their toe pads, and possess a specialised toe pad morphology (directional fluid channels on the pad periphery) which may contribute to better performance in flooded conditions. Torrent frogs utilise large areas of ventral skin to stay attached on overhanging surfaces, while tree frogs display a reduction in contact area resulting in a failure to stay attached. This combination of ability and behaviour

will help torrent frogs to stay attached on the rough and flooded surfaces that make up their waterfall habitat.

On rough surfaces, tree frogs showed improved (compared to smooth surface performance) performance on smaller scale roughness (asperity size $<10\ \mu\text{m}$), and poorer performance on the larger scale roughnesses tested ($30 - 425\ \mu\text{m}$). Interference reflection microscopy (IRM) revealed that larger asperities result in pad fluid being unable to fill the larger gaps of such surfaces, which was confirmed by adding water to rough surfaces to improve attachment performance. The soft pad does however aid in conforming to some rough surfaces, which could account for the better performance on the smaller scale roughness.

Many plant surfaces exhibit hydrophobic properties, and so the adhesive performance of tree frogs on hydrophobic surfaces was compared to that on hydrophilic surfaces. It was found that the toe pads could produce similar adhesive and frictional forces on both surfaces. The pad fluids contact angles were then measured on hydrophobic surfaces using IRM, where droplets of pad fluid formed lower contact angles (and are therefore exhibiting higher wettability) than water. Though the exact composition of pad fluid is unknown, some form of surfactant must be present which aids wetting of surfaces (either a surface modification or detergent present in the fluid) to allow wet adhesion to occur - goniometer experiments of water on dried footprints on hydrophobic surfaces confirmed this.

The ability to stick in a variety of conditions could provide inspiration for 'smart' adhesives, which mimic the adaptable adhesion of tree frog toe pads.

Table of Contents

1. General Introduction	12
1.1 Advantages to climbing	13
1.2 Climbing with adhesive pads	13
1.2.1 Dry adhesion	15
1.2.2 Wet adhesion	18
1.2.3 Adhesion in insects and spiders	21
1.2.4 Adhesion in tree frogs	23
1.3 Challenges for adhesive pads	26
1.3.1 Fast, effortless detachment	27
1.3.2 Self-cleaning properties of adhesive pads	29
1.3.3 Sticking under wet conditions	30
1.3.4 Adhesion to rough surfaces	31
1.4 Bioinspiration	34
1.5 Aims of this thesis	36
2. General Materials and Methods	37
2.1 Introduction - adhesion measuring techniques	38
2.1.1 Whole animal force measurement techniques	38
2.1.2 Smaller scale force measurements	39
2.2 Materials and methods	41
2.2.1 Frog species and care	41
2.2.2 Whole animal experimentation methods	42
2.2.3 Single toe pad experimentation methods	45
2.3 Conclusions	48
3. Evidence of self-cleaning in the adhesive toe pads of tree frogs	49
3.1 Introduction	50
3.2 Materials and methods	52
3.2.1 Study animals	52
3.2.2 Contamination	52
3.2.3 Force measurements	53
3.2.4 Statistics	55
3.3 Results	56
3.3.1 Single toe pad force recovery	56
3.3.2 Contact area and bead deposition	58
3.4 Discussion	61
3.4.1 Occurrence of self-cleaning	61
3.4.2 Mechanisms of self-cleaning in tree frogs	64

3.4.3 Comparisons with other animals	65
3.4.4 Biomimetic implications	66
4. The attachment abilities of torrent frogs on rough and wet surfaces	68
4.1 Introduction	69
4.2 Materials and methods	71
4.2.1 Experiments from 2010 study	71
4.2.2 Study animals and location	73
4.2.3 Force measurements	75
4.2.4 Morphology investigation using SEM	76
4.2.5 Statistics	76
4.3 Results	77
4.3.1 Force measurements of toe pads, belly and thigh skin	77
4.3.2 Skin morphology	79
4.4 Discussion	82
4.4.1 Effect of surface wetness and roughness on climbing frogs	82
4.4.2 Contact area on a tilting board	84
4.4.3 Force measurements analysis	86
4.4.4 Linking force measurements with contact area	88
4.4.5 Pad and skin morphology	90
4.4.6 The role of body mass	91
4.5 Conclusions	92
5. Analysis of tree frog performance on rough surfaces	94
5.1 Introduction	95
5.2 Materials and methods	97
5.2.1 Experimental animals	97
5.2.2 Climbing performance in free-climbing frogs	98
5.2.3 Measuring forces of single toe pads	99
5.2.4 Rough surfaces	100
5.2.5 Visualising pad contact using IRM	105
5.2.6 Statistics	108
5.3 Results	108
5.3.1 Attachment abilities of free climbing tree frogs	108
5.3.2 Individual toe pad force measurements	112
5.3.3 Using IRM to visualise pad contact	115
5.3.4 Climbing performance on a rough and wet surface	118
5.4 Discussion	120
5.4.1 Rough surface effects on adhesion and friction	120

5.4.2 Whole animal experiments	121
5.4.3 Single pad force measurements	123
5.4.4 The role of fluid	125
5.4.5 Surface contact on a rough surface	127
5.4.6 Comparing performance with other climbing organisms	128
5.5 Conclusions	129
6. The effect of surface wettability of surfaces on the adhesive abilities of tree frogs toe pads	130
6.1 Introduction	131
6.2 Materials and methods	134
6.2.1 Frog species used for experiments	134
6.2.2 Surfaces tested	135
6.2.3 Force per unit area measurements	137
6.2.4 Contact angle measurements using goniometer	138
6.2.5 Contact angle measurements of ‘footprint’ fluid droplets	139
6.2.6 Statistics	140
6.3 Results	141
6.3.1 Force measurements of single toe pads	141
6.3.2 Contact angles using the goniometer	143
6.3.3 Contact angles using IRM	146
6.4 Discussion	149
6.4.1 Wet adhesion and fluid properties	149
6.4.2 Fluid composition	151
6.5 Conclusions	154
7. General Discussion	155
7.1 Research summary	156
7.2 Future frog research	159
7.3 Adhesive replicate design	160
7.4 Biomimicry	162
7.5 Concluding remarks	166
Appendices	167
References	177

List of Tables

4.1 Combined force measurements and contact areas for tree and torrent frogs	89
5.2 Average roughness values (R_a) for surfaces used for experiments	102
6.1 Chemicals present in the secretions of tree frogs using GC-MS	152

List of Figures

1.1 Wet adhesion schematic	20
1.2 Toe pad morphology in tree frogs	24
1.3 Cellular structures of toe pads	25
1.4 Setae contact on rough surfaces	33
2.1 Whole animal experimental setup	43
2.2 Single toe pad force measurement experimental setup	45
2.3 Example of single toe pad force measurement plot	47
3.1 Images of the beads used for contamination	53
3.2 Diagram of 'drag' program	54
3.3 Diagram of 'dab' program	54
3.4 Images of contaminated toe pads	55
3.5 Boxplot of pad force recovery after contamination	57
3.6 Boxplot displaying pad force recovery after partial contamination	58
3.7 Boxplot comparing various results from 'drag' and 'dab' trials	59
3.8 Correlation between number of beads deposited and area of pad in contact	60
3.9 Images of deposited beads after 'drag' movements	61
3.10 Boxplot of whole animal friction force recovery after contamination	62
3.11 Boxplot of whole animal adhesive force recovery after contamination	63
4.1 Diagram of torrent frog tilting experiment setup	72
4.2 Images of rainforest study location	73
4.3 Images of torrent and tree frogs in study	74
4.4 Friction and adhesion force measurements for various body parts	77
4.5 SEM images of torrent frog toe pad structures	79
4.6 SEM images comparing toe pad cells in tree and torrent frogs	80
4.7 SEM images comparing thigh and belly skin in tree and torrent frogs	81
4.8 Attachment performance of tree and torrent frogs	83
4.9 Contact area of tree and torrent frogs on a tilting platform	85
4.10 Attachment performance of male and female torrent frogs	91
5.1 Diagram of tilting platform with rough surfaces	98
5.2 Diagram of the single toe pad force measurements setup for rough surfaces	99
5.3 Diagram of PDMS surface topographies	103

5.4 SEM images of PDMS surfaces	104
5.5 IRM image of toe pad cells in contact	105
5.6 IRM images of the toe pad in contact with the glass surrounding an asperity	108
5.7 Slip angles of climbing tree frogs on varying rough surfaces	110
5.8 Fall angles of climbing tree frogs on varying rough surfaces	111
5.9 Mean slip and fall angles plotted on a log axis	112
5.10 Single toe pad forces on rough surface replicates	113
5.11 Force measurements of single toe pads on PDMS rough surfaces	114
5.12 IRM image of toe pad in contact around a glass bead	115
5.13 Scatterplot showing correlation between asperity size and pad contact	116
5.14 Slope analysis of pad around an asperity	117
5.15 Boxplot of attachment performance of tree frogs in varying conditions	119
5.16 IRM image of a small glass bead stuck within the channels	124
5.17 Diagram predicting toe pad contact on different rough surfaces	126
6.1 Diagram of contact angles of water on different solid surfaces	135
6.2 Contact angle measurements of water on varying surfaces	136
6.3 Diagram of the goniometer setup	138
6.4 Boxplots showing forces generated on OTS and glass	141
6.5 Boxplots showing forces generated on PDMS with differing surface energies	142
6.6 Images displaying water droplets on different surfaces	143
6.7 Boxplot showing contact angles of water on clean OTS and on footprints on OTS	144
6.8 Images showing the contact angles of different fluids on OTS	145
6.9 Boxplot displaying the contact angles of differing fluids on OTS	146
6.10 Images of pad fluid on an OTS surface	146
6.11 Reconstruction of the shape of pad fluid droplets on an OTS surface	147
6.12 Contact angles of pad fluid on glass and OTS	148
6.13 Diagram showing a cross section of the toe pad in contact with a surface	149
7.1 Images of tree frogs toe pads and some examples of bioinspired surfaces	165
A.1 Profiles of various surfaces	171
A.2 Diagram of the configuration of a monolayer of beads on a surface	172

Acknowledgements

Firstly, I'd like to thank my supervisor W. Jon P. Barnes, who provided me with this great opportunity to do exciting and interesting research on tree frogs. His advice and dedication to my work have helped enormously. Credit is also due to my co-supervisor Mathis Riehle, whose guidance and thoughts have helped to steer me during my PhD.

I would like to thank the other members of the tree frog group. I owe an enormous amount of gratitude to Thomas Endlein, who has helped me through all aspects of this thesis. He was a constant supply of ideas, as well as an excellent teacher, and was there whenever I ran into problems. He has also been a great friend. Thanks as well to Diana Samuel, who was always helpful with scientific discussions, as well as being a good friend and colleague. Of course, thanks to the frogs themselves; although frustrating to work with at times, I've still enjoyed working with them.

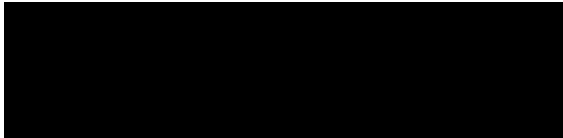
Thanks to all members of the CCE department. It has been an immense privilege to have studied and worked with you, and I've made many lifelong friends in the group. In particular, thanks to Mark for his friendship and all the lunches and banter.

This thesis was funded by a research grant from the Deutsche Forschungsgemeinschaft (DFG).

For their continued support throughout my thesis, I'd like to thank my family. I've always been supported in doing my PhD, which I am grateful for. Finally, thank you to my wife Caitlin; she has provided constant love and support, and has had to put up with repeated stories of how tree frogs stick to things. I wouldn't have got this far without you.

Author's declaration

This thesis is submitted for the degree of Doctor of Philosophy. The research reported within is my own work (unless otherwise stated) and is not being considered elsewhere for any other academic qualification.



Niall Crawford

February 2016

Publications

Some of the following research has been published in original research publications with are co-authored by the candidate:

Crawford, N., T. Endlein and W. J. P. Barnes (2012). "Self-cleaning in tree frog toe pads; a mechanism for recovering from contamination without the need for grooming." The Journal of Experimental Biology **215**(22): 3965-3972.

Endlein, T., W. J. P. Barnes, D. S. Samuel, N. A. Crawford, A. B. Biaw and U. Grafe (2013). "Sticking under Wet Conditions: The Remarkable Attachment Abilities of the Torrent Frog, *Staurois guttatus*." PLoS ONE **8**(9): e73810.

Conference Proceedings

2012 International School and Conference on Biological Materials Science

Potsdam

‘The self-cleaning properties of the toe pads of tree frogs’

2013 COST workshop (European Cooperation in Science and Technology)

Cluj-Napoca

‘The adhering abilities of tree frogs on rough surfaces’

2013 SEB

Valencia

‘The adhering abilities of tree frogs on rough surfaces’

2014 COST conference (European Cooperation in Science and Technology)

Istanbul

‘When the going gets rough... the effect of surface roughness on the attachment abilities of tree frogs’

2014 SEB

Manchester

‘When the going gets rough... the effect of surface roughness on the attachment abilities of tree frogs’

2015 SEB

Prague

‘How does the wettability of a surface affect tree frog adhesion?’

1. General Introduction

“Sometimes, if you pay real close attention to the pebbles you find out about the ocean”

- Lords and Ladies, Terry Pratchett

“As Crake used to say, ‘Think of an adaptation, any adaptation, and some animal somewhere will have thought of it first’”

- Oryx & Crake, Margaret Atwood

1.1. Advantages to climbing

In the natural world, the ability to climb is a tremendous advantage for a species to possess, as it provides new resources and environments to aid the survival of the organism. Obstructions such as trees, steep cliffs and high walls can act as a barrier to those who cannot climb with ease (or fly). Climbing allows for greater predator evasion, access to a greater variety of safer nesting sites, foraging or hunting, and a more efficient mode of travel - particularly in dense forest (Cartmill 1985). In order to be able to successfully scale such environments, organisms often need to have evolved specialised equipment or techniques. Despite the specialised adaptations necessary, the animal kingdom is filled with examples - from insects to apes - in which climbing is an essential and natural part of their lifestyle. Invertebrates as varied as stick insects, snails and crabs all have species which show climbing behaviours. Mangroves play host to climbing killifish, and arboreal salamanders and tree frogs are found worldwide. Some bird species (despite possessing the ability to fly) even show climbing behaviours; this is seen in species such as parrots, woodpeckers and juvenile hoatzin. The methods of climbing are just as varied as the species, with several techniques involved (Peattie 2009). However, all climbing methods involve propulsion (jumping, pulling or brachiating), and some form of fall prevention. This refers to gripping, interlocking or frictional forces with the surface, as well as bonding with the surface using adhesion. Most organisms which need to move will possess feet, pads and other surfaces which have a textured surface or claws for gripping and interlocking, but on some surfaces, such as inclined or vertical smooth surfaces, further attachment using adhesive and frictional forces is necessary.

1.2. Climbing with adhesive pads

For some organisms attachment to a surface that is permanent is required, and for this certain adhesive qualities are necessary. Many vine specimens of plants will use adapted roots to attach themselves to surfaces using a strong adhesive protein/polysaccharide mix, which binds to the surface and acts like a cement (Groot, Sweeney *et al.* 2003). Sessile animals also utilise strong adhesives for permanent attachment to surfaces - for example barnacles will produce a

cement-like material (Walker 1981). These organisms live in a marine environment where wave action can easily dislodge them or predators can try to pull them from the surface, therefore adhesives need to be strong. The byssal thread adhesives used by mussels, which are effective both in dry and wet conditions (as the mussels can be exposed to air and underwater conditions when living in the tidal area), are so effective that they have become inspiration for underwater adhesive design (Waite and Sun 2005). However, for most animals where continuous movement is needed whilst sticking (referred to as dynamic adhesion, for example with climbing), permanent adhering by a glue-like substance is not suitable - although starfishes adhesion is an exception to this (Flammang 1996). Recently there has been a growing interest in the adhesion techniques of animals which can climb vertical surfaces, including smooth ones, without incurring any slipping or falling (Emerson and Diehl 1980). Dynamic adhesion is especially important for climbing animals which require speed and agility to either catch prey or evade predators, or when it is used as a defence mechanism to prevent being pulled from a surface (as has been shown in the beetle species *Hemisphaerota cyanea* (Eisner and Aneshansley 2000)).

Dynamic adhesion can be formed through several different mechanisms, for example via suction, interlocking, frictional forces, wet adhesive and dry adhesive systems. Suction involves the creation of a lower pressure by increasing the volume within an enclosed space between the organism (often as a cup or dome) and the substrate, and can produce large adhesive forces. Octopuses utilise suction in their tentacle suckers by using an array of muscles to reduce the pressure in each sucker (Kier and Smith 2002). However as this can be difficult to implement whilst climbing, this technique is typically more suited for a longer attachment period, for example in roosting Spix's disk-winged bats (Riskin and Fenton 2001). Mechanical interlocking is often deployed through claws in several climbing organisms like squirrels, but this is reliant on a rough surface that fits the dimensions of the claw well (or that the substrate will be soft enough to allow penetration of the claw into the surface).

Many organisms deploy attachment devices which utilise adhesion and/or friction to stick whilst climbing. Adhesion is defined as the attractive force between two different substances; in the case of climbing organisms, it is measured by the forces required to perpendicularly separate two surfaces (the attachment force). Frictional force (sometimes known as shear force or shear resistance) is the force resisting the parallel movement of two surfaces against each other; this can be split into static friction (when the surfaces are non-moving) and kinetic friction (forces produced by two surfaces that are moving). With rubber-like substances, a greater level of force is required to pull it across a surface (this is named rubber friction), due to the adhesive interaction (and energy dissipation) between the rubber and the surface, and the deformations of the rubber to the contours of the surface in contact (Persson 1998). Soft adhesive surfaces (such as those seen in tree frogs or some insects) can exhibit such characteristics due to the nature of their pads. Rubber friction forces scale with real contact area, and in some cases in climbing organisms are based on the pull of gravity to create the necessary parallel pull on the surface. This means that friction will have its greatest impact on a vertical surface, and will be reduced on overhanging surfaces (Emerson and Diehl 1980)(although this applies to an inanimate object on a surface, not an actively climbing organism *per se*). Organisms then often utilise an adhesive system which incorporates adhesion and friction forces when climbing, which can be divided into two categories: dry and wet adhesion.

1.2.1. Dry adhesion

As said, there are two predominant variations of dynamic adhesion seen in the natural world, which differ in how attachment forces are produced. One of these is termed dry adhesion, which involves the use of hairy pads to create adhesion by attraction via van der Waals forces (attractive forces between charged molecules), and is used by geckos to great effect (Autumn and Peattie 2002). Dry adhesion works by van der Waals forces forming collectively strong bonds (despite a single bond being far weaker than a covalent bond, for example) when the two surfaces (the feet and the substrate) are in extremely close contact (Casimir and Polder 1946). Direct contact at a molecular level greatly aids the formation of these forces (Kinloch 1987), which can be difficult to

achieve on uneven surfaces. In geckos, a high level of conformity is achieved through multiple contact points, using hierarchical structures beginning with hairs or setae (130 μm in length and about one tenth the width of a human hair (Autumn, Liang *et al.* 2000)) on the adhesive pads, which split into fine, densely packed spatulae on a nanoscopic scale (typically less than 10 nm in geckos) (Autumn, Sitti *et al.* 2002).

A gecko's spatulae possess an asymmetrical structuring, which results in a flattened tip which comes into contact with the surface. The flattened tip is not parallel with the substrate in its free form, and will only come into contact (and therefore become 'active' as adhesives) when they are perpendicularly dragged on the surface to bend and align them. Indeed, when experiments were first conducted on individual setae (Autumn, Liang *et al.* 2000), Autumn *et al.* struggled to make the setae stick. The setae were found to require a perpendicular preload, then a small drag of the setae parallel to the surface (somewhere between 5 μm (Autumn, Liang *et al.* 2000) and 10 μm (Gravish, Wilkinson *et al.* 2008)) was needed to activate friction and other adhesive forces. This provided the maximum level of force, and allowed a large number of the spatulae to attach. The implications for a gecko are that it can adapt its attachment so that the feet will only stick when needed, and the ultrahydrophobic setae can remain in a non-adhesive default state until activated (Autumn 2006). The design of the setae - a hierarchical branching from the bottom upwards - means that self-sticking is greatly reduced, and allows for better conformity to some rough surfaces as the contact splitting allows setae to bend and attach to asperities (Huber, Gorb *et al.* 2007). An important reason for hairy pads being so effective is that splitting of the contact area into smaller sections could have two possible effects: firstly the assumption that work of adhesion increases as the width (or perimeter) of the contact area is increased (as adhesive forces scale with the length of the adhesive edges as opposed to the area in contact), and secondly the splitting of the contact area results in 'crack arresting', so that if one area becomes detached then peeling does not occur across the entire contact area because they are made up of smaller (and separate) segments (Federle 2006).

For dry adhesive pads (though not exclusively), friction force also plays a role in climbing and attachment. Static friction can occur when there is no sliding of the surfaces as opposed to kinetic friction which occurs when there is sliding (Autumn, Dittmore *et al.* 2006). Presence of both forces can lead to stick-slip behaviour of the surfaces as they slide (often due to pinning and unpinning of one surface on another), where they will move and slide according to the strength of the static friction (Persson 1999). In many climbing organisms, shear forces have been shown to be important as they lead to an increase in adhesive forces, and allow the pad to detach easily without the need for excessive force.

Although the climbing abilities of geckos had been noted as far back in time as Aristotle, the mechanics behind their incredible abilities were not known until the 20th century. The specialised setae (composed of β -keratin (Autumn, Sitti *et al.* 2002) with some α -keratin parts (Rizzo and Hallahan 2006)) allow geckos to freely climb without complications on many surfaces regardless of what angle the surface is at. The foot of a Tokay gecko can have a setae density as high as 14,400 per mm² (Autumn, Sitti *et al.* 2002), with spatulae that can number from 100 to 1,000 per single setae, which allows for several thousand individual adhesives points. Studies show that geckos front feet will take 10 N of force on an area of 100 mm² of setae (Irschick, Austin *et al.* 1996, Autumn, Liang *et al.* 2000), meaning that the force of one seta should be 6.2 μ N on average (Autumn and Gravish 2008). However, single setae produced an adhesive force of 200 μ N (Autumn and Peattie 2002), and a whole foot could potentially bear 130 kg of weight, which is a greater level of adhesion than needed in order to hold the weight of the gecko (typically 150 - 300g). This huge over-compensation of force acts as a safety factor, designed to allow adhesion to still occur on different levels of surface roughness, when the number of setae attached would decrease (Huber, Gorb *et al.* 2007). The extra force created could also help in extreme circumstances, such as high winds or a recovery from falling using one foot. Stress distribution has also been found to be non-uniform throughout the adhesive area of the foot, which could help explain how a gecko connects and releases its feet whilst climbing (Eason, Hawkes *et al.* 2015).

1.2.2. Wet adhesion

The other common form of dynamic adhesion seen in nature is wet adhesion, whereby a fluid is produced which aids attachment by holding together the two solid surfaces with interacting forces (Emerson and Diehl 1980). The fluid is not necessarily a glue, but properties of the fluid being between two solid layers mean that adhesion to the surface occurs (a good example would be putting wetted paper on a window; the water is not a glue, but it can hold the paper onto the glass).

Two principal forces are thought to contribute to the sticking in wet adhesion: these are capillary forces and viscous forces (sometimes termed as Stefan adhesion) (Emerson and Diehl 1980). Capillary action relies on the ability of the liquid to spread on the surface. Surface tension produces a meniscus of the fluid at the interface between air, liquid and the solid surfaces (Butt and Kappl 2009). In any fluid, surface tension exists at the air-water interface, and is caused by the cohesive nature of the fluid. The meniscus layer forms an angle when it touches the solid surface, known as the contact angle. The amplitude of the contact angle is dependent on the varying surface energies of substrates (in the presence of the third medium, air) (Emerson and Diehl 1980), which changes the nature of the surfaces, i.e. whether they are hydrophobic (high contact angle) or hydrophilic (low contact angle). When two parallel surfaces meet with a liquid layer between them, a bridge will form around the edge, therefore lowering the pressure within the liquid (also known as the Laplace pressure) and causing the two surfaces to draw together and adhere. Using the contact angle, the fluid viscosity and the distance between the two surfaces, a force value for capillary action can be calculated. Similar to van der Waals interactions, if the distance between the two surfaces increases, the capillary force decreases. As mentioned above, an increase of fluid will also decrease capillary forces. Several different equations exist which attempt to explain the adhesive forces involved in wet adhesion (Hanna and Barnes 1991, Endlein and Barnes 2015). Betz and Kölsch (Betz and Kölsch 2004) use the following equation to explain the capillary forces produced by two solid surfaces with a fluid layer between them (modelled on circular plates), written as:

$$F_{\text{surface tension}} = \frac{(\cos \theta_1 + \cos \theta_2)A\gamma}{d} \quad (1)$$

where θ = the contact angles of the fluid with the surface, A = contact area, γ = surface tension of the fluid, and d = the distance between the surfaces.

Stefan adhesion relies on the viscosity of the liquid between the two solid layers to create a pull between two separating surfaces. When two surfaces are pulled apart with a fluid layer between them, then the flow of the fluid as they separate (and the velocity at which they separate) will contribute to adhesive force. Stefan adhesion is calculated as follows (when separating two stiff, circular plates):

$$F_{\text{Stefan adhesion}} = \frac{3\pi r^4 \eta v}{2d^3} \quad (2)$$

where r = radius of the contact surface, η = fluid viscosity, v = rate of separation, and d = distance between the two surfaces. Stefan adhesion relies heavily on a close proximity of the two surfaces, as the attractive force decreases significantly with separation, as well as there being no interruptions in the fluid layer (Smith 1991). The two above equations assume that the fluid has spread ubiquitously throughout the area with the same thickness, that the surfaces are flat and stiff disc shapes, and that the contact angles are constant around the perimeter.

Both surface tension from capillary forces and viscosity from Stefan adhesion play a role in wet adhesion (*Figure 1.1*) (Hanna and Barnes 1991), and as can be

seen by these equations both rely on the distance between the surfaces being small. In a similar manner to dry adhesion, the mechanics of wet adhesion rely on a very small distance between the two adhering surfaces (Federle, Barnes *et al.* 2006). Most models and equations explaining wet adhesion are made assuming that the two separating layers are rigid and flat, but in many species the pads are soft and rounded, which could affect the dynamics of the adhesive area. Soft pads in insects and tree frogs tend to follow the Johnson-Kendall-Roberts (JKR) model of elastic contact (Johnson, Kendall *et al.* 1971), where the deformation of the surface results in an increase in contact area as load increases; this can increase the frictional forces due to the increase in contact area as well (as opposed to being load dependent).

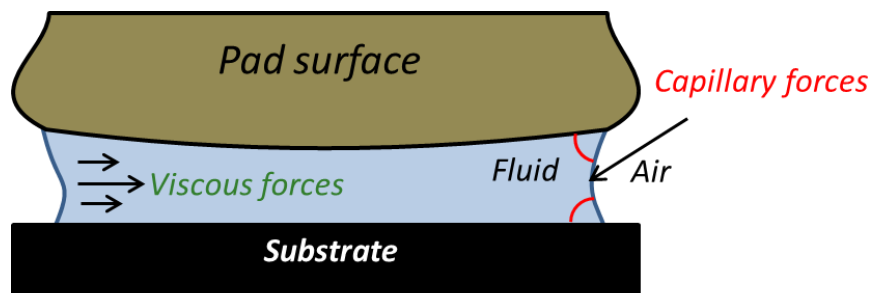


Figure 1.1: Simplified diagram showing how wet adhesion works. An air/fluid meniscus is formed around the perimeter of the contact area, which lowers the pressure within the fluid and holds the two surfaces together. The viscosity of the fluid increases the force required to separate the two, depending on the speed of separation.

This system occurs on a smooth pad, as seen in tree frogs and some insects (Federle, Barnes *et al.* 2006), but fluid based hairy pads do exist as well (Federle 2006, Barnes 2007). Wet adhesion relies on the spreading of a thin layer of liquid across the surfaces, which can only happen when the surface energy between the liquid and solid is favourable for the liquid to spread - surfaces such as Teflon or waxy cuticles (with comparatively low surface energies) are not suitable when water is the intermediate fluid (Emerson and Diehl 1980). Insects which use adhesive pads to climb use wet adhesion to stick to surfaces, and the fluid produced has been shown to consist of oil and aqueous components (water in oil immersion) (Vötsch, Nicholson *et al.* 2002, Dirks, Clemente *et al.* 2010); this is thought to aid in friction force production, particularly in smooth pads

with little or no topography (Dirks, Clemente *et al.* 2010). This is thought to provide friction forces for smooth pads, although many wet adhesive systems can produce friction due to the structuring of the surfaces.

1.2.3. Adhesion in insects and spiders

Insect adhesive structures fall into two principal forms, based on their structure: setae-based hairy pads seen in the Coleoptera, Dermaptera and Diptera orders (Gorb 2005); and smooth, soft pads seen in Hymenoptera, Phasmatodea, Orthoptera and some Hemiptera and Lepidoptera (Gorb 2007). The class of insects provides the greatest volume of adhesive climbers in the animal kingdom. The four largest orders of insect - Coleoptera, Diptera, Lepidoptera and Hymenoptera - between them accrue over 500,000 species, and many of those species will possess adhesive pads on their tarsus. Evolution of both pad types has been spread throughout the insect Phylum, so hairy and smooth pads appear in various places, and sometimes both are found within the same Order of insect, for example in Lepidoptera (Gorb 2008). The presence of insects on Earth for such a long time may account for the large variation in adhesive pads found today. As insects have evolved adhesion over a long time, many have developed complex or intricate dynamics with plant surfaces, either showing special adaptations for climbing (as seen with the *Camponotus* ant and its host the *Macaranga* plant (Federle, Maschwitz *et al.* 1997)) or inducing slipping (as seen with *Nepenthes* plants (Bohn and Federle 2004)). Current research often forms around such interactions, or is at least inspired by them, as they display instances where adhesion is specifically triumphing or failing.

Structures which aid climbing can be found throughout the tarsal and pretarsal areas of insect legs (Beutel and Gorb 2001), though there are variations within each leg depending on location due to their function (Labonte and Federle 2013). Attachment devices are frequently found all down the leg of insects; Beutel and Gorb (Beutel and Gorb 2001) give several examples of differing leg attachment devices, such as distally placed arolium, pulvilli and eversible bladders, as well as structures placed more proximally further up the leg. 'Friction pads' found in the tarsus region can provide added friction for pushing

forces in climbing insects (Labonte, Williams *et al.* 2014). Some insects, such as the mosquito, do possess tarsi which have the dual purpose of allowing adhesion to a smooth surface, and water repulsion to allow them to walk on the surface of water (Wu, Kong *et al.* 2007).

The method of adhesion in the smooth and hairy pads of insects is similar, with a fluid being produced to create forces by wet adhesion. The morphological characteristics of both systems allow for effective adhesion by conforming on many surfaces (Beutel and Gorb 2001). The stiff setae will bend to allow for maximum contact in hairy systems, while the very soft cuticle of smooth pads will mould to the contours of the surface. Despite the hairy insect systems bearing a resemblance to the feet of geckos, they use different adhesive systems (although a fluid has been shown to be produced by geckos pads, it is still considered to be van der Waals attraction which provide the forces (Hsu, Ge *et al.* 2012)). Removing the fluid from the insects pads results in a big drop in adhesive force, indicating that the fluid is either the main contributor to adhesive force (Beutel and Gorb 2001), or at least aids in maintaining close surface contact for other adhesive forces to occur. The ultrastructure of the soft smooth pad contains fibrous material, set at an angle in a similar manner as the stiff hairy pads, which indicates the two pad types could be closely connected (Gorb 2007). The smooth pads are often patterned or ridged, which will provide added friction (by direct contact with the surface) or directionality to the pads that can stick better when dragged in one direction (Gorb 2007). Patterning of the contact area allows for more efficient drainage of excess fluid, which will provide the close contact necessary to produce larger frictional and adhesive forces (Scholz, Baumgartner *et al.* 2008). In ants the fluid film is kept small by drawing it out when the feet slide, which forms large static forces (Federle, Riehle *et al.* 2002).

In spiders, a hairy pad system that is similar to insects is seen. (Kesel, Martin *et al.* 2003). Most research agrees that the tarsi of the spider utilise the same techniques for climbing as geckos (Federle 2006), possessing extremely similar spatulae-tipped setae which use dry adhesion, and also using claws for rough surface attachment (Niederegger and Gorb 2006). The setae are arranged radially on each leg, which should provide a better sticking success rate (Wolff

and Gorb 2013), and spiders have been shown can utilise their eight legs in order to produce high friction forces in opposing legs (which other climbers are likely to do) (Wohlfart, Wolff *et al.* 2014). However, some recent research discovered thin layers of fluid being deposited by the tarsus of spiders and other arachnids, which implies that an adhesive mechanism more like the one seen in various insect species. The tarsus did not always secrete a fluid, with the tarsus displaying periods of dryness (also seen in insects), and so the adhesion used could be interchangeable between a wet system and a dry system, although at this point it is still unclear (Peattie, Dirks *et al.* 2011). The adhesive properties of spiders silk are tested and studied more frequently than their adhesive pads.

1.2.4. Adhesion in tree frogs

Like insects, tree frogs utilise a wet adhesion system using fluid produced from pores on specialised toe pads (*Figure 1.2*). (Federle, Barnes *et al.* 2006). The exact composition of tree frog toe pad fluid is unknown, but a fluid made up of long-chained molecules could increase viscosity and allow for a greater degree of friction and adhesive forces to take place (Hanna and Barnes 1991). The toe pad surface exhibits hydrophilic properties, and so the pad fluid should spread across the whole of pad easily if it is mainly aqueous in composition. Early work speculated that the fluid acted like a glue (a method utilised by echinoderms (Flammang 1996)), but this theory has since been dispelled by experimentation (Emerson and Diehl 1980). A tree frog's sticking ability is greatly reduced after being fully immersed in water (Emerson and Diehl 1980), which is used as evidence that the forces through wet adhesion are used for sticking (Federle, Barnes *et al.* 2006)(although dry adhesive systems also decrease in effectiveness in wet systems). Capillary forces were first proposed as the method of sticking by Emerson and Diehl, although it was accepted that some other mechanisms must be in play for frogs to stick, particularly on challenging surfaces such as rough surfaces.

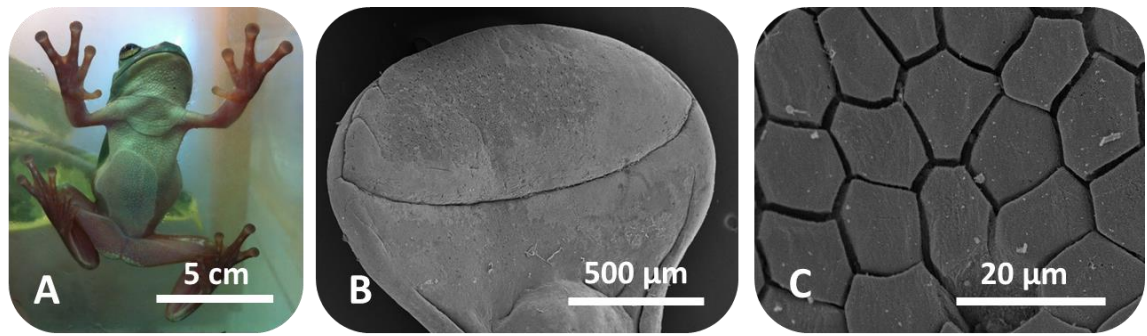


Figure 1.2: Toe pad morphology in tree frogs, which are used for climbing (Image A). The toe pads are an enlarged area on the distal end of each toe (Image B), which are composed of polygonal cells with channels running through them (Image C). Images B and C taken using scanned electron microscopy.

The adhesive pads of tree frogs are flat, disc-shaped ends placed distally on each toe (Figure 1.2), which are significantly larger than other areas of the foot (Federle, Barnes *et al.* 2006), and possess a specialised layer of epidermal cells (Green 1979). The pad's microstructures - polygonal shaped columnar cells (approx. 10 μm in diameter), are soft (<30 kPa) and extremely malleable, and are coupled with relatively deep channels (1 μm wide) connected to pores, which allows pad fluid to spread throughout the toe pad (Federle, Barnes *et al.* 2006). Each polygonal protrusion appears flat topped, but the cells are covered in peg shaped nanostructures (100-400nm in diameter) which are thought to provide close contact and friction with the surface (Figure 1.3) (Barnes, Baum *et al.* 2013). The tops of the polygons, with their nanostructures, will then produce significant levels of frictional force which a smooth surface would not. The nanopillars could be multifunctional in purpose: the structuring could aid in conformation when coupled with the softness of the pad, the small channels between the dimples could help to drain the contact zone, and the concave shape may act as small suction cups for additional adhesive forces (Barnes, Baum *et al.* 2013). This polygonal pattern of cells is remarkably similar to the pads found in other climbing organisms, such as some smooth-padded insects like crickets (Barnes 2007). Structurally, the toe pads show internal fibrillar structures underneath the polygonal patterns, which bear a resemblance to the hairy pad systems of insects and geckos (Barnes, Baum *et al.* 2013). The channels between the polygonal cells are thought to aid both the spreading of the liquid throughout the pad (as they are connected to the pores), and also to remove excess fluid (whether that be pad fluid, water or other fluids) to maintain a close proximity between the two adhering surfaces (Federle, Barnes

et al. 2006). Close contact between the surface and these pads significantly increases the shear forces, as even a small layer of fluid can act as a lubricant which would reduce the boundary friction forces of the cells. High friction forces measured for the pad mean that direct contact is likely to be occurring between the pad and the substrate (Federle, Barnes *et al.* 2006), although the pad fluid may play a role in friction production like in insects (Dirks, Clemente *et al.* 2010).

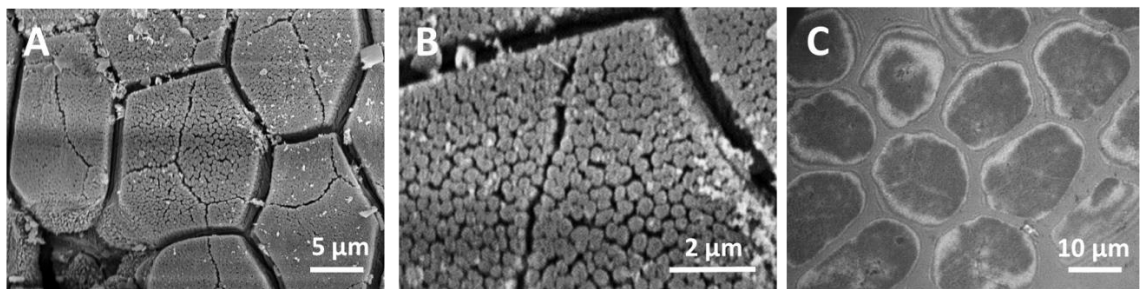


Figure 1.3: The toe pads of tree frogs are made up of polygonal cells (image A), which are topped by nanopillars (image B). The top of the cells come into direct contact with the surfaces, which can be seen as dark patches using interference reflection microscopy (IRM) (image C). Images A and B taken using scanned electron microscopy, and image C taken using interference reflection microscopy.

The pads will also change shape when adhering, due to the softness of the surface (an elastic modulus of approximately 35.5 ± 4.1 kPa (Barnes, Baum *et al.* 2013)). This means that that pad can display rubber-like friction with the surface, and allows extremely close contact and therefore better adhesion (Federle, Barnes *et al.* 2006). The softness of the pad will aid in expulsion of excess fluid by squeezing and therefore narrowing the channels of the pad. Studies measuring the softness of the pad (measured as the effective elastic modulus, or E_{eff}) have shown that the pad overall acts as a very soft material (with an E_{eff} of 4-20 kPa)(Barnes, Goodwyn *et al.* 2011). The outer epithelial layers of the pad appear to be stiffer (33.5 kPa), where the keratin filaments of the outer layer provide the pad surface with a relatively stiffer outer layer (Barnes, Baum *et al.* 2013). Deeper down the pad is composed of many blood capillaries, which will provide the pad with its soft properties. This provides the pad with a material that will conform well when necessary, but has an outer layer which provides some degree of protection from wear and tear (Barnes, Baum *et al.* 2013).

Adhesive toe pads in frogs have evolved independently in several frog families, principally from Hylidae (known as 'true' tree frogs) and Rhacophoridae (bush or shrub frogs) (Duellman and Trueb 1986); they are also found in Microhylidae, Leptodactylidae, Hyperolidae, Centrolenidae and Dendrobatidae (Barnes, Baum *et al.* 2013). This is considered by some as evidence of convergent evolution (although it may be argued that frogs are still too closely related for this to be convergent evolution), with toe pads of all families showing highly similar structuring (Barnes, Oines *et al.* 2006). These species can vary hugely in size: smaller species can measure only 1 cm in length, while larger species (such as the Wallace's flying frog) can measure over 10 cm in length. However as tree frogs increase in size, it becomes increasingly difficult for them to stay attached. Studies on a variety of organisms, including tree frogs (Barnes, Oines *et al.* 2006), have shown that the adhesive surface area is linked to the total weight it can carry; this is due to area being squared when increased in larger animals, whilst volume of the organism will be cubed. Allometric scaling studies showed that larger frogs compensate for a larger mass by having comparatively larger toe pads, although still not efficient enough to perform equally with smaller frogs (Barnes, Oines *et al.* 2006). Frogs have also been known to use the large surface area of their stomach and midriff to aid in sticking when resting in a vertical position, as the larger contact area helps by producing friction with the surface. However, wet adhesion using the pads and their fluid appears to be a more important aspect of their sticking, as sticking ability is greatly reduced when the frogs were immersed in water (Emerson and Diehl 1980).

1.3. Challenges for adhesive pads

There have been several examples of studies of natural adhesives concerning their mechanism of attachment/detachment and how much force they can withstand. However, these are often conducted under certain testing conditions, where the surface that is being stuck to is generally clean, smooth and dry; typically the surface tested on is glass, as a smooth surface illustrates the capabilities of an adhesive pad without interactions like interlocking of claws coming into play. Whilst climbing in the natural world, a whole array of surfaces

will be encountered which will exhibit many different characteristics. Often the characteristics of a surface are in place to prevent an organism from climbing on it, such as a plant which would not want herbivorous insects to eat it. Waxy layers on plant leaves can have crystals loosely attached to the surface which will potentially impede contact with a surface, and in general natural surfaces will have loose dirt and dust on them. Very rarely will a surface be as smooth as glass, and so roughness will constantly be a challenge to adhesion as well. The wetness of surfaces can also vary hugely, particularly in a humid environment like the rainforest where water droplets can form on leaves and surfaces, and leaves can possess hydrophobic outer layers which will allow water to roll from the surface. Failed adhesion for a climbing organism can result in falling, or failing to reach food sources and safety, which can affect the survival of that individual. What this means is that although an organism may have shown good adhesive ability when tested on glass, its performance could be very different depending on the environment. Recent research is increasingly interested in the climbing capabilities of animals in difficult environments, such as wet conditions, rough surfaces and contaminated surfaces. There is a noticeable gap in the research field in how tree frogs adhesion is adapted for such challenges.

1.3.1. Fast, effortless detachment

An efficient detachment method is as equally important as sticking ability in dynamic adhesive systems. When sticking to a surface, an organism cannot afford to become too attached to the surface, as too much friction and adhesion with a surface can negatively affect movement and be expensive energetically, as well as potentially damaging to the pad (Federle and Endlein 2004). Even though there are many strong adhesive systems in nature, for climbers the detachment speed is often very rapid (15 milliseconds detachment time in geckos), nor is there any large degree of detachment forces impeding pad removal. In order to allow for efficient dynamic adhesion, many organisms have developed specialised techniques of toe pad removal; an example of one of these is peeling of the adhesive surface. In tree frogs, the peeling of the foot begins at the proximal end of the pad and moves towards the distal end, which has evolved so that it can efficiently occur whilst taking a step forward (Hanna and Barnes 1991). The fibrillar structures within the pads of stick insects and

tree frogs can provide directionality much in the way that setae do in hairy pads, as they could act as stiff structures within the pads that will give when the pad is peeled from the proximal end. This is contrasting to what occurs in geckos, where they curl their toes upwards (distal end first, peeling to the proximal end) to detach their setae (Autumn and Peattie 2002). In geckos, by peeling off setae at an angle (30°) and individually, much less force is needed, and so can be done with little trouble as the setae move into an “unsticking” state (Tian, Pesika *et al.* 2006). The adhesive pads of many insects have evolved for efficiently and only sticking when necessary. In the case of ants, the retractable arolium can be regulated, which gives the ant a ‘preflex’ to change its adhesive capabilities depending on circumstances (e.g. a gust of wind, being turned upside down) by changing the area in contact passively and almost instantaneously (Federle and Endlein 2004). In flies, varying movements (pulling, shifting, lifting and twisting) of the tarsus and pretarsus allow for an easier detachment, and the movement used depends greatly on what leg is being removed (Niederegger and Gorb 2003). The adhesive pads of ants also display highly variable detachment movements, but as their pads are a soft, non-hairy material which only extends when needed (Federle, Brainerd *et al.* 2001) a peeling mechanism is more possible too.

Peeling an adhesive surface allows a strongly bonded surface to be removed from the substrate without the large force necessary to remove the entire surface at once. The force is concentrated along the peel zone instead of over the entire adhesive area, which means it requires less force. A good example of this is sticky tape - it requires much less force to peel the tape from one end than it does to try and remove the whole piece of tape. The detachment force at the peel zone for a simple adhesive system being peeled off is characterised by the following equation:

$$F_{peel} = \frac{b\Delta\gamma}{1 - \cos \alpha}$$

(3)

where b = width of the peel zone, $\Delta\gamma$ = the constant adhesive energy of the tape, and α is the peeling angle (Endlein, Ji *et al.* 2013). This assumes a constant peeling force and speed, and is referring to the peeling of tape from a surface (which is not strictly the same as the peeling of a toe pad). The angle of peel greatly affects the amount of force needed; again with the tape analogy, it is much easier to peel off tape when the angle is perpendicular compared to a low angle. From personal experience, when trying to removing a tree frog from a surface, it is much more difficult by pulling backwards, compared to pushing which can be done with relative ease (Hanna and Barnes 1991). Climbing frogs tend to keep their toe pads facing up when on a tilting board, or at least at as low an angle as possible (constant readjustment of the pads is often necessary to do this)(Endlein, Ji *et al.* 2013). Tree frogs deploy a sprawled posture on overhanging surfaces to prevent peeling of the pads and to create frictional forces by pulling the pads inwards. This results in the peel angle of the pad increasing, therefore the foot is repositioned away from the centre of mass (Endlein, Ji *et al.* 2013). The frog's toe pads themselves are often very manoeuvrable, with joints being able to bend to accommodate many stances (Hanna and Barnes 1991). The pads of tree frogs are detached whilst climbing using peeling, so that the strong adhesive forces of the pad can be quickly overcome by fast detachment, and therefore allow easy climbing (Hanna and Barnes 1991).

1.3.2. Self-cleaning properties of adhesive pads

An important aspect of any adhesive pad based climbing is keeping pads, feet and climbing appendages clean. Many adhesive pads possess microstructures or a secretion which should cause contaminants to stick. Contamination in the wild can be caused by dirt and particles becoming stuck to the adhesive pads. The presence of contaminants can detrimentally affect the contact area between pad and surface which is essential for effective adhesion. In fact, many plant species utilise this to keep away some animals but allowing those adapted to it to stay. The *Macaranga* trees of South-East Asia possess a layer of waxy crystals, and yet the ant species which live on it can easily climb in those difficult conditions (Federle, Maschwitz *et al.* 1997). Although some organisms shed skin

or show grooming behaviour, a mechanism to clean the pads passively as they climb would be advantageous.

Evidence of self-cleaning pads has been shown in some climbers already. In geckos, pads which have lost adhesive ability due to particulate can recover most of those forces after four steps on the surface (Hansen and Autumn 2005). The loose particles were more attracted to the surface than they are to the setae (due to energetic disequilibrium between the surface and the few setae in contact), which have a very low energy surface, and so particles are easily deposited with each step. The peeling detachment technique of their feet also flicks loose particulate from the feet to aid in cleaning (Hu, Lopez *et al.* 2012). Insects utilise a shearing movement of the pads to displace contaminants, which helped recover most adhesive ability after eight steps (Clemente, Bullock *et al.* 2010). The presence of a fluid also aids in the recovery of forces, by filling the gaps formed by the contaminant to allow wet adhesion to occur (Clemente and Federle 2012). The hairy pads were shown to be more efficient at this, although varying particle size showed that contaminants of a certain size (10 μm) will get stuck between the hairs. Smooth pads in general took longer to recover, and were more reliant on the shear movement to remove contaminant than hairy pads were. However on surfaces with low surface energy the smooth pads showed better self-cleaning properties than hairy pads, and so the variance in pad type in insects could be explained by this difference (Orchard, Kohonen *et al.* 2012). Contaminant size is restricted by the positioning of the arolium in ants, between the tarsal claws (Anyon, Orchard *et al.* 2012).

1.3.3. Sticking under wet conditions

Many man-made adhesive surfaces struggle to stick when surfaces are wet, and so it would make sense that climbing organisms would also struggle in the presence of water. The adhesive setae of geckos are hydrophobic, and remove fluid from their pads by flicking away balled up water via hyperextension (in a similar manner to their self-cleaning mechanism) (Stark, Wucinich *et al.* 2014). Nevertheless, long exposure to water causes the pads to change in properties and lose their sticking ability (Stark, Badge *et al.* 2013). Van der Waal forces are

relatively weak in submerged conditions (Ditsche and Summers 2014), which means that geckos feet cannot stick effectively in a fully wet environment (many gecko species possess claws to interlock with a surface, which may be good enough for attachment in such circumstances). Insects are thought to stick using a wet adhesion system. If the system is fully submerged in water, then these forces are limited, and would negatively affect the adhesive forces. Some water-living beetles overcome this by trapping air within the tarsal hairs to de-wet the pad area, therefore allowing wet adhesion to function again (Hosoda and Gorb 2012). The presence of fluid can cause a drop in friction forces, as the excess fluid causes the feet to aquaplane on the surface, leading to slipping. This is utilised by *Heliamphora* pitcher plants which combine directional hairy trichomes with a highly hydrophilic nature, making a slippery surface to catch insects with (Bauer, Scharmann *et al.* 2012). As a consequence to wet adhesion not being very effective in wet conditions, interlocking, suction and permanent glues are more prevalent for adhesion in submerged environments.

Conversely there are frogs with adhesive pads which live on waterfalls, generally a very wet environment. Torrent or rock frogs, such as *Staurois guttatus* of the South East Asian rainforests, live in an environment where water is constantly flowing over the surface of their pads, which should disrupt the adhesive properties of fluid based adhesion. A morphological comparison of the structures on the toe pads indicated a variance in the patterning of the toe pads compared to tree frogs, which could have some effect on the draining qualities of the pads (Ohler 1995). Further studies on torrent frogs' toe pads and their adhesive capabilities could show new insights into dynamic adhesion, which could help to explain climbing in wet environments for other organisms.

1.3.4. Adhesion to rough surfaces

Part of the adaptive nature of dynamic adhesive mechanisms is to allow for effective adhesion on uneven or rough surfaces. Most surfaces that climbers will scale will possess roughness (Ditsche and Summers 2014)(even surfaces such as glass will possess a degree of roughness), and yet many organisms have little difficulty in adhering to various surfaces whilst climbing. For most dynamic

adhesive systems, effective adhesion is reliant on the adhesive surface and the substrate being within close proximity. This includes dry adhesive systems, which rely on Van der Waals forces, and for wet adhesive systems, which require a constant micro-thin layer of liquid to obtain capillary and viscous forces. Presence of 'peaks' and 'channels' within a rough surface can potentially cause large gaps to appear in the adhesive area and therefore reduce adhesive forces, which could potentially weaken the adhesiveness of a pad. Rough surfaces can also drain fluid from wet adhesive contact areas, which could negatively impact the forces produced by the pad. Finally rough surfaces can be abrasive and therefore damaging to body surfaces in contact with them, particularly as some adhesive surface are made from soft tissues.

To adapt to this, organism's adhesive pads feature morphological characteristics which help to conform; smooth adhesive pads are made of very soft material to adapt to the rough contours, potentially acting like an elastic body on the rough surface (Persson and Zilberman 2002), and hairy pads possess a hierarchical structure and several arrays of setae, which although are made of hard materials can act like a soft material by bending (Jagota and Bennison 2002) to stick to the rough topography. This is coupled with interlocking of the surface with pad contours and increasing frictional forces. This though relies on the level of roughness of the surface suiting the pad, and roughness can vary from nano-through to macro-roughness. In geckos when a surface has small levels of roughness (<100 nm) or very high levels of roughness (>300 nm) then spatulae adhesion is not affected (see *Figure 1.4*), but intermediate levels of roughness will cause the contact area of the spatulae to be decreased, leading to a reduced adhesive force (Huber, Gorb *et al.* 2007).

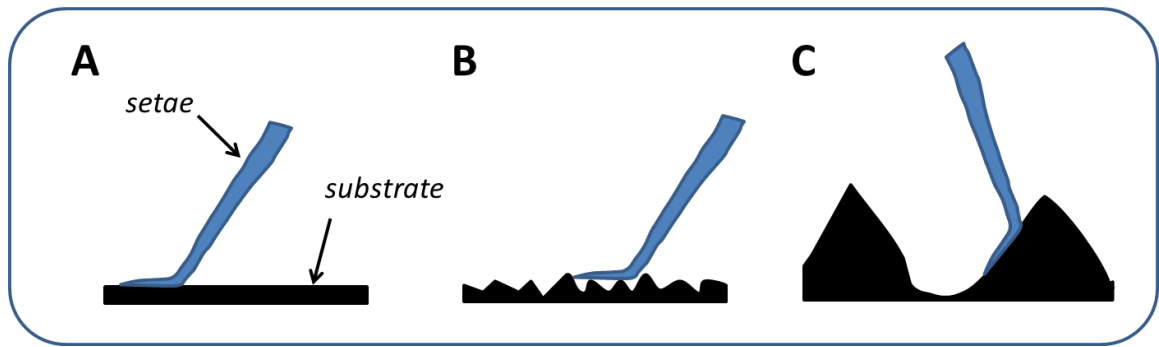


Figure 1.4: diagram showing setae contact on surfaces with different topographies. On a smooth surface (A) the setae can make full contact, which is also true for large asperities (C). However on an intermediate roughness (B) full contact cannot be made, therefore hindering adhesion.

For some insects, large scale surface roughness is gripped with tarsal claws (Dai, Gorb *et al.* 2002). In some cases, such as ants, the tarsal claws are controlled depending on the movement of the arolium (Endlein and Federle 2008). This allows adhesion when necessary, and stops the tarsal claws from getting in the way when unused. For hairy adhesive pads to stick on varying levels of roughness, adhesive hairs need to be long and fine. However this can lead to hairs clumping together, so to counteract some hairy systems display hierarchical branching (Bullock and Federle 2011). Beetles display a minimum force production on nano-rough surfaces, in the same way that gecko pads are less effective at an 'intermediate' roughness. Insect pads also use a fluid for adhesion, and so the fluid can play a role by filling the gaps in the rough surface, therefore maintaining a continuous fluid film for adhesion (Dirks and Federle 2011). Conversely large volumes of fluid on a *smooth* surface can decrease overall forces; consequently insect adhesion on natural surfaces, which can constantly vary in roughness, relies on careful control of fluid production. The density of pillars on rough surfaces can dictate whether the hairy and smooth pads of insects will form a full contact or a partial contact with the surface. This means that the pads fail to make contact with the surface between the pillars, which results in a decrease in adhesive forces (Zhou, Robinson *et al.* 2014).

The effect of rough surface on the performance of the toe pads of tree frogs remains a much less studied field when compared to other dynamic adhesive systems. A brief test of the performance of tree frogs on a wood surface (although no indication of roughness was given) was compared with performance

on various smooth surfaces; the tree frogs were found to adhere poorly to wood (Emerson and Diehl 1980). Unpublished data of the performance of various frog species from Trinidad on different rough surfaces showed that frogs would display decreased climbing performance on an intermediate roughness (asperity size approx. 100 μm). Models predict that the pad fluid plays an important role on rough surfaces, similar to insect adhesion. The fluid will fill the surface gaps upon contact (essentially smoothing out the contact surface), creating its thin layer across the pad and preventing 'cracks' from appearing in the contact area which would weaken adhesion. However, large channels on a surface may prevent the fluid from successfully filling the gaps, and instead it remains within the channels and limits adhesion (Persson 2007). The pad is also a very soft material, which could play a role in maintaining close contact (Federle, Barnes *et al.* 2006). Friction forces could play a large role on rough surfaces, with the mucus channels and the dimple geometry on the hexagonal blocks providing interlocking on a micro- and nano-scale (Federle, Barnes *et al.* 2006).

1.4. Bioinspiration

One of the potential drivers for studies in the field of natural world dynamic adhesion is the wish to replicate them and make innovative bio-inspired surfaces, which are highly efficient and multi-functioning. An example of this is the design of wind turbine blades based on fin shape of marine mammals such as whales. This is known as biomimicry, which is to gain inspiration for inventions or innovations from nature. Lotus leaves exhibit superhydrophobic properties, where water balls up and rolls from the surface very easily. The surface is covered in an epicuticular wax, which is coupled with a microstructure that means that water forms contact angles up to 160° . This helps to clean the surface, because as the water rolls off the surface they will pick up dirt particles and contaminants from the surface and remove them from the leaf surface (Neinhuis and Barthlott 1997).

The idea of dynamic adhesives which will work in a variety of environments, and still detach easily from the surface when needed is a highly appealing prospect. However, designing a micro-structured adhesive which can work on rough, wet,

or contaminated surfaces, and still be reusable for thousands of repeats is a major challenge. Despite these difficulties, the discovery of gecko, spider, insect and tree frog adhesive systems has instigated the advent of biomimicry of adhesive surfaces for several potential applications. An important step in designing such surfaces is to understand the exact parameters which are best suited to the environment the adhesive is needed for. Many organisms which need adhesives to climb show such specialisations, as has been noted above, and understanding how nature copes with the challenges faced by adhesion aids smart surface design. Tree frogs present a sticky surface which could potentially be used for inspiration, but this requires an understanding of their capabilities which is currently lacking. So far the micro-patterning of the toe pads have aided in design of many surfaces, including tyre design (Barnes 2007). Splitting of the contact area can improve friction forces by removing excess fluid, and it helps to split the peel front into separate parts. This prevents cracks from forming in the adhesive area, which will improve performance. The hope would be that the experiments in this thesis would help to contribute to any potential surface designs.

Gecko adhesion in particular has been the subject of many biomimetic investigations, as their adhesive system involves no additional fluid. Mushroom shaped microstructures (approx. 20 μm in diameter) show a greater pull off force than a smooth structure of the same material (Gorb, Varenberg *et al.* 2007). Angling of microfibers can also help prevent buckling of the structures (Aksak, Murphy *et al.* 2007). Forming surfaces which possess spatula-like tips or mushroom topped structures dramatically increase the pull off force of micropillars (del Campo, Greiner *et al.* 2007). One of the difficulties of creating surfaces which mimic gecko adhesion is the complexity of the hierarchical structures, where the branching of the setae prevent clumping or self-sticking. Most attempts at hierarchical structuring in smart adhesives, whilst showing superior adhesive performance to non-hierarchical surfaces, are still not as sophisticated as the pads of geckos (Bhushan 2007). The adhesive pads of tree frogs present an alternative adhesive system which could potentially be more replicable. If this is the case, then a thorough understanding of the dynamics of tree frog adhesion can only help the development of such surfaces.

1.5. Aims of this thesis

The current accepted mechanism for tree frog adhesion is wet adhesion, whereby the frogs secrete a fluid from the pads to produce forces to stick. The specialised morphology of the pad aids in spreading the fluid round the pad, but allowing for frictional forces to be made by the pad in contact with the surface. Previous studies have shown this pad structure exists in all tree frog species, and the adhesive forces of tree frogs on glass have been well tested. Despite this, very little is known about how well tree frogs can stick and climb on surfaces similar to natural conditions. This includes whether the pads can self-clean after getting contaminated (and whether contamination has a negative effect on adhesion), or how well tree frogs can climb on surfaces with differing roughnesses. Natural surfaces will also frequently exhibit hydrophobic properties, or can be hydrophilic and therefore have water on the surface. The aim of this thesis is to investigate how well tree frogs can stick under these conditions. This will be tested using specialised force measuring equipment, along with microscopy techniques and climbing performance experiments.

This PhD was funded by the Deutsche Forschungsgemeinschaft's (DFG) Priority Programme, SPP1420 'Biomimetic Materials Research: Functionality by Hierarchical Structuring of Materials', as part of a collaboration project between the University Of Glasgow (UK) and the Max Planck Institute for Polymer Research in Mainz (Germany). The project aimed to investigate the abilities of tree frogs, and to gain inspiration to manufacture adhesive surfaces which would work in a similar way.

2. General Materials and Methods

For many of the following experiments conducted, there are common frog species, materials and techniques used. Along with the history of adhesion measurements, the techniques used are written in the following chapter. Any variations between studies are noted within individual chapters.

2.1. Introduction - adhesion measuring techniques

2.1.1. Whole animal force measurement techniques

Despite scientific interest in climbing adhesion existing for a long time (Hooke 1665), there were few studies of the forces involved in adhesion until later in the 20th century, with Kerkuts' study of starfish adhesion in 1953 being an exception (Kerkut 1953). Various techniques have been used, depending on both the organism being studied and in relation to how the forces bear significance (e.g. self-cleaning properties of adhesive structures). Force plates (often termed as sensors or transducers) are frequently used, by translating bending of the surface in contact into adhesive values. However, several experiments used the forces created by the weight of the organism to test their adhesive ability, usually by tilting and rotating the platforms to which the organism is sticking to see at what angle the organism fails to adhere at. This technique was commonly used in studies on tree frogs (Emerson and Diehl 1980, Hanna and Barnes 1991, Barnes, Oines *et al.* 2006, Smith, Barnes *et al.* 2006, Smith, Barnes *et al.* 2006), but has also been used on lizards (Zani 2001) and aphids (Kennedy 1986). An elegant study by Endlein *et al.* (Endlein, Ji *et al.* 2013) combined the tilting platform with an array of force plates, allowing forces to be measured at different tilting angles. In a similar vein to the rotating method, Ishii tested the adhesive ability of upside down ladybirds by adding weights to their bodies, therefore testing their adhesive capabilities (Ishii 1987). For both of these methods, gravity plays a role in the measuring of adhesive ability.

Centrifuges can also be used to measure whole animal adhesive force, as the centrifugal forces produced by a rotating tube or platform tests the adhesive and frictional forces of the organism. Cameras or fibre optic sensors are deployed to determine the moment of detachment. First described in 1990 (Dixon, Croghan *et al.* 1990), centrifuges have been repeatedly used to test the dynamic adhesive forces in climbing organisms, mainly insects such as ants (Federle, Rohrseitz *et al.* 2000, Federle, Riehle *et al.* 2002), flies (Gorb, Gorb *et al.* 2001), beetles (Voigt, Schuppert *et al.* 2008, Bullock and Federle 2011), moths (Bitar, Voigt *et al.* 2009), cockroaches (Lepore, Brambilla *et al.* 2013) and insect larva (Voigt and Gorb 2012). Whilst it has been a common technique for smaller invertebrates, centrifuge experiments on larger climbing organisms such

as geckos and tree frogs are lacking. This is likely due to the experiments being seen as stress inducing for larger organisms, which could harm the animal in some way.

A common technique is to tether or attach the organism to thread, wire or hair, and then test the adhesive ability by pulling with a known force. The organism can be attached to weighing scales, known weights or to sensitive force sensors or plates to measure the maximum adhesive or frictional force. This was often used on marine organisms such as limpets (Grenon, Elias *et al.* 1979), barnacles (Yule and Walker 1984), periwinkles (Davies and Case 1997) and the tubules of sea cucumbers (Flammang, Ribesse *et al.* 2002). Being tied or glued to a tether to measure forces is prevalent in arthropods as well, particularly in measuring frictional forces. Originally used by Stork on beetles (Stork 1980), several other studies used the technique on a variety of arthropods, including blowflies (Walker, Yule *et al.* 1985), aphids (Dixon, Croghan *et al.* 1990), several other beetles studies (Betz 2002, Dai, Gorb *et al.* 2002, Gorb, Voigt *et al.* 2008, Gorb, Hosoda *et al.* 2010, Hosoda and Gorb 2011, Prum, Seidel *et al.* 2011, Voigt, Schweikart *et al.* 2012, Prum, Bohn *et al.* 2013), as well as some recent tests on spiders (Wolff and Gorb 2012, Wolff and Gorb 2012, Wolff and Gorb 2013, Wohlfart, Wolff *et al.* 2014). There have also been a few studies involving lizards (Irschick, Austin *et al.* 1996, Niewiarowski, Lopez *et al.* 2008, Stark, Sullivan *et al.* 2012) and frogs (Green 1981) where the organism has been held or tethered and pulled against a force measurer of some sort, although they are less common and understandably so, given the difficulty in tethering these organisms. Whole animal tethering is useful as it allows the overall adhesive ability of the organism to be measured, however the organisms' behaviour (and unwillingness to hold on) can affect the reliability of these results as maximum capabilities. This method will test all adhesive mechanisms collectively (for example, claws and pads) rather than simply the adhesive pads of the organisms.

2.1.2. Smaller scale force measurements

All of the previous techniques involve testing force measurements on a whole animal scale, but some techniques involve looking at force measurements for a

specific region like single toe pads. This is useful in gaining understanding the capabilities of solely the pads, and could help to explain the differing roles of adhesive appendages.

Atomic force microscopy (AFM) is a useful technique which involves a thin cantilever (within the nanometre range in size) coming into contact with the surface. The tips can be varied in shape depending on the experiment, and AFM can be used to map the topography of a surface, or for measuring forces on a nanoscale. AFM is often used to test the adhesive abilities of single celled organisms (Ong, Razatos *et al.* 1999). AFM proves to be a useful technique when measuring the forces of a very small area such as the adhesive hairs of spiders (Kesel, Martin *et al.* 2003, Kesel, Martin *et al.* 2004), flies (Langer, Ruppertsberg *et al.* 2004) and geckos (Huber, Gorb *et al.* 2005). AFM (along with other probes such as glass beads on cantilevers) also provides useful information on the surface properties of adhesive pads, particularly the elastic modulus of smooth pads (Scholz, Baumgartner *et al.* 2008).

As noted above, force plates (also termed force sensors and force transducers) are commonly used in testing adhesive ability. One highly effective method is to immobilise the organism and test the pad by manipulating the pad on the surface, to measure the maximum adhesive and/or frictional forces. In this way, the behaviour of the animal is no longer a factor, and the pad can be tested in a repeatable manner. Since 2000, there has been a flurry of papers using this method to measure adhesive forces; from geckos toes and setae (Autumn, Liang *et al.* 2000, Liang, Autumn *et al.* 2000, Autumn, Sitti *et al.* 2002, Hansen and Autumn 2005, Gravish, Wilkinson *et al.* 2008, Gravish, Wilkinson *et al.* 2009, Gillies, Lin *et al.* 2013), to tree frogs pads (Federle, Barnes *et al.* 2006, Barnes, Pearman *et al.* 2008), and arachnids (Mizutani, Egashira *et al.* 2006, Niederegger and Gorb 2006), as well as a plethora of studies on insects (Gorb, Jiao *et al.* 2000, Drechsler and Federle 2006, Bullock, Drechsler *et al.* 2008, Frantsevich, Ji *et al.* 2008, Clemente, Bullock *et al.* 2010, Dirks, Clemente *et al.* 2010). Some variations include transparent surfaces and cameras to allow contact area to be

measured simultaneously with force (Drechsler and Federle 2006), which is the setup utilised in many of the following experiments.

2.2. Materials and methods

2.2.1. Frog species and care

As the dynamic adhesive system of tree frogs works by the frogs secreting a fluid, adhesive tests work best when studied *in vivo*. As such, live tree frogs are used for the majority of the studies in this thesis. Several of the following experiments involved using tree frogs which are kept at the University of Glasgow; the species *Litoria caerulea* (Family Hylidae), which is also known by the common names Australian green tree frog and White's tree frog. Compared to other tree frog species, *L. caerulea* exhibit docile behaviour whilst being handled by humans, and so are an excellent species for studies in biomechanics. The use of the same species in related studies allows for continuity between data that is collected, and *Litoria* has been used in several relevant studies in the past (Federle, Barnes *et al.* 2006, Platter, Pearman *et al.* 2007, Scholz, Barnes *et al.* 2009).

The frogs were bought from a local exotic pet shop (Partick Aquatics & Reptiles, Glasgow), and were kept in the laboratory. They were housed in glass vivaria (30 cm wide x 45 cm long x 76 cm high), which were designed and furnished to provide a comfortable and suitable environment for the frogs. The temperature in the vivarium was maintained at 28°C during the day and 24°C at night using a combination of electric heat mats and room heating. Each vivarium contained a gravel base, a rubber tree plant for the frogs to sit and climb on, and a basin of copper and chlorine free water for the frogs to submerge themselves in. Humidity is kept at a high level using a Honeywell BH-860E2 humidifier (Berkshire, UK). The frogs were fed three times a week on live silent house crickets, which were dusted with a calcium balancer and multi-vitamin supplement (Nutrobal, purchased from Peregrine Live Foods, Essex, England).

Preceding any experimentation, the frogs were washed in water to remove any contaminant or loose dead skin which may be present on their toes and bodies, and carefully blotted dry to prevent the excess water from affecting any friction or adhesion measurements and therefore the frogs' performance.

The general force measurements and experiments used throughout this thesis were non-invasive, and non-stressful. Therefore, they did not come under the Animals (Scientific procedures) Act (1986).

2.2.2. Whole animal experimentation methods

Adhesive capabilities of whole tree frogs were tested using a rotating tilting board - a procedure which was introduced by Emerson and Diehl (1980). The setup (*Figure 2.1*) consists of a wooden board (30 cm long and 20cm wide), to which different surfaces can be attached. The board is screwed to an axle connected by gears to a Stuart SB3 rotator (Bibby Scientific Ltd, Staffs, UK). The motor system allows the board to be rotated at a constant rate (rotation speed was recorded as $4 \pm 1^\circ \text{ s}^{-1}$) as the board moves from horizontal (0°), through vertical (90°) and then finally to upside down (180°). Angles were measured either by viewing a needle on a mounted 360° protractor, or by the use of a potentiometer attached to the back of the rotating board - in this way the angle was recorded using a customised labVIEW interface (LabVIEW Inc., National Instruments, Austin, Texas).

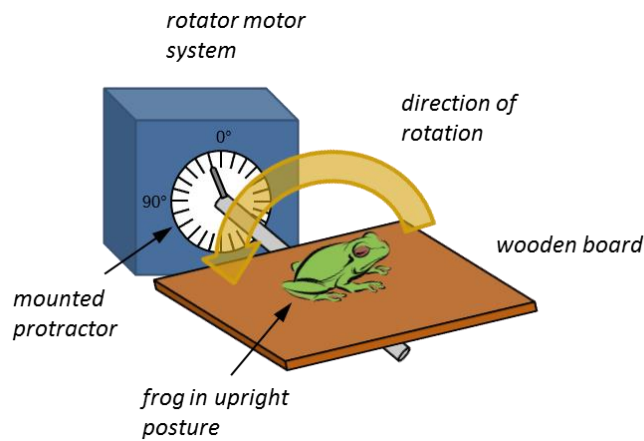


Figure 2.1: diagram of the whole animal experimental setup. The diagram shows the rotating board used for measuring adhesive abilities in whole organisms.

The frogs were placed on the board in a 'head up' orientation, so that as the board rotates the head will be facing uphill. Naturally the frog would occasionally want to jump from the surface rather than hold on, and this was discouraged by either a gentle hand waving over (but not actually touching) the larger species of frog, or a small plastic box if the frog studied is particularly small.

The experiments would begin with the frog at a horizontal position, and as the angle increases the frogs were observed to see at what angles the frog would begin to slip, and eventually fall from the platform. As the board rotates, the frog has to use its adhesive pads to stay on, as the mass of the frog working with gravity increases the frictional and adhesive forces necessary to keep the frog on the board are greater. The two angles measured - the slip and the fall - were recorded for each run of the experiment. These angles represent the maximum amount of friction (from the slip angle) and adhesion (the fall angle) being produced by the frog in this experiment - if the frog is slipping, then friction forces have peaked, and similarly if the frog has fallen from the platform then adhesion has failed. So these are the maximum performance levels by the frog in this experiment. Through using the mass of the frogs and the force of gravity, the angles measured can be used to calculate shear and normal forces using trigonometry (Barnes, Oines *et al.* 2006). These are calculated using simple formula -

For measuring shear force, where $0^\circ < \theta < 90^\circ$:

$$F_{friction} = \sin(\theta) * mg$$

(4)

For measuring normal force, where $90^\circ < \theta < 180^\circ$:

$$F_{adhesion} = -\cos(\theta) * mg$$

(5)

In these equations, θ equals the angle of tilt of the board, m equals the mass of the frog, and g equals the acceleration of gravity. Because of this relationship, the raw data of the angles the frog slips and falls can be used as indicators of their sticking performance.

It is important to note that if the frog is able to avoid slipping beyond 90° , then the maximum level of friction for this test has been reached, as at 90° all of the mass of the frog is working parallel to the pads. This is not necessarily the maximum level of friction force that the pads can produce, but it is the maximum friction force measurable in this test. This is also true for the falling angle of the frog - since at 180° the entire mass of the frog is working through gravity perpendicularly to the pad. If the frog reaches 180° , then the experiment is stopped, as the frog has performed to the maximum measurable adhesive forces. When using angles to calculate force in the above formulae, slip angles greater than 90° were scored as 90° , and fall angles less than 90° or greater than 180° were scored as 90° and 180° respectively. The addition of weights to the frogs would increase the force acting against their pads, but this was too difficult to carry out on small slippery frogs.

For any climbing experiments, if the frogs were lethargic or did not seem to be climbing to their usual ability (this can occasionally happen if a frog is shedding

its skin, for example), then the data for that frog is considered void. The frog is returned to the enclosure, and given a rest from experimenting until normal behaviour has resumed (this can take up to a week).

2.2.3. Single toe pad experimental methods

The single toe pad experimental setup used extensively throughout this thesis was a development of the force measurement setup described by Drechsler and Federle in their 2006 study into attachment forces in insects with smooth pads (Drechsler and Federle 2006). A custom built 3-Dimensional force transducer, designed and built by Thomas Endlein, was used to measure 2 dimensions of force - adhesive (also known as normal force, on the z axis) and frictional (also termed lateral force, on the x axis) forces - created by a single adhesive pad in contact with the bottom of the force plate (*Figure 2.2*).

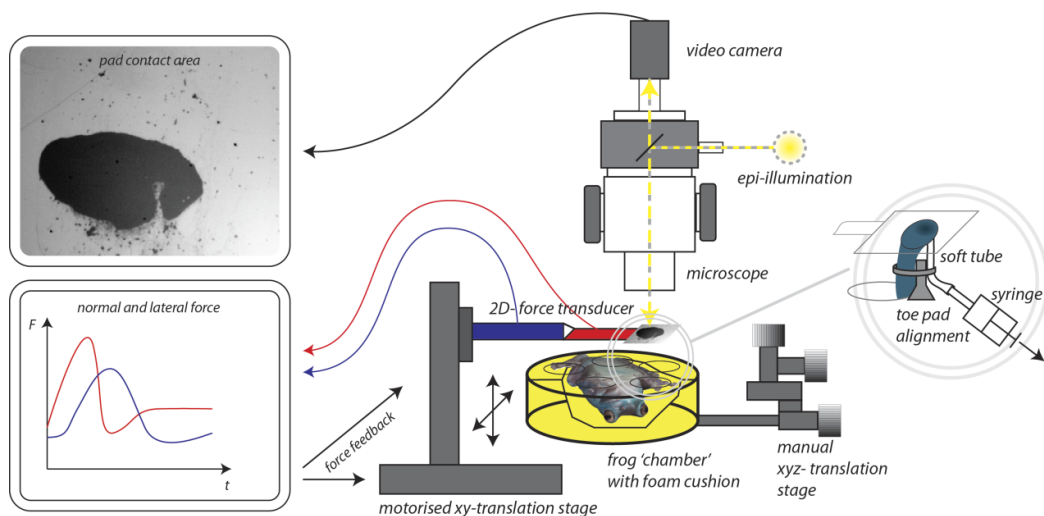


Figure 2.2: Diagram of the single toe pad force measurement experimental setup. The frog is restrained (using a foam cushion) inside a petri dish, and moved using a micromanipulator. An individual toe pad is held so as to be aligned with the force plate (see inset). Adhesive abilities can be measured by a home-built 2D-force transducer, which is moved using a computer controlled motorised stage. Pad contact is visualised using a digital video camera through a binocular microscope lit by epi-illumination. Reproduced from Crawford et al. (Crawford, Endlein et al. 2012).

The force transducer consisted of a bending beam fitted with semiconductor strain gauges (Micron Instruments, CA, USA), two of which are attached to each axis to accurately measure any bending. The beam is part of a wheatstone bridge configuration, with a full bridge made up from four strain gauges. A glass

cover slip (20 x 20 x 0.1 mm) is glued to the end of the beam to provide a flat, transparent surface for the pad to come into contact with - though this surface can be changed for others depending on the experiment. The beam is calibrated by hanging weights to measure specific loads, and by measuring beam displacement along the force plate using weighing scales. This gives a measure of the stiffness of the beam (51 N/m on the longest axis) and the number of oscillations per second (resonance frequency - z axis: 96 Hz, x axis: 125 Hz). The resolution of the force plate is well below the adhesive forces being measured (± 0.2 mN average for both axes).

The force transducer can make precise movements, as it is attached to a 2 dimensional motorised translation stage (M-126 High-Resolution Translation Stage; Physik Instrumente, Karlsruhe, Germany). The motors are run from a custom-built LabVIEW program interface (National Instruments, Austin, TX, USA), providing precise movements of distances in the mm range. As the beam is bent during experimentation, the sampled data is amplified via an amplifier (Gould 57-1340-00 DC Amplifier, Gould Electronics, Eichstetten, Germany), visualised live on an oscilloscope (DL1540 Digital Oscilloscope, Yokogawa electric corporation, Tokyo, Japan) and fed into a data acquisition board (NI BNC-2110; National Instruments). The data is then fed back into the computer that the LabVIEW program is on, completing the loop. This loop allows for force feedback, which allows for a constant load force during friction measurements where the plate moves in a lateral direction. A calibration file run with the program provides information to LabVIEW regarding the beam stiffness, length and the crosstalk (unwanted signal on one of the axis coming from another axis) measured by the beam; this means that these parameters are part of the calculation of the forces measured.

The force transducer setup allows for contact area to be seen whilst measuring forces - this is recorded using a video camera (A602F, Basler, Ahrensburg, Germany), recording at 100 frames sec^{-1} (unless stated differently). The camera is attached to an epi-illuminated binocular microscope (Wild Heerbrugg, Heerbrugg, Switzerland), which provides high contrasting images where the pad

in contact shows as a dark spot (Federle, Riehle *et al.* 2002). The videos are recorded using a Streampix program (NorPix Inc., Montreal, Canada), and are triggered with the camera so that videos and force measurements can be synchronised. Analysis of the videos and force measurement are conducted through a customised MATLAB script (Mathworks, Natick, MA, USA), where peaks in forces and area in contact can be visualised simultaneously to give force per unit area or stress (mN/mm^2 , or kPa). Data is displayed as a plot of forces over the time of the measurement, as in *Figure 2.3*.

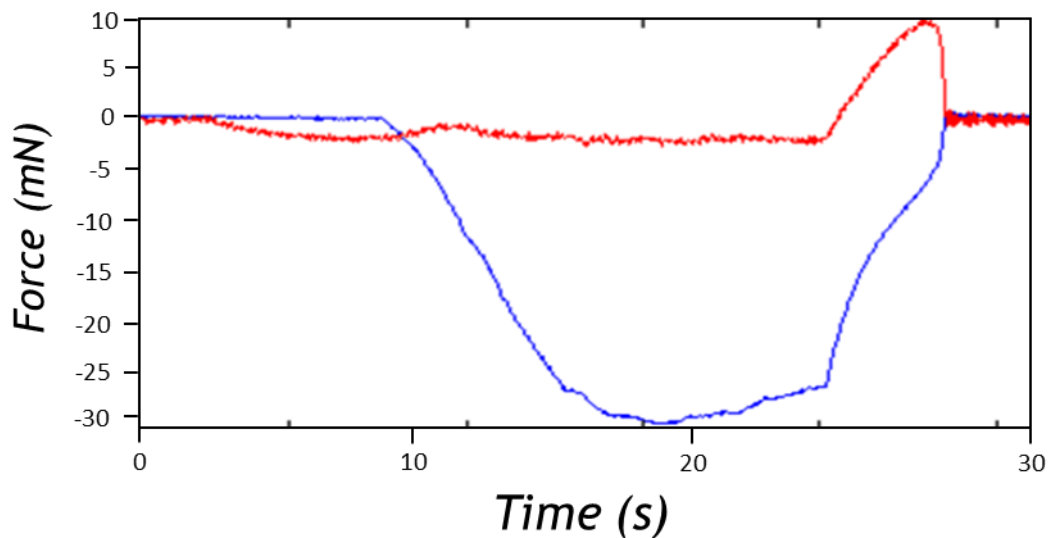


Figure 2.3: Typical output from the force experiments, showing the adhesive (red) and frictional (blue) forces produced throughout the experiment time. Peak values can then be extracted from the data.

To allow force measurements to be conducted on a single toe pad, the frog has to be restrained within a Petri dish, being held in the one spot by a foam cushion acting as padding around the body. The Petri dish is positioned upside down underneath the force plate, and can be accurately positioned directly below the plate using a micromanipulator. In order for the toe to be orientated properly for force measurements, the leg is held in position by a small piece of plastic tubing, acting as a cast for the frog's leg. Due to the bending nature of the toe as well as the leg, it is necessary to restrain the toe pad from unwanted movement as well. A single toe pad is then held in position by deploying light suction (provided by a hand held syringe) on the dorsal side of the toe pad, which orientates the pad in a parallel position with the force plate (see inset of *Figure 2.2*). The toe pads of *Litoria caerulea* are of a suitable size for this

technique of pad alignment, however for smaller species this technique is not possible.

2.3. Conclusion

The use of the force transducer has proved to be an effective and highly reliable method for adhesion measurements, and so it is an excellent technique to use for tree frogs in the following set of studies. However, it is important to see what effect this has on a climbing organism *whilst it is climbing*. The tilting platform test allows this to be tested in tree frogs, as other techniques (centrifuges or organism tethering experiments) are deemed too difficult to conduct on frogs. Both techniques, separately and combined, serve to improve our understanding of tree frog climbing abilities.

3. Evidence of self-cleaning in the adhesive toe pads of tree frogs

The experiments in this chapter have been published in the article detailed below, and has been adapted with permission from the Journal of Experimental Biology. All figures in this chapter have been taken from this publication. The whole animal experiments in the paper (involving the rotating platform) were conducted during a Masters project in 2010; for this reason, they are not present in the results. They are shown in the discussion, as they form part of the overall study into self-cleaning.

N. Crawford, T. Endlein and W. J. P. Barnes (2012). "Self-cleaning in tree frog toe pads; a mechanism for recovering from contamination without the need for grooming." The Journal of Experimental Biology **215**(22): 3965-3972.

Summary

The toe pads of tree frogs will become contaminated by loose particles during use when climbing, and subsequently lose adhesive ability due to loss of contact area. However, frogs can still climb afterwards and maintain their sticking ability. Therefore, there must be a cleaning mechanism in place to aid this. This study showed how the toe pads of tree frogs are capable of self-cleaning whilst in use (a process which naturally occurs whilst the pads are used), which helps to recover adhesive ability lost through contamination. Forces produced by individual toe pads were tested on glass surfaces, and the pads were contaminated with glass beads and repeatedly tested to look for recovery. The results were compared with a previous study looking at whole animal performance. In each case the frogs recovered adhesive forces within a few steps. The use of a shear movement on the surface aided adhesive force recovery, and the presence of the pad fluid could potentially allow for contaminant to be quickly removed with each step.

3.1. Introduction

With tree frogs' toe pads, one would expect them to get dirty over time during use. Whilst climbing about in the wild, tree frogs will encounter a variety of particles of different sizes. The nature of the toe pads - the presence of a secretion and the network of channels found throughout the pad - lends itself to them becoming contaminated easily by loose particulate such as dirt, pollen and other microscopic matter. Several species of plant possess waxy crystallised layers which have the role of deterring climbing organisms; for example, *Macaranga* plants which deter certain species of ants from climbing by producing a layer of epicuticular wax crystals along the stem (Federle, Maschwitz *et al.* 1997). Contaminants can negatively affect adhesive pads by reducing the area of real pad contact as obstructions, and therefore not allowing the close contact necessary to allow toe pads to work. With man-made adhesives, once contamination occurs then the adhesive abilities are significantly reduced, and therefore tapes are often only useful for one or two contacts before losing their stickiness. In contrast, climbing organisms which use adhesive pads (such as ants, geckos and tree frogs) need to use their pads several hundred times a day,

and will repeatedly encounter dirty surfaces. Whilst grooming of pads or shedding of skin can help, these solutions are not always immediately available if the animal is mid-climb. Consequently if adhesive pads are getting dirty regularly, there must be a self-cleaning mechanism (the process of adhesive pads becoming cleaner whilst in use) in place to remove contaminants.

So far, self-cleaning has been documented in both geckos and insects. Geckos, with their nanoscopic hair-like setae on their toes, show a rapid recovery after contamination of shear forces (described as clinging forces) after only four simulated steps in one study (Hu, Lopez *et al.* 2012). The hypothesised mechanism for self-cleaning - digital hyperextension - shows another uniquely distinct role for the setae; however, particles could also be shed due to greater attraction forces to the surface being climbed on (Hansen and Autumn 2005). For insects, adhesive force recovery reached at least 53.4% after eight simulated steps. The morphology of adhesive pads in insects is split into two forms - 'hairy' and 'smooth' pads - and whilst they perform similarly in adhesive performance, the hairy pads are more efficient at cleaning by showing a 98% recovery of forces for 'hairy' pads (the 'smooth' pads showed the previously quoted 53.4% recovery) (Clemente, Bullock *et al.* 2010).

Although tree frogs' climbing abilities have been well documented, prior to this study there had been none looking into self-cleaning. As tree frogs use a wet adhesive system like insects do, looking at the self-cleaning abilities (if they exist) in tree frogs would be an interesting comparison. Ubiquitous self-cleaning in adhesive systems throughout the animal kingdom would suggest that it is a key component of any dynamic adhesive system, and an important consideration when designing manmade 'smart' adhesives.

In this study, the presence of self-cleaning abilities was investigated through experiments on free climbing tree frogs, and force measurements on individual toe pads. The aim of the experiment was to 1) establish whether any form of self-cleaning occurs, and 2) look into the mechanisms involved in the process.

Using glass beads as an artificial contaminant, the tree frogs' self-cleaning performance can be studied and therefore compared to similar studies done on geckos and insects.

3.2. Materials and methods

3.2.1. Study animals

Five tree frogs (*Litoria caerulea*) were used in the following *in vivo* experiments - the housing and care of the frogs are described above in Chapter 2. The frogs (aged between 2 and 4 years old) were weighed throughout the experimenting timeline using a digital scale (mean mass and standard deviation: $29.095 \text{ g} \pm 9.635 \text{ g}$), and the snout-vent length of each frog was measured as well using Vernier calipers (mean length and standard deviation: $69.5 \text{ mm} \pm 9.5 \text{ mm}$). As described in the general methods, the frogs were cleaned in a submerging tub in order to clean the pads prior to experimenting. This prevented any unwanted contaminants from being present. The frogs were then blotted dry so that additional water did not affect the frogs' performance.

3.2.2. Contamination

Contamination of the frogs' toe pads was done using glass beads (Ballotini beads, Jencons, VWR International, Leicestershire, UK). The circular beads had the average diameter of $50 \text{ } \mu\text{m}$ ($\pm 15 \text{ } \mu\text{m}$), which was small enough to be a suitable microscale contaminant whilst still being visible through the microscope used. For this experiment, the beads were arranged on a glass cover slip ($60 \times 20 \text{ mm}$) - this was done by statically charging the slip (rubbing on cloth material) and dipping it into the beads, thereby creating a monolayer of beads on the slip (*Figure 3.1*). The electrostatic charge would last long enough to allow for pad contamination, usually done immediately after the beads have been stuck to the surface.

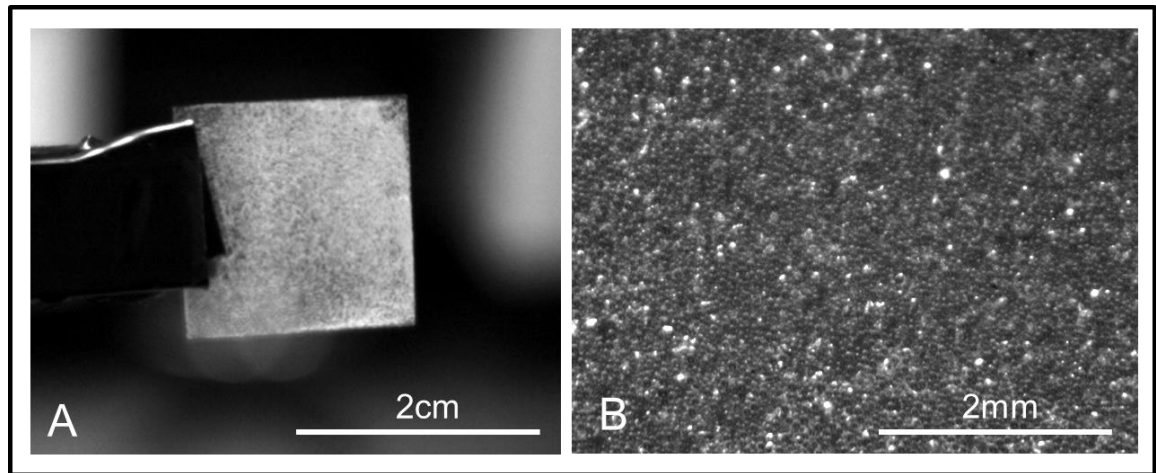


Figure 3.1: Images of the beads used for contamination of a single toe pad in the experiment. Image A shows the glass beads as a monolayer on a glass cover slip. Image B shows a close up shot of the bead monolayer. Images were taken using a digital camera and zoom lens. Reproduced from Crawford et al. (Crawford, Endlein et al. 2012)

3.2.3. Force measurements

The adhesive forces produced by the pad were measured using the force transducer setup described in the general methods section. The setup still contained the force transducer, the feedback loop with the LabVIEW program and the camera with microscope to visualise contact area. However, a couple of added modifications have been made when necessary for experiments involving self-cleaning.

The movement of the force plate is controlled by a motorised stage, so that specific movements of the plate in relation to the pad could be done. In order to test what kind of movements aid self-cleaning, two separate programs were run. The first program (*Figure 3.2*) included a horizontal drag (along the x-axis), and is termed the 'drag' movement. This program involved firstly pushing the pad onto the surface (*Figure 3.2a*) using the force feedback loop, with 2 mN of force being applied (an approximate estimate of the force applied to one pad when the frog is climbing). The pad was then dragged across the surface proximally for 4 mm (at approx. 0.375 mm s^{-1}), with the force being maintained throughout the drag (*Figure 3.2b*). Finally, the pad is pulled away from the force plate at a 30° (*Figure 3.2c*), an angle which shows high levels of adhesive forces.

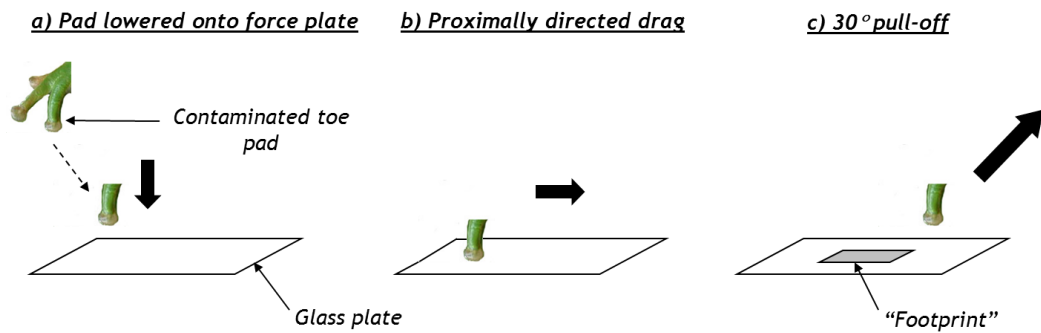


Figure 3.2: The lateral 'drag' program used. (a) The individual toe pad is pushed onto the force plate. (b) The toe is moved in a proximally-directed shear drag (horizontal movement towards the body). (c) Finally, the pad is pulled off the surface at a 30° angle. Reproduced from Crawford et al. (Crawford, Endlein et al. 2012)

The second program used did not have a lateral drag on the surface (Figure 3.3), and was termed the 'dab' sequence. The movement consisted simply of the pad being pushed onto the force plate (with the same 2 mN of force), and then removing the pad vertically. Four repeated measurements were done along the plate, as part of the repetitions explained below.

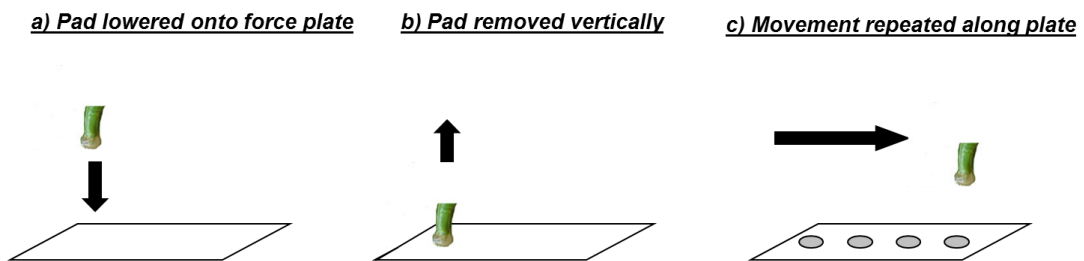


Figure 3.3: 'Dab' program, with no shear movement involved. (a) The pad is brought into contact with the force plate, and is then removed vertically (b). (c) 4 measurements were repeated along the plate. Reproduced from Crawford et al. (Crawford, Endlein et al. 2012)

In order to measure any comparative recovery of adhesive forces in the single toe pad, a control measurement was required prior to any contamination of the pad. With the frog held in position in the petri dish, as described previously, 3 control measurements of an uncontaminated toe pad were taken (4 controls were taken in the case of the 'dabs' measurements) by carrying out the movements described above without the pads being contaminated ; an average value for the control was then calculated. Having the control before each

contamination meant that the same toe can be measured before and after contamination, which acts as a way of standardising the testing, and it provides an indicator for 100% force recovery of that pad. The pad was contaminated with the glass beads by attaching the cover slip with the monolayer of beads onto the force plate, and pushing the pad onto the surface with a desired amount of force - when the pad was pushed on with 2 mN of force, it was described as ‘full’ contamination; when the pad was pushed on with 0.5 mN of force, it has been labelled a ‘partial’ contamination. The difference in contamination levels can be seen in *Figure 3.4*, and were used in tests to see the effects that different levels of contamination has.

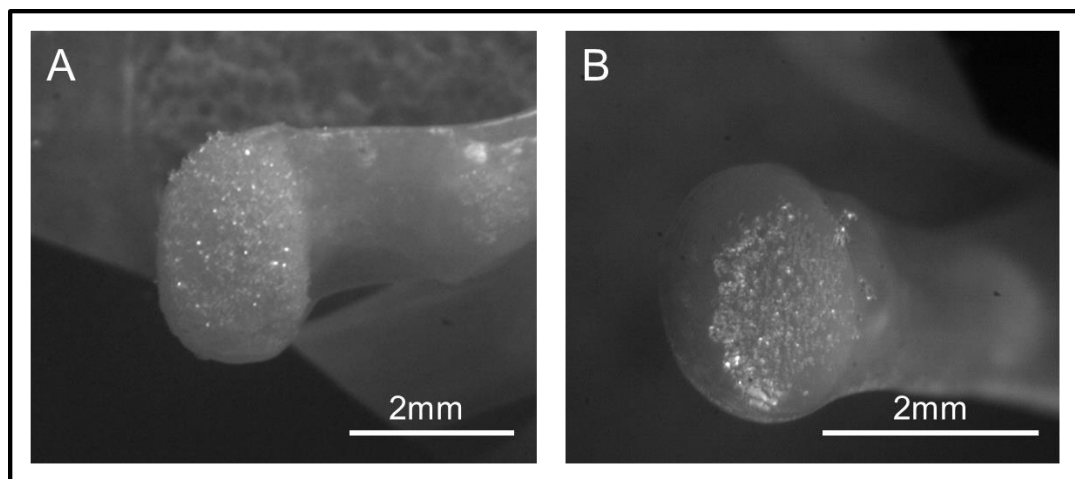


Figure 3.4: Images of frog pads contaminated with glass beads at two different levels of contamination. Image A shows a pad pushed onto the beads with 2mN force (fully contaminated). Image B shows a pad pushed onto the contaminant with 0.5mN of force (partially contaminated). Reproduced from Crawford et al. (Crawford, Endlein et al. 2012)

3.2.4. Statistics

Page’s non-parametric L test was used for this experiment, as it tests for progressive increases or decreases (i.e. trends) between sequential measurements (Page 1963). The results are written as $L_{m,n}$, where m = number of conditions, and n = sample size (along with a p number). After being tested for normality, comparative tests between data sets were conducted appropriately. Two sample Student t -test and Mann-Whitney U tests were used for comparisons, and correlation between bead deposition and contact area was tested using a Spearman correlation test. Statistical analyses for both experiments were done

using MINITAB 15 (State College, PA, USA), and the statistical toolbox in MATLAB 7.6.0 (version R2008a, Mathworks Corp., USA). Ranges of values are indicated by mean \pm standard deviation. For the boxplots - on each box, the central line is the median, the boundaries of the box are the 25th and 75th percentiles, the whiskers extend to include 99.3% of the data for a normal distribution (defined by Matlab), while outliers are plotted individually. Statistical tests are sometimes shown above plots, and the results are denoted as follows: NS = not significant, * = $p < 0.05$, ** = $p < 0.01$, *** = $p < 0.001$.

3.3. Results

3.3.1. Single toe pad force recovery

An initial study on self-cleaning showed that tree frog adhesion was indeed badly affected by contamination, and that the frogs can recover adhesive ability over repeated subsequent steps. This was enhanced by the frogs using their pads, as opposed to remaining stationary (Crawford, Endlein *et al.* 2012). This implies that through use, the pads will clean and therefore be able to stick effectively after becoming contaminated. These results form part of the published material, but were conducted during a Masters project, and so are not included in this thesis. The graphs from those results are shown in this chapter's discussion (*Figure 3.10* and *Figure 3.11*).

In order to gain added insight to the self-cleaning seen, experiments involving single toe pads were carried out on the frogs. The first experiment involved looking at recovery of adhesive forces of a pad which had undergone full contamination. A comparison was done between the two simulated steps described above - the 'drag' and the 'dab' programs (*Figure 3.5*). Contamination of the pads resulted in a large drop in forces for both steps tested, with adhesive force down to 5.93% and 6.35% for the 'drag' and 'dabs' trials respectively. Including this immediate measurement, a sequence of eight sequential measurements was recorded. In the 'drag' trials, a significant trend of recovery was seen (Page's trend test, $L_{8,15} = 2856$, $p < 0.001$), while in the 'dabs' trials there was no significant recovery (Page's trend test, $L_{8,18} = 2714.5$, $p = 0.99$), with adhesives forces remaining too low to allow for effective adhesion. Paired

comparisons of the two experiments at each measurement showed that, for the first three measurements, there was no significant variation between them. By the fourth measurement, a significant difference could be seen ($n = 18$, $z = 2.04$, $p = 0.041$), and this difference continued for all of the subsequent comparisons made, with ‘drags’ producing significantly higher forces than the ‘dabs’ (for all tests, $n = 18$: fifth - $z = 3.74$ $p = 0.0002$, sixth - $z = 4.57$ $p < 0.0001$, seventh - $t = 6.05$ $p < 0.0001$, eighth - $z = 4.11$ $p < 0.0001$). By the final eighth measurement, 75.58% (mean value for all measurements) of the pre-contamination adhesive forces had been recovered by the ‘drag’ technique.

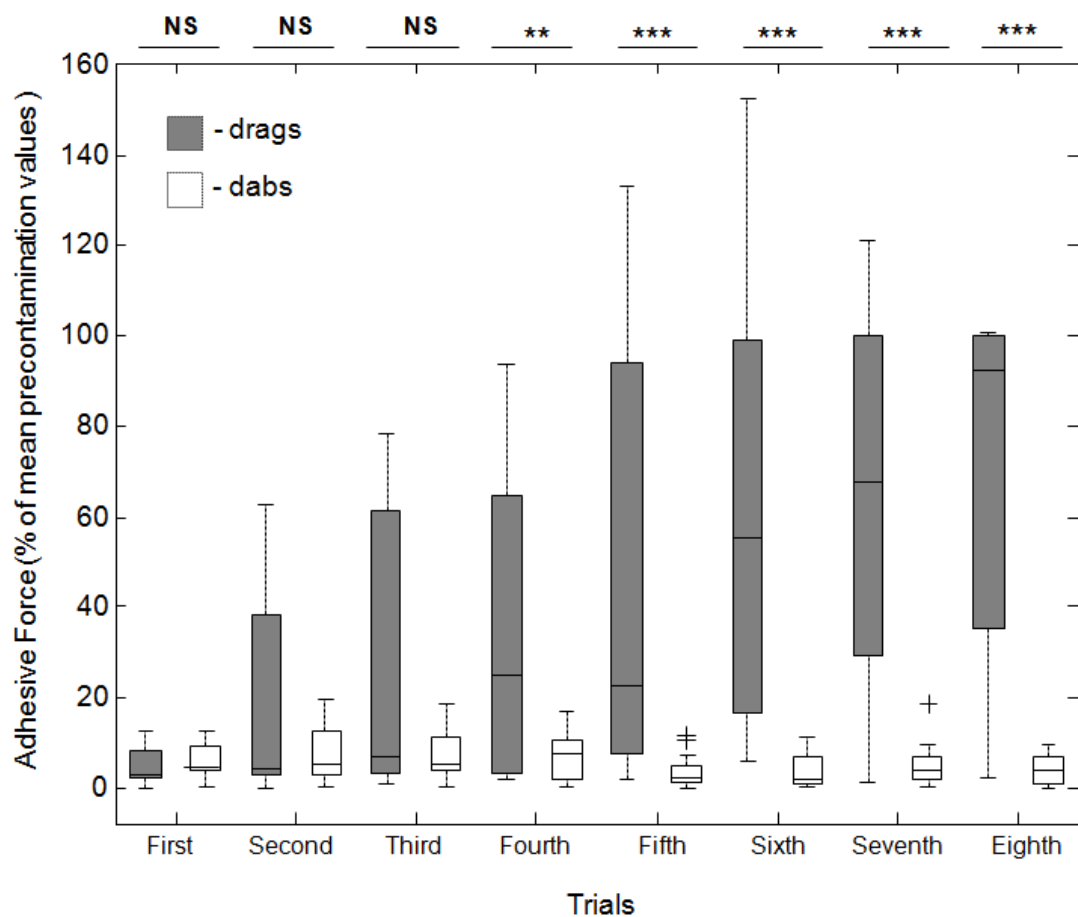


Figure 3.5: Recovery of forces following full contamination. A comparison of adhesive force (normal component of pull-off force) as a percentage of the mean pre-contamination values for both the ‘drag’ (filled boxes) and ‘dab’ (open boxes) forms of the experiment) during recovery from full contamination in single toe pads. The boxes represent consecutive simulated ‘steps’ taken by the toe pad on the force plate following pad contamination. Statistical tests were conducted on each pair, with the results for each shown above the plots. Reproduced from Crawford et al. (Crawford, Endlein et al. 2012)

With full contamination, the ‘dabs’ trials showed no recovery of forces, as seen in *Figure 3.5*. However, in experiments involving partial contamination of the pad, there was a significant recovery of forces over eight consecutive measurements (Page’s trend test $L_{8,13} = 2428.5$, $p < 0.001$) (*Figure 3.6* open boxes). For the ‘drag’ movements, there was no loss of forces when the pads were partially contaminated (*Figure 3.6*, filled boxes). The results from the full and the partial contamination experiments indicate that force recovery differs greatly between the ‘drag’ movements and the ‘dabs’ movements; ‘drags’ are more effective at self-cleaning.

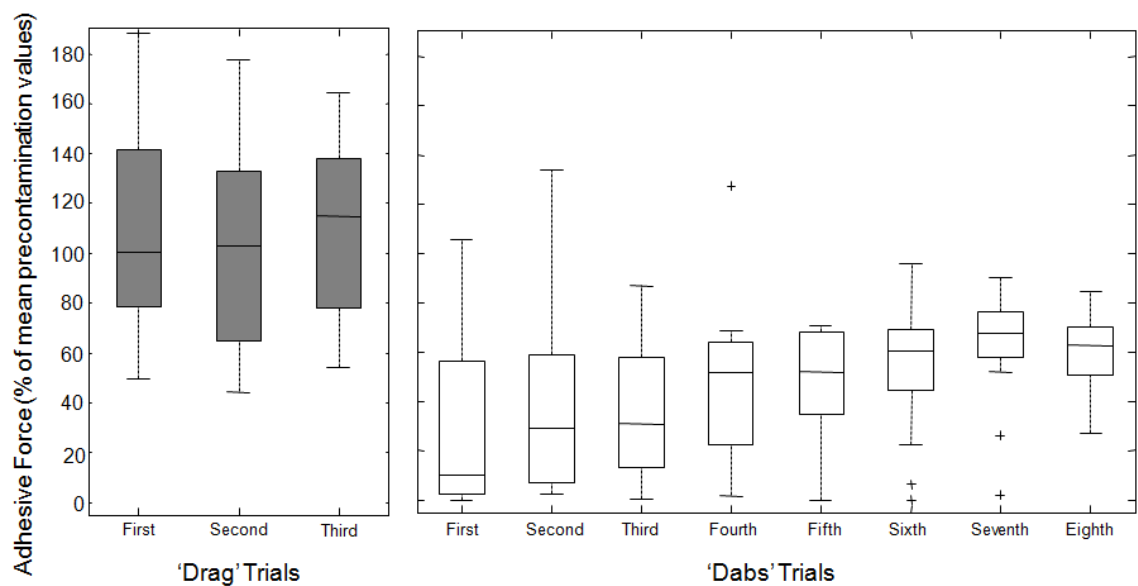


Figure 3.6: Recovery of forces following partial contamination. Boxplot comparing adhesive force (normal component of pull-off force) as a percentage of the mean pre-contamination values for both the ‘drag’ (filled boxes) ‘dab’ (open boxes) forms of the experiment during recovery following a partial contamination in single toe pads. The boxes represent consecutive simulated ‘steps’ taken by the toe pad on the force plate following pad contamination. Reproduced from Crawford et al. (Crawford, Endlein et al. 2012)

3.3.2. Contact area and bead deposition

Another method of quantifying the self-cleaning abilities of tree frogs is to measure the contact area and number of beads being deposited (or ‘cleaned’ off), whilst also measuring the adhesive forces. The same comparison ‘dab’ versus ‘drag’ trials was conducted, for pads which had been partially contaminated (as rate of recovery was faster when the contamination was smaller) as well as pads which are fully contaminated (new measurements rather than the same from the previous experiments). As had been noted before, there

was a significant variance in the forces produced between the different trials (Figure 3.7c), while there was also a significant variance in the number of beads deposited by each step (Figure 3.7a) and in the percentage of the total pad area in contact with the surface (Figure 3.7b). The ‘drag’ movement resulted in more beads being deposited, a greater area of pad in contact, and greater overall adhesive forces when compared to the ‘dab’ movement.

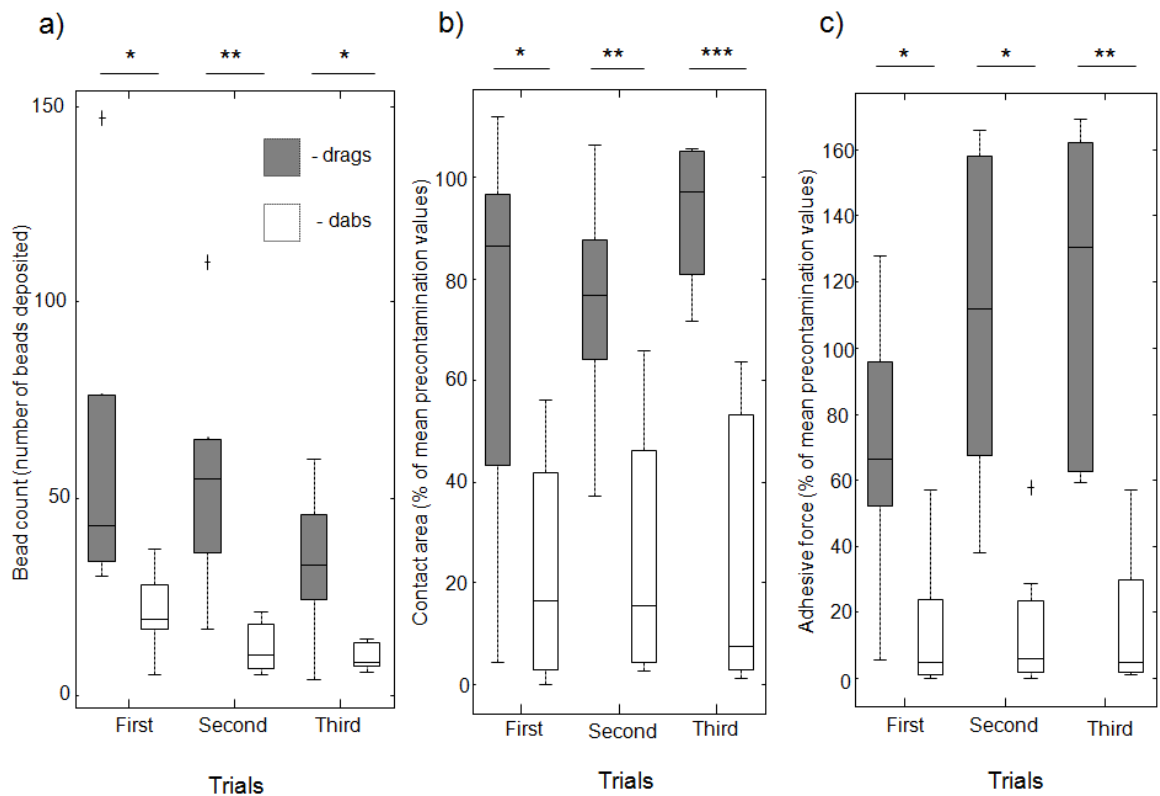


Figure 3.7: Boxplot comparing various results for both the ‘drag’ (filled boxes) and ‘dab’ (open boxes) forms of the experiment during recovery from partial contamination in single toe pads. The boxes represent consecutive ‘steps’ taken by the (Crawford, Endlein et al. 2012) toe pad on the force plate following pad contamination. Graph a) shows the bead deposition rate of each trial, b) shows the contact area as a percentage of the pre-contaminated pads, and c) shows the adhesive forces as a percentage of the pre-contaminated pads. Statistical tests were conducted on each pair, shown above the plots. Reproduced from Crawford et al.

For the bead deposition tally, the cumulative numbers in individual successive trials were correlated with the visible pad contact area (Figure 3.8). For the ‘drag’ trials, a significant correlation was found (Spearman correlation test; $\rho = 0.5711$, $p = 0.0185$), while for the ‘dab’ trials there was none (Spearman correlation test; $\rho = -0.1496$, $p = 0.5175$). A correlation in bead removal and pad contact indicates that more beads being removed results in a larger area of pad in direct contact with the surface, which is associated with higher adhesive

forces. The deposition of beads is evident from the 'drag' trials (seen in *Figure 3.7a* and *Figure 3.8*), and images of the force plate post trial in *Figure 3.9* are further evidence of contaminant being removed effectively. The evidence of all of the following experiments appears to show that the 'drag' movement of the pad is highly effective at removing contaminant and therefore at self-cleaning, and is more effective than the 'dab' movement.

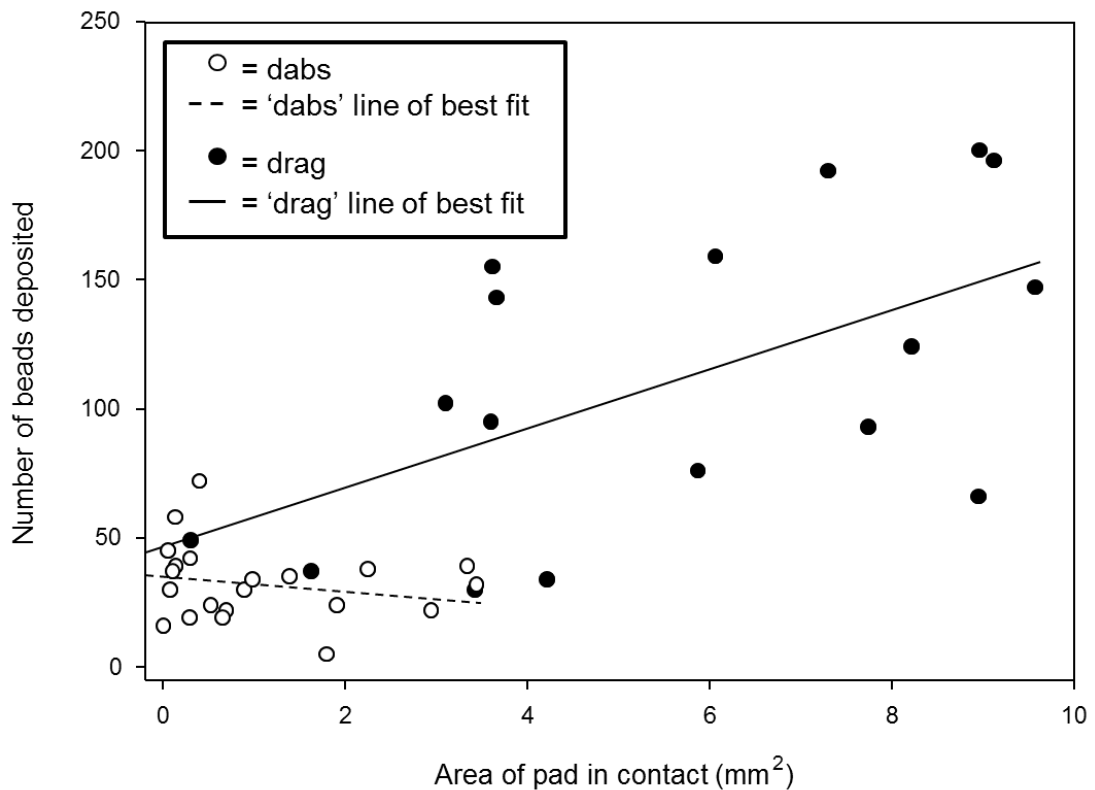


Figure 3.8: Scatter plot showing the correlation between number of beads deposited on the glass force plate (a cumulative total of beads from successive trials, i.e. the first trial = x beads, the second trial = $x + y$ beads, the third trial = $x + y + z$ beads) and the area of pad in contact with the glass surface (mm²). Lines of best fit were calculated for both trial variations - with the 'drag' trials showing a correlation significantly differing from zero (Spearman correlation test, $p < 0.05$), while the 'dab' trials show no significant correlation (Spearman correlation test, $p > 0.05$). Note that 'dab' trials (open circles) often result in removal of fewer beads and are associated with lower contact areas, while 'drag' trials (filled circles) show more bead deposition and higher contact areas. Reproduced from Crawford et al. (Crawford, Endlein et al. 2012)

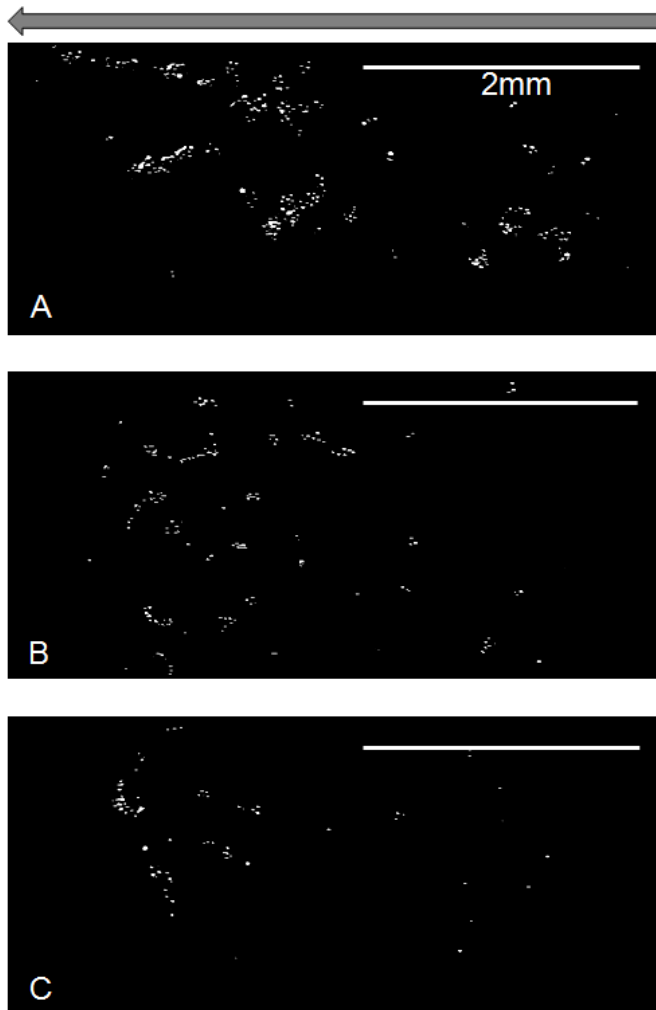


Figure 3.9: Illuminated beads (illuminated by a lamp directed onto the surface to highlight the beads) which have been deposited in a 'drag' movement, as seen through the microscope; A, the 'first' trial; B, the 'second' trial; C, the 'third' trial. Beads are deposited in characteristic 'footprints', and frequently towards the end of the 'drag' in clusters caused by the pad fluid. The arrow indicates the direction of the drag. Scale bars = 2 mm. Reproduced from Crawford et al. (Crawford, Endlein et al. 2012)

3.4. Discussion

3.4.1. Occurrence of self-cleaning

The experiments described above, coupled with an initial study on whole animal performance, provide evidence that self-cleaning occurs in the toe pads of tree frogs as they climb. The initial study involved testing adhesive ability (as explained in the methods chapter), with pads contaminated so that rate of recovery could be recorded. The initial study showed that frogs which use their pads frequently will display adhesive force recovery quicker than frogs which remain stationary, and so the self-cleaning property must be inherent with the adhesive abilities of the pads. By the 4th whole body trial, 91.9% of all adhesive

forces had been recovered (*Figure 3.11*), and 98.5% of original frictional forces (*Figure 3.10*) were being used by the frog.

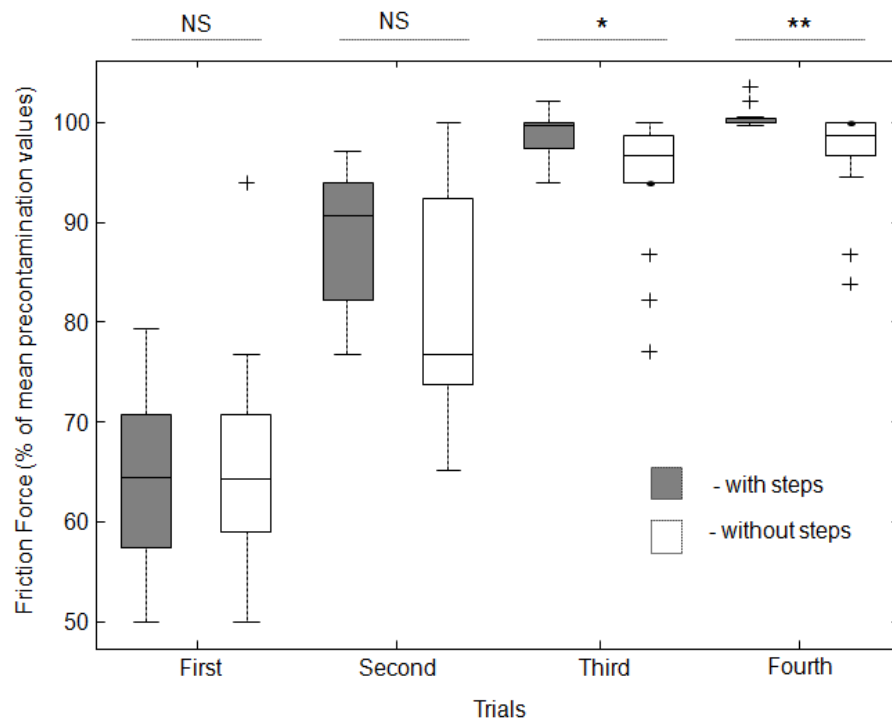


Figure 3.10: Boxplot showing the recovery of whole body frictional force for both 'with steps' and 'without steps' forms of the experiment as a percentage of the mean pre-contamination values. The filled boxes show measurements on walking frogs, while the open boxes are measurements for 'without steps' trials. The first measurement occurred immediately after contamination, and each subsequent measurement was separated by either a one minute rest or a minute where the frog was allowed to take some controlled steps. Statistical tests were conducted on each pair, with the results for each shown above the plots. Reproduced from Crawford *et al.* (Crawford, Endlein *et al.* 2012)

It appears that self-cleaning is universal in organisms which use dynamic adhesion - evidence has already been supplied for geckos (Hansen and Autumn 2005, Hu, Lopez *et al.* 2012) and various insects (Clemente, Bullock *et al.* 2010, Orchard, Kohonen *et al.* 2012). Despite being present in many adhesive systems, some organisms will show grooming behaviour - a study by Hosoda and Gorb (2011) showed that when the pads are not functioning well, grooming behaviour is triggered in beetles. However, grooming is not seen in organisms such as geckos and tree frogs, which will rely solely on self-cleaning. Self-cleaning is a highly effective and useful trait, which is present in organisms beyond adhesive climbers. Many plants, for example lotus leaves are ultrahydrophobic in nature (a hydrophobic wax layer coupled with micro-roughness), which means that during rainfall dirt particles are washed away in water rolling off the surface

(therefore the systems is driven by fluid rolling across the surface). In the case of tree frogs, the pads stick using a watery fluid, and so hydrophobicity or low surface energy (like in geckos' feet) is unlikely to be the source of their self-cleaning abilities. The pads do however produce a fluid, and so are likely to have fluid them also.

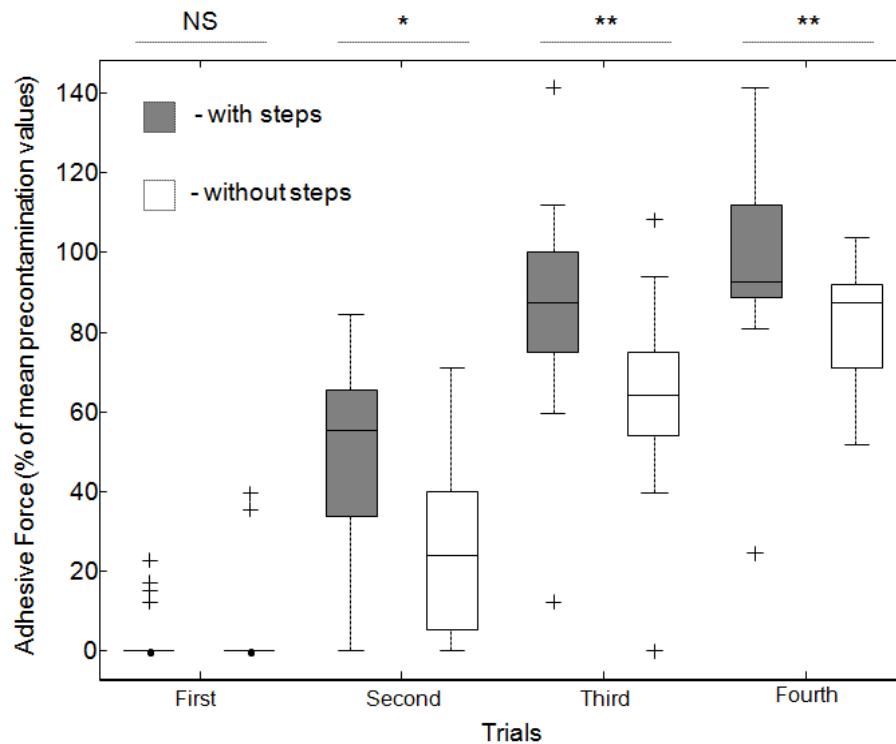


Figure 3.11: Boxplot showing the recovery of whole body adhesive force for both 'with steps' and 'without steps' forms of the experiment as a percentage of the mean pre-contamination values. The filled boxes show measurements on walking frogs, while the open boxes are measurements for 'without steps' trials. The first measurement occurred immediately after contamination, and each subsequent measurement was separated by either a one minute rest or a minute where the frog was allowed to take some controlled steps. Statistical tests are shown above the plots. Reproduced from Crawford et al. (Crawford, Endlein et al. 2012)

The single toe pad experiments provided further evidence of self-cleaning, although this appears to occur at a slower rate than that seen in the free climbing frogs in *Figure 3.10* and *Figure 3.11*. Whilst the reasons for this are not fully known, an unrestrained frog would have a greater range of movements available to it, including a longer shear movement, which could allow for more effective cleaning of the pads whilst in movement. The trial are also not directly comparable, as the whole animal experiments involved multiple movements by

the frogs during and between trials, and the time scale for the different experiments will vary as well.

3.4.2. Mechanisms of self-cleaning in tree frogs

The single toe pad experiments offer some idea of the mechanism behind the self-cleaning process seen in tree frogs. The 'drag' movements are shown to improve adhesive forces after 8 consecutive measurements after the full contamination, whereas the 'dab' trials showed no significant recovery, as can be seen in *Figure 3.5*. However, there was evidence of self-cleaning with the 'dab' trials, when the pad was only partially contaminated (*Figure 3.6*). What these tests show is that shear movements of the pad on the surface are important for cleaning the pads. Frogs pads naturally slip whilst the frog is climbing (personal observation), which is likely caused by its weight pulling the frog downwards by gravity. Frogs whose pads slip on a surface will constantly reposition them whilst clinging on, as a constant shear movement on the surface aids adhesion (Endlein, Ji *et al.* 2013). This means that 'drag' movements of the pad are a common behaviour by a climbing frog, therefore self-cleaning is quite easily incorporated into the natural techniques of the frog and can therefore occur quickly. Even a simple pull off can quickly clean a partially contaminated pad, as was shown in *Figure 3.6*, and so pads are well equipped with dealing with contamination. As is explained further on, the shear movements move the beads to the periphery of the contact area and/or deposit them onto the surface. This model was proposed by Persson (Persson 2007), and has been shown to be true in insects as well (Clemente, Bullock *et al.* 2010).

The additional experiments involving the recording of pad contact area and bead deposition show a correlation between adhesive force and contact area (*Figure 3.7*) - this means that the adhesive force per unit area (or normal stress) does not significantly differ between measurements (force per unit area values for 'drag' controls (1.08 ± 0.24 mN/mm²) and contaminated pads (0.94 ± 0.36 mN/mm²) were tested for variance; Kruskal-Wallis test: $p = 0.0929$). The conclusion from this is that contaminants reduce the adhesive abilities of toe pads by reducing the area of pad which is in close contact with the surface. As a

measure of self-cleaning, the number of beads deposited on the surface positively correlates with both the contact area and adhesive force produced (*Figure 3.8*) - this relationship is highlighted in *Figure 3.7* as well. This relationship shows the need for close contact between the pad and the surface for adhesive forces to work. The addition of the contaminant is likely to prevent the fluid from filling the space fully and allowing forces to be produced, therefore reducing adhesive ability. *Figure 3.9* displays the beads grouped together at the end of the 'drag', which indicates the role of sliding is bringing together the beads to be removed *en masse* (alluded to by *Figure 3.9* and seen in the live videos of the step). The sliding action of the pad moves the beads to the distal end, which allows for the beads to be left behind in pad fluid footprints on the surface. The pad fluid could therefore have a 'flushing' effect by helping to move and then remove dirt particles; this however has not been quantified, and further work would be required to test this.

3.4.3. Comparisons with other animals

The experimental technique used in this study is highly similar to that used in the study by Clemente, Bullock *et al.* (2010). The similarity means that the results for both experiments can be used for comparison, as the insects tested both use wet adhesion despite having differing pad morphologies (the beetles have 'hairy' pads, whilst the stick insects have 'smooth' pads). With the smooth pads of the stick insects, contamination reduced adhesion by reducing contact area, and recovers as beads are removed - this mirrors the findings in tree frogs.

As with the tree frogs, adhesive fluid was left behind by the insects as they climbed, and the contaminant was left there in large quantities. Fluid production appears to be continuous, and friction of the pad on the surface means that particles get cleaned away (Clemente, Bullock *et al.* 2010). The fluid in insect pads plays an important role in filling gaps between the pad and surface created by either contaminants or rough asperities (Clemente and Federle 2012). In tree frogs, the production of fluid on the pad seems to be sporadic (Ernst 1973), although fluid is left behind with each step, just as with the insects. The randomness of fluid production could affect the rate of self-

cleaning depending on the volume of liquid under the pad. As the pad fluid is essential for frogs' climbing abilities, it can be seen to have a dual role in self-cleaning as well.

The utilisation of a 'drag' movement also forms another similarity, with both insect pad forms showing more effective cleaning when a shear movement is involved than when it is absent (Clemente, Bullock *et al.* 2010). As the method of adhesion in geckos is different (they adhere using dry adhesion), the self-cleaning method also differs (and the precise mechanics of both remain unclear). Dirt particles are shed due to the theory that they bear a greater affinity to the climbing surface than to the hydrophobic surface of the gecko's foot (Hansen and Autumn 2005). Recent studies have given strong evidence that the curling detachment of the gecko's toe by hyperextension also removes particles by flicking them from the toe (Hu, Lopez *et al.* 2012). Although comparisons are difficult, due to there being different techniques or contaminants used in other self-cleaning studies, it seems that tree frogs can self-clean their pads as efficiently as others studied so far (Hansen and Autumn 2005, Clemente, Bullock *et al.* 2010, Hu, Lopez *et al.* 2012, Orchard, Kohonen *et al.* 2012).

3.4.4. Biomimetic implications

Synthetic bio-inspired adhesives have been proposed and created in vast amounts since the discovery of climbing animal's adhesives, with gecko inspired surfaces in particular being a well-researched area (Boesel, Greiner *et al.* (2010)). This is also true for tree frog adhesion, with several adhesive surfaces citing tree frogs as an inspiration (Drotlef, Stepien *et al.* 2012, Tsipenyuk and Varenberg 2014). However, despite being a highly useful and relevant trait, there are as yet no studies on tree frog inspired adhesives which show self-cleaning; Lee and Fearing (2008) providing the only man made surface with some self-cleaning properties with a surface inspired by gecko feet. Any man made surface which can match the impressive self-cleaning properties of tree frogs and their effortless climbing abilities, would be overcoming one of the biggest challenges to modern day adhesives - contamination of the surface. As the pads

utilise shear movements and are likely to use the fluid to remove contaminants, man made adhesives would need to replicate these properties, which may be difficult considering the pads of tree frogs are continually being replenished with pad secretions. Conventional adhesives are unable to produce continual supplies of fluid, and so contaminants are unlikely to be 'flushed' away. Until such times, the self-cleaning properties of the tree frogs toe pads can only act as inspiration.

4. The attachment abilities of torrent frogs on rough and wet surfaces

This chapter includes experiments which have been published in the article detailed below (permission is not required as the paper is open access). The work was conducted in conjunction with Thomas Endlein, Jon Barnes, Diana Samuel and Ulmar Grafe; the other authors all contributed in various degrees to experimental design, data collection and analysis, discussions on the work and writing of the paper. Most of the figures in this chapter have been taken from this publication (Figure 4.2 and Figure 4.5 are the exceptions).

T. Endlein, W. J. P. Barnes, D. S. Samuel, N. A. Crawford, A. B. Biaw and U. Grafe (2013). "Sticking under Wet Conditions: The Remarkable Attachment Abilities of the Torrent Frog, *Staurois guttatus*." PLoS ONE **8**(9): e73810.

Summary

The adhesion of tree frogs is characterised by a thin layer of fluid between the pad and the surface - often termed wet adhesion. Wet habitats such as waterfalls will have a regular flow of water over the surface, which could potentially disrupting the air-fluid interface necessary for frog adhesion. Here, the adhesive abilities of a torrent frog (*Staurois guttatus*) were compared to those of a tree frog (*Rhacophorus pardalis*) - to see if torrent frogs possess special adaptations for living in and around waterfalls. Individual force measurements were taken for various body parts, and were compared with results from previous experiments (whole animal tilting experiments). Torrent frogs performed better than tree frogs on rough and wet surfaces, and while the individual forces did not appear different, the torrent frogs used a bigger proportion of their body to contact the surface. The toe pads were also shown to have a specialised structuring which differed from tree frogs and the belly and thigh skin were also investigated (and found to have skin which differed from the studied tree frog). The overall conclusion of the study is that torrent frogs have adapted to adhering to wet/rough surfaces, which allows them to fill niches unavailable to other frogs.

4.1. Introduction

The wet adhesion system, regarded as the mechanism for adhesion in tree frogs, relies mainly on the coordination of capillary and hydrodynamic forces (although the exact mechanism and importance of these forces is still unclear) (Hanna and Barnes 1991). Tree frogs maintain these forces by producing a thin layer of fluid between the pad and the surface it is adhering to. The capillary forces rely on the air-fluid interface which exists around the edge of the pad, while hydrodynamic forces work within the thin layer and are reliant on the gap between the pad and surface being small. The mucosal fluid secreted via pores on the pad (Ernst 1973) acts as the fluid joint necessary for effective adhesion. While the exact composition of the fluid is unknown at the moment, it has been described as a watery solution (Federle, Barnes *et al.* 2006). If the pad is in contact with a surface where this air-fluid interface is disrupted by excessive water, the adhesive abilities of the frog should be reduced. Indeed, it has been

shown previously that tree frogs perform poorly when submerged, indicating the presence of capillary forces (Emerson and Diehl 1980).

Given this, torrent and rock frogs (of the Ranidae family) have become an enigma. They live in and around waterfalls in the rainforest - sitting on leaves beside the water flow at night, but during the day clambering and jumping round on the rough and flooded surface of the waterfall. If the adhesive forces of torrent frogs are affected the same way as tree frogs when submerged, then how can they stick to waterfalls? The solitary study looking at their toe pads was Ohler in 1995 (Ohler 1995), where the morphology of several species were investigated. The cells on the toe pad were found to be elongated and tapered (in the proximo-distal direction), and it was speculated that these anatomical differences could contribute to adhesion on the wet surfaces of waterfalls. An initial study on the stream frog *Mannophryne trinitatis* indicated that they performed well on rough and wet surfaces, and better than on smooth and wet surfaces (Barnes, Smith *et al.* 2002).

The waterfalls in which the torrent frogs live have water flowing over them constantly, with varying levels of flow rate. The rocky surface of the waterfall will also possess different roughnesses which torrent frogs will have to navigate whilst climbing. Previous studies have noted the poor performance of frogs on dry rough surfaces (Emerson and Diehl 1980, Hanna and Barnes 1991), but investigations of how torrent frogs deal with rough *and* wet surfaces would provide a clearer indication of their abilities in conditions similar to their habitat. As mentioned, some studies show good performance on rough/wet surfaces (Barnes, Smith *et al.* 2002), while others find poor performance on dry rough surfaces (Hanna and Barnes 1991). The waterfalls inhabited by torrent frogs often have overhangs and vertical surfaces, meaning that frog pads must be able to produce friction and adhesion in order to stay attached.

In this chapter, the abilities of a torrent frog are investigated, and compared to a tree frog. A research field station in Brunei Darussalam provided access to primary rainforest (and its wealth of frog species) with lab facilities in close proximity for these studies (Grafe and Keller 2009). The first aim of this study

was to see if there is a difference in the attachment abilities between tree and torrent frogs, when roughness and fluid levels are varied. The tree frogs' performance can act as a control, as their adhesion has been well studied previously. The hypothesis is that torrent frogs show superior performance in conditions mimicking waterfalls. The second aim is to gain an insight into what, if any, adaptations torrent frogs have to climbing on waterfalls. Either the frogs will exhibit special behaviours, or have evolved specialised structures which help them stay attached to difficult surfaces.

4.2. Materials and methods

4.2.1. Experiments from 2010 study

An initial study was done prior to this one in 2010, in the same location. In this study, whole animal adhesive abilities were tested using a tilting board setup modified from the one used by previous tree frog studies (Hanna and Barnes 1991, Smith, Barnes et al. 2006), and described in the Methods chapter. In the initial study, the tree and torrent frogs were tested in conditions attempting to mimic the waterfalls that torrent frogs inhabit (*Figure 4.1*). This includes varying the roughness of the surface using polishing discs (30 μm roughness) and a surface coated with a monolayer of glass beads (Ballotini beads, $1125 \pm 125 \mu\text{m}$), as well as a glass sheet as a smooth surface. A water flow was also set up, so that water would flow over the surface and the frogs as they attempted to stay attached. Flow rate was controlled by use of a clamp on the tube which fed in the water, and the overall flow rate could then be measured (volume of water produced over time). Flow rate was varied between no flow (dry), light flow (roughly 50 ml/min, termed 'low') and full flow (roughly 4000 ml/min, termed 'high'). The performance of the tree frog and the torrent frog in these varying conditions could then be compared (5 individual frogs for each species tested 10 times in each conditions, so that $n = 50$).

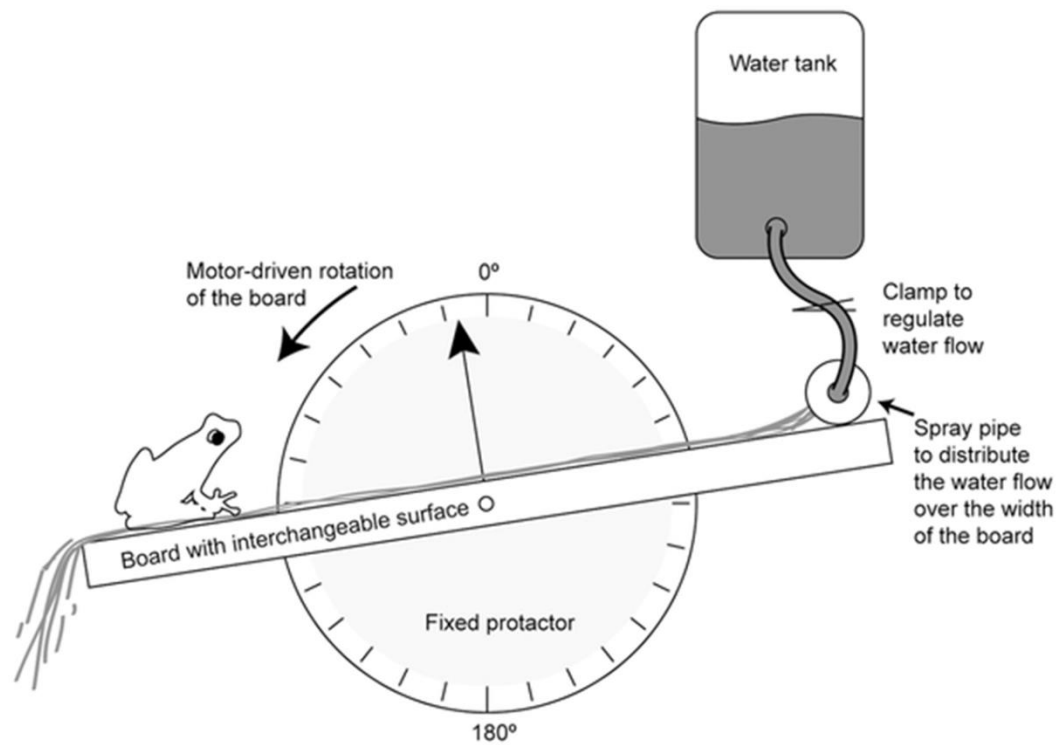


Figure 4.1: Diagram displaying the tilting platform experiment, not drawn to scale. Reproduced from Endlein et al. (Endlein, Barnes et al. 2013)

The other experiment conducted along with the tilting experiment allowed contact area to be seen at different angles of tilt, to see if different strategies are used by tree and torrent frogs. This involved having the frog attempt to stay attached to a smooth glass surface as it is rotated, while light is internally reflected through the glass (with no light escaping). Only at points where contact is made by the frog will light be released and therefore will shine brightly. This can then be recorded and analysed to see what sort of contact area the two species use at different angles of tilt. This technique could only be used on dry surfaces, as water on the surface would also illuminate and show as contact area.

Although these two experiments were not carried out during this PhD, the results formed part of the analysis when combined with the following studies; therefore the results are referred to in the discussion.

4.2.2. Study animals and location



Figure 4.2: Images of the rainforest of Brunei (left) and the waterfall habitats of the torrent frogs, which have a constant flow of water over them (right).

The experimental work (not including the microscopy) carried out for this study was conducted at the Kuala Belalong field studies centre, which is owned by the Universiti Brunei Darussalam. The field station is located in the Ulu Temburong National Park, which consists of large areas of Dipterocarp primary rainforest (Figure 4.2). The rainforests of Borneo are one of the most biodiverse locations on Earth, with several species of amphibians inhabiting trees, the forest floor and the river systems (Keller, Rodel *et al.* 2009). The locality of the field station to the habitats of the frogs allowed for experiments to be carried out, and the frogs returned to their natural habitat quickly after experimenting.

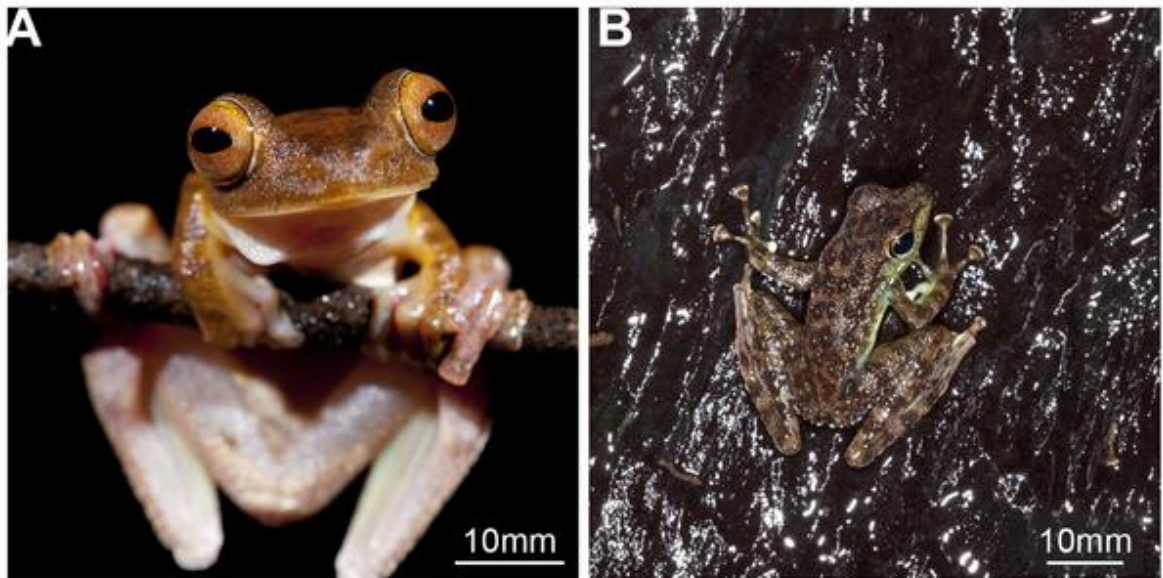


Figure 4.3: Frog species used in study. A is the tree frog *Rhacophorus pardalis*, and B is the torrent or rock frog *Staurois guttatus*. Photos provided by T. Endlein. Reproduced from Endlein et al. (Endlein, Barnes et al. 2013)

For the study a comparison was conducted between two frog species (Figure 4.3): one a torrent frog (often termed as a rock frog) called *Staurois guttatus* (of the Ranidae family), known as the Black spotted rock frog ($n = 39$); and the tree frog *Rhacophorus pardalis* (family Rhacophoridae), known as the Harlequin tree frog ($n = 34$). Both species were commonly found in locations near to the field station, which meant that frogs could be collected on night excursions. *R. pardalis* were typically found near intermittent freshwater ponds, while *S. guttatus* (well documented for their foot flagging behaviours (Grafe and Wanger 2007)) were found on leaves near to waterfalls at streams at night. Both species (referred to from here as the tree frog and the torrent frog) were abundant and easy to catch, and of the species found locally were the closest in size and mass (meaning a fairer comparative study). Both species are classed as “least concern” for their conservation statuses. Captured frogs were brought to the lab, where they were kept in tanks with suitable moisture, substrate and leaves. As the lab where the frogs were kept was *in* the rainforest, the temperature and the humidity of the lab were the same as the conditions the frog lived in. Frogs were weighed using electronic scales (Mettler, Leicester, UK) and the snout-vent length (SVL) was measured using callipers - the torrent frogs (mass = 2.7 ± 0.3 g, SVL = 34 ± 1 mm) were overall smaller than the tree frogs

(mass = 4.0 ± 0.4 g, SVL = 45 ± 2 mm). Frogs were kept for no longer than 48 hours before being released back into the wild in the location they were found.

4.2.3. Force measurements

To test how much force different parts of the body can produce for both species, force per unit area measurements were taken using a setup similar to the one described in the methods chapter which is used for single toe pad force measurements. As this setup had to be transported to the field station in Brunei, a few adjustments were required to make the setup transportable. As described before, frogs are held in position beneath the force plate in a petri dish, orientated so that the desired body part would come into contact with the force plate (the areas tested were the toe pads, the thigh skin and the belly skin). The force plate was illuminated by an array of micro LED lights which were attached around the perimeter of the force plate - this meant that any contact by the frog could be visualised by the light escaping the surface, and recorded using a digital video camera (Basler A602f, filming at 10-30 frames per sec.) and the program Streampix (Norpix, Montreal, Canada). Force measurements and video recordings were collected simultaneously (videos were synchronised with the forces using a manual trigger switch) using a portable data acquisition board (NI 9237, National Instruments, Austin, USA), with a LabVIEW interface being used to view and save the force recordings. Movements to measure adhesion and friction were carried out by using a micromanipulator, with recordings of movement being fed into the LabVIEW script by affixed potentiometers. In this way, the distance the frog is moved and the amount of load force applied are recorded and can be controlled (in the original setup, this was done by motors which are run by programs in LabVIEW).

As said previously, force measurements were taken from the toe pads, the belly skin and the thigh skin. For the toe pad measurements, a flat force plate was used (made from polyethylene, 15 x 15 mm); however for the thigh and belly skin measurements a curved spherical surface (diameter = 18 mm, radius of curvature = 9 mm) was used, as this prevented the force plate from getting caught on other body parts as the measurements were taken. To test the effect

of water on the adhering abilities of the frogs, a small drop of water (~10 µl) was pipetted onto the area tested before coming into contact with the force plate; this was then compared with 'dry' measurements (no water added). Force measurements were measured by pushing the pad/skin into contact with the plate, moving horizontally on the surface (to create frictional forces) and then removing it vertically (to produce adhesive forces) - these movements were done using the micromanipulator. As this was done by hand, this meant that there is some variation in the movements, measured as - drag distance = 2.9 ± 0.7 mm, velocity = 1.4 ± 1.1 ° s⁻¹.

4.2.4. Morphology investigation using SEM

To see if there are morphological differences between tree and torrent frogs in this study, scanning electron microscopy (SEM) was conducted on the different parts of the body tested in the adhesive tests (the toe pads, the belly skin and the thigh skin). The precise protocol for euthanasia, fixation and mounting for SEM are in detail in the appendix.

5 individuals were used, being euthanized with a lethal dose of benzocaine. Samples of the toe pads, the belly and the thigh skin were dissected out (feet were severed at the wrist/ankle joints, and rectangular sections of belly and thigh skin were carefully cut away) and fixed using a phosphate buffer and 2.5 % gluteraldehyde fixative. The samples were then dehydrated through an acetone series, critical point dried and attached to mounts with double-sided tape. Finally, the samples were sputter coated with a gold-palladium alloy. The samples were then examined using the scanning electron microscope (JSM-7500F (JEOL, UK Ltd.)) at 6 kV; images were taken using the SEM software (Scandium Universal SEM Imaging Platform, version 5.0; Olympus Soft Imaging Solutions GmbH, Germany).

4.2.5. Statistics

Statistical tests for all of the above experiments were done using the statistical toolbox in MATLAB 7.6.0 (version R2008a, Mathworks Corp., USA). To compare

between samples (i.e. between species) for all the experiments, Mann-Whitney U tests were used. For the boxplots - on each box, the central line represents the median, the boundaries of the box are the 25th and 75th percentiles, and the whiskers extend to include 99.3% of the data, with outliers plotted individually. Statistical tests are shown above plots, and the results are denoted as follows: n.s. = not significant, * = $p < 0.05$, ** = $p < 0.01$, *** = $p < 0.001$. The Bonferroni correction has been implemented on data which is used for multiple tests.

4.3. Results

4.3.1. Force measurements of toe pads, belly and thigh skin

Upon observing the tree and torrent frogs climbing, it was noticed that various body parts came into contact (personal observation). Using a sensitive force transducer, these various body parts (the toe pads, the belly and the thigh) were tested for the adhesive and frictional forces produced. The results are shown below (Figure 4.4). The different body parts were tested for both species, and under 'wet' and 'dry' conditions.

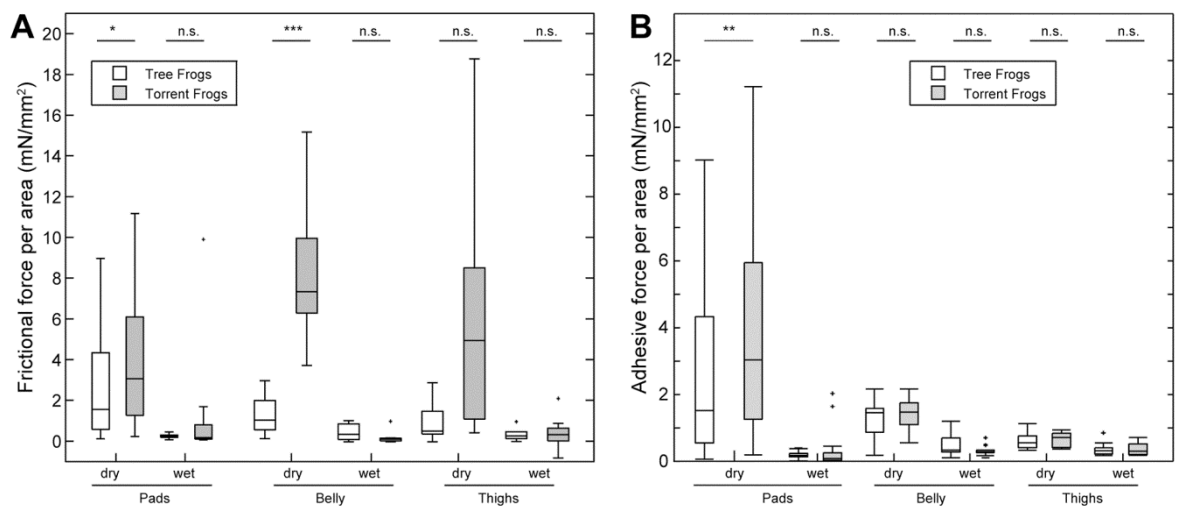


Figure 4.4: Friction and adhesive forces per unit area (mN/mm²) for different body parts in the tree (white boxes) and torrent (grey boxes) frogs, under wet and dry conditions. Particularly for the belly and thigh measurements, low n numbers for statistical tests ($n = 11$) could explain the lack of statistical variance when it would seem that there would be (e.g. testing frictional forces of dry thigh skin). Reproduced from Endlein et al. (Endlein, Barnes et al. 2013)

In dry conditions, the toe pads of both species produced high levels of adhesive and frictional force -outperforming any tree frogs which have been tested in past studies. Adhesive force per unit area (mN/mm^2 , or kPa) measured for the tree and torrent frogs yielded means of 1.5 and $3.0 \text{ mN}/\text{mm}^2$ respectively; these are higher than previous measurements in various hylid tree frogs which were $0.7\text{-}1 \text{ mN}/\text{mm}^2$ (Barnes, Oines *et al.* 2006) (although different techniques for force measurements were used), and higher than those measured in *Litoria caerulea* in the self-cleaning experiments in chapter 3 (mean of $1.08 \text{ mN}/\text{mm}^2$)(Crawford, Endlein *et al.* 2012). So both species performed well, but torrent frogs' pads produced a higher force per unit area than the tree frogs. When compared with each other ($n = 34$), it was found that the torrent frogs produced a higher adhesive ($z = -2.2, p < 0.01$) and frictional force ($z = -2.28, p < 0.05$) per area than the tree frog.

Forces produced by belly and thigh skin have previously been untested in any climbing frogs. Whilst they did not produce the kinds of adhesive forces seen in the toe pads, both areas of skin still showed some significant forces which could contribute to staying attached to a surface. This was particularly true of frictional forces, with forces reaching levels similar to those seen in toe pads. The skin of the torrent frogs in particular produced high levels of friction, with the belly skin producing significantly higher levels of friction than in the tree frogs ($z = 3.87, p < 0.001$). The looseness of the skin contributed to this - the skin of torrent frogs tended to wrinkle up a lot during testing, and it is feasible that this is an adaptation of the skin to help increase contact area and/or static friction forces.

As torrent frogs climb on flooded surfaces, the performance of all body parts were tested under wet conditions; this was achieved by pipetting a small amount of water onto the surface tested before measuring forces. What was found was that adhesive and friction forces dropped significantly across the board - both in tree and torrent frogs. The adhesive force of toe pads dropped by one order of magnitude from those measured under dry conditions, with any difference between species of the sticking forces of the pads disappearing ($n = 11$,

adhesion: $z = 0.37$, $p > 0.05$; friction: $z = 0.37$, $p > 0.05$). There were similar low force measurements of belly ($n = 13$) and thigh skin ($n = 12$) in wet conditions, with both species producing low forces (For belly - adhesion: $z = -1.53$, $p > 0.05$; friction: $z = 1.81$, $p = 0.06$. For thigh - adhesion: $z = 0.019$, $p > 0.05$; friction: $z = 0.25$, $p > 0.05$). The poor performance of tree frogs under wet conditions is not surprising, as previous studies have shown this to be true as frogs rely on capillary forces and therefore an air-fluid interface. The results for this particular experiment show that torrent frogs, which live in flooded environments, adhere poorly when there is excess water between the pad and surface, which appears to contrast with earlier studies and what is seen in the wild.

4.3.2. Skin morphology

A closer look was taken of the toe pads, belly and thigh skin of both species studied, to look for any morphological specialisations using SEM. Selected images are shown in *Figure 4.5*, *Figure 4.6* and *Figure 4.7*.

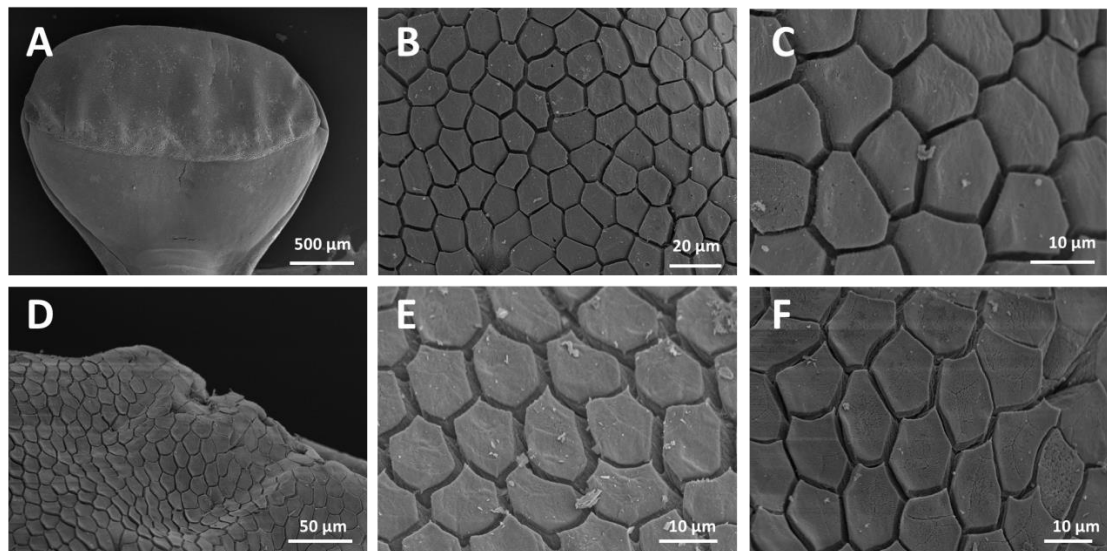


Figure 4.5: SEM images of a torrent frog toe pad. Image A) shows the whole pad, B) and C) show the cells located centrally on the pad, D) E) and F) show the cells with directed channels found near the edges of the pad.

Figure 4.5 shows the cellular structure of the toe pads seen in torrent frogs. The pads on the toe are proximally placed (*Figure 4.5A*), with a small but pronounced

circumferal groove around the pad. This groove extends down the pad towards the toe before disappearing. Although the circumferal groove is thought to be the result of pads becoming larger and more efficient (Green 1979), it could be that a well-established circumferal groove around the pad could aid in adhesion to wet surfaces. The structures of the cells in the centre of the pad (Figure 4.5B and C) are very similar to those seen in other tree frogs (Green 1979, Green 1980, Smith, Barnes *et al.* 2006); composed of polygonal cells typically as wide as they are long (i.e. a ratio close to 1). There are channels between the cells, and at each junction where channels meet, the straightness of the channels mean that fluid could move through either channel, because there is no directionality. Moving to the periphery of the pad (Figure 4.5D), the cells begin to specialise in shape; becoming more pointed in the direction away from the centre of the pad, and rounded in the side facing the centre (Figure 4.5E and F). This alludes to a possible specialisation which would help to channel excess fluid away from the centre of the pad to the edges (although experimental evidence of this has not been shown and so is still unclear). This morphological variance has been noted before in other torrent frog species (Ohler 1995).

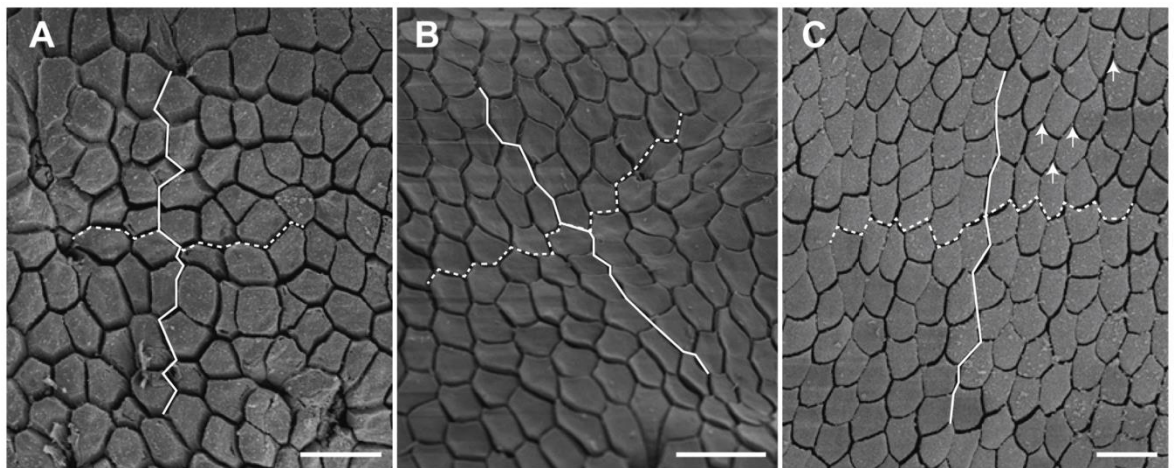


Figure 4.6: SEM images of toe pad cells in different frog species. Image A) is from the tree frog *R.pardalis*, B) is from the torrent frog *S.guttatus*, and C) is from the torrent frog *O. hosii*. The white lines indicate hypothetical routes of fluid between the cells - the solid white line indicates the vertical transect, and the dashed line indicates the horizontal transect. Arrows (on image C) indicate pointed edges seen in the cells of torrent frogs' pads. Image C was obtained by D. Samuel from the first trip to Brunei. Pads are orientated in the same way in each picture, with the distal end of the pad facing upwards. Scale bars = 20 μ m. Reproduced from Endlein *et al.* (Endlein, Barnes *et al.* 2013)

Figure 4.6 highlights this morphological variance further, by comparing images of the pads of the tree frog *R.pardalis* (Figure 4.6A), of the torrent frog *S.guttatus*

(Figure 4.6B), and from another torrent frog species from the Ranidae family *Odorrana hosii* (Figure 4.6C). In the images, pictures of cells from similar locations on the pads are compared under the same magnification. The white lines on each image indicate a typical route through the channel system in each direction - hypothetically this is a route that fluid could take when being squeezed out. In the tree frog sample (Figure 4.6A), vertical and horizontal transects are similar in deviation, whilst in the torrent frog sample (Figure 4.6B) the vertical transect is straighter and therefore easier for fluid to follow. This contrast is also seen in the *O.hosii* sample (Figure 4.6C), a Bornean species which also spends a large amount of time in or near flowing water. The curved channels create points in the cells, which could direct water flow away from the pad.

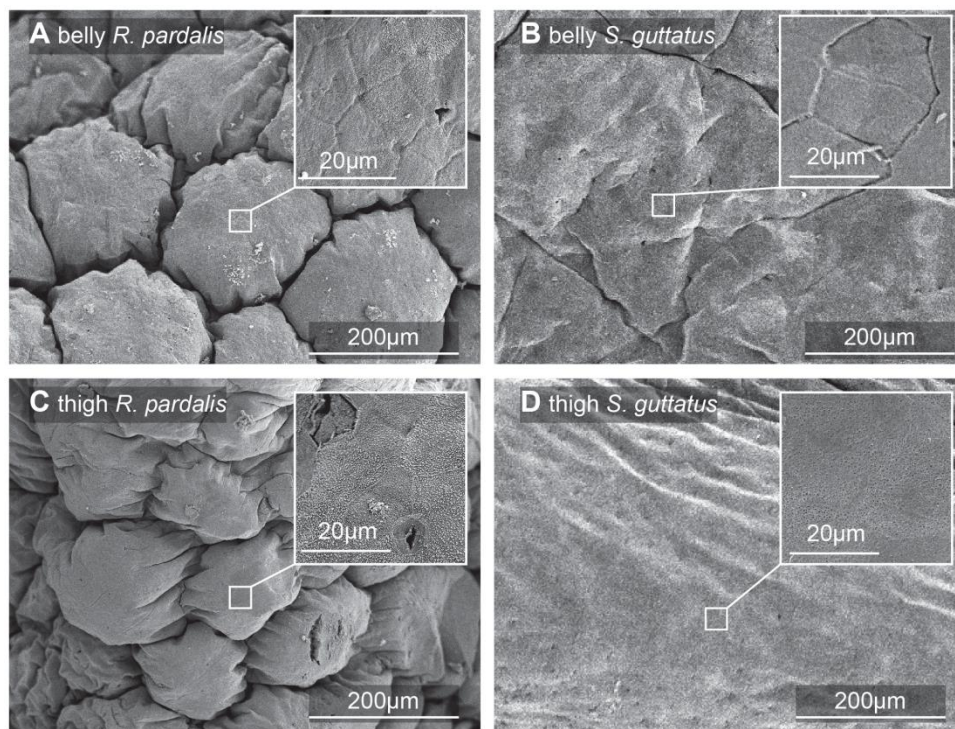


Figure 4.7: SEM images of the thigh and belly skin of tree and torrent frogs. Images A) and B) are belly skin, C) and D) are thigh skin; tree frog samples are on the left hand side, and torrent frogs on the right. Close up images of each sample are insets within each image. Reproduced from Endlein et al. (Endlein, Barnes et al. 2013)

The force measurement experiments showed that the belly and thigh skins of both frogs produce significant adhesive and frictional forces. This means that the morphology of these locations is of interest, as there could be adaptations to help with attaching. Images of the belly and thigh skin in both the tree and

torrent frog studied are shown in *Figure 4.7*. The skin on the ventral side (both the belly and thigh skin) of the tree frog is characterised by large dome-like bumps (approx. 200 μm in diameter). In some respects they mimic the cells and channels seen in the toe pads, but on a larger scale with each bump being composed of several relatively flat epidermal cells. In the torrent frogs, the skin is relatively flat, and made up of typical epidermal cells (which would be expected to make drainage of fluid from the surface more difficult). The skin also looks wrinkled, although this could be an artefact from the fixing process. From the force measurements and the images, it is unclear how the skin on the ventral side of the frogs aids in adhesion. Certainly whilst measuring forces, it was noted that the skin on the torrent frog would wrinkle up easily as it was very loose, which lead to the skin being pinned and subsequently producing high frictional forces. This was less apparent in the tree frog skin measurements, and this could be a result of the differing morphologies.

4.4. Discussion

On the first excursion to Brunei in 2010, the climbing abilities of the torrent frog *Staurois guttatus* were observed in the wild, and tested using the tilting apparatus described above. The experiments conducted on the second trip to the field station (analysed in the above results section) attempted to gain an understanding of how the torrent frog is capable for such climbing feats. The following discussion will try to bring together all that was found from all testing, to try and paint a picture of how torrent frogs stick.

4.4.1. Effect of surface wetness and roughness on climbing frogs

In the initial study of 2010, the attachment abilities of free climbing frogs were challenged using a tilting board, with roughness of the surface varied and water flow over the board being controlled. Various combinations of the conditions were tested for both tree frogs and torrent frogs - the results are shown in *Figure 4.8*. Graph A shows comparisons of slip angles between the frogs, which relates to the friction forces being produced. There was no significant difference found between the frogs when water was either absent or flow rate was low (roughly

50 ml/min), with both frogs performing beyond the limitations of the test (no slipping before 90°). Both frogs suffered a drop in performance at high flow rates (roughly 4000 ml/min), but the torrent frogs could prevent slipping until a steeper angle than tree frogs could, on all surfaces tested (as can be seen from *Figure 4.8*).

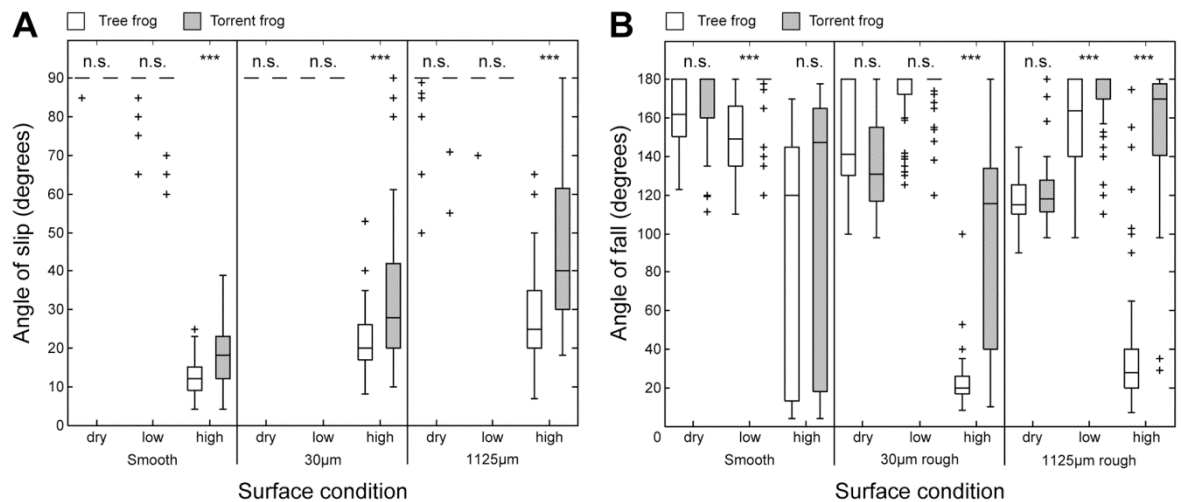


Figure 4.8: Boxplot showing attachment performance of the two frog species under varying conditions - a comparison of slip angles (graph A) and fall angles (graph B) between the tree frog (*Rhacophorus pardalis*) and the torrent frog (*Staurois guttatus*) on different flow rates and roughnesses (indicated on the x axis). Statistical tests between the two frog species are shown above each pair. Reproduced from Endlein et al. (Endlein, Barnes et al. 2013)

The fall angles of the frogs in the same experiment showed a greater variation in the performances. The fall angle of the frog corresponds to the adhesive abilities of the frog, with maximum forces being produced at 180° . Under dry conditions, the adhesive performance decreased with increasing roughness for both species. The introduction of fluid on the smooth surface generally diminished performance in both species, but torrent frogs could withstand the low flow rates, leading to a better performance than the tree frogs. On the 30 µm rough surface, both species performance improved significantly when a low flow rate was introduced. On a high flow rate, both species' performances dropped, yet the torrent frogs outperformed the tree frogs again. On the roughest surface (1125 µm), the torrent frogs performed significantly better than the tree frogs under both flow rates, and performed better than when the surface was dry.

From this experiment it appears torrent frogs perform significantly better than the tree frogs when surfaces are rough and have a high flow rate - which is exactly the conditions they inhabit when they are climbing on waterfalls. Under dry conditions, both species performed best on a smooth surface and showed a decrease in adhesive performance with increasing roughness. Although the role of surface roughness is investigated further in a later chapter, here we see some of the effect roughness can have. It is likely that the rough surface deprives the frogs of real contact when the pad is in contact, as the fluid from the pad cannot fill the gaps (as has been speculated to be the effect in tree frogs (Persson 2007)). This theory is strengthened by the improvement in performance by both species when a low level of fluid is present - the fluid could help to fill the gaps between the pad and the rough surface. On the smooth surfaces, the lack of roughness meant that the introduction of fluid resulted in both frog species slipping on the surface, and falling at a lower angle. The fluid is likely to have a lubricating effect on the pads which will diminish their adhesive abilities. The biggest difference in performance is seen on the roughest and high flow rate conditions, where the torrent frog stay attached to almost 180° , while the tree frog only on a few occasions managed to stay attached beyond 90° . The precise reasons for the better performance on the rough surfaces are unclear, but being smaller and therefore possessing smaller toe pads which can potentially grip around asperities could play a role in better performance on rougher surfaces.

4.4.2. Contact area on a tilting board

The second experiment from the 2010 study looked at the contact area of both the tree frogs ($n = 42$ trials from 6 frogs) and the torrent frogs ($n = 33$ trials from 6 frogs) on a tilting illumination board (with no water on the surface)- the results are shown in *Figure 4.9*. Between horizontal (0°) and fully inverted (180°), there are dramatic but differing changes from both species. The tree frogs begin with a large proportion of the body in contact, with the thigh skin as well as pads in contact. An initial increase in contact area occurs when belly skin attaches, but by the time the frog is upside down, all the frog can maintain on the surface are the pads. These amount to a very small amount of contact area

and have to be constantly pulled towards the body and then reattached further away. This is an anti-peeling technique that tree frogs use to prevent pads from detaching easily, and to raise contact area and friction forces to stay attached (Endlein, Ji *et al.* 2013).

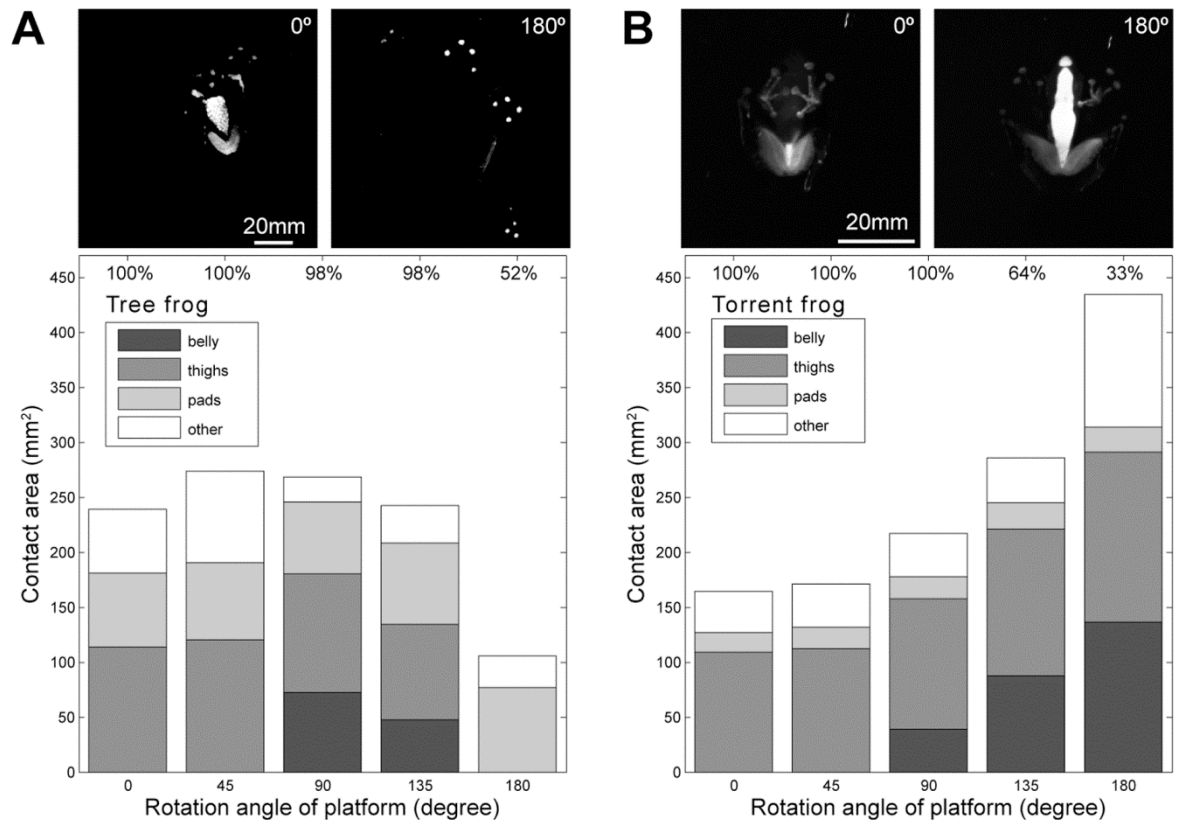


Figure 4.9: Contact area of tree (A) and torrent (B) frogs at different tilting angles. The areas of different body parts are denoted by the different shades. The images above show contact at 0° and 180°. Contact area becomes illuminated upon contact with the surface. Reproduced from Endlein *et al.* (Endlein, Barnes *et al.* 2013)

As a contrast to the tree frogs, the torrent frogs employ a different tactic when faced with an inverted surface. When tilted beyond 90°, the torrent frog brings more of its body into contact with the surface, and by 180° has more than doubled its contact area. The fact that torrent frogs produce a larger area of contact than the tree frogs is remarkable, as generally they are smaller in size than the tree frogs (torrent frog SVL = 34 ± 1 mm, tree frog SVL = 45 ± 2 mm). This ‘hunkering down’ technique was also seen in the other tilting experiment, and so could be perceived as a common method of maintaining attachment for torrent frogs.

4.4.3. Force measurements analysis

The force per unit area measurements conducted on the pads of tree and torrent frogs indicate that both species can produce high adhesive and friction forces; these forces are higher than those previously seen in other climbing frogs (Barnes, Oines *et al.* 2006, Crawford, Endlein *et al.* 2012). The torrent frogs pads were more efficient than the tree frog pads (produced a higher force per unit area), but the reasons for this as yet are unclear. Although differences in toe pad efficiency have been noted before, they are usually associated with an increase in frog size (Smith, Barnes *et al.* 2006) (it is also worth noting that the torrent frogs are smaller than the tree frogs in this test). Contact splitting is known to increase efficiency in hairy adhesive systems (Arzt, Gorb *et al.* 2003), but a variance in cell size (and therefore a potential increase in contact splitting) has not been observed in this comparison. Similarly, keeping pad film as thin as possible (particularly on a smooth surface) would increase efficiency (Labonte and Federle 2015); therefore possessing an efficient drainage system for excess fluid and being able to squeeze out said fluid would help in achieving this. Certainly, it is known that tree frogs can bring their pads into very close contact with the surface (Federle, Barnes *et al.* 2006), and it may be that torrent frogs can do this more efficiently than tree frogs (although this has not been tested).

The high forces produced by the belly/thigh skins indicate an important role in staying attached in high flow rates, despite the exact reason for the high forces being unknown. The loose nature of the torrent frogs' skin would help to conform and stay attached on a rough waterfall surface, and the increase in contact area with these body parts could aid the overall attachment abilities of the frogs. The high friction forces measured could be due to the loose nature of the skin staying attached to the force plate and therefore pulling on the beam. While the tree frogs' belly and thigh skin also produced high forces, it appears that they are less likely to bring these body parts into contact when inverted - most likely due to the mass of the frog pulling the body away from the surface by gravity. Subsequently these frogs cannot perform as well, as was seen in both

tilting experiments (and has been noted in previous studies (Hanna and Barnes 1991, Endlein, Ji *et al.* 2013)).

The force measurements also showed a dramatic drop when fluid is added between the body part and the surface in contact, with forces dropping to almost negligible forces. As with the water in the tilting experiments, the excess fluid will act as a lubricant which prevents the pads from making close contact. This means that capillary forces are reduced (as the meniscus surrounding the pad is disrupted), and pad contact is removed so friction from the cell tops in contact with the surface will not occur. Poor performance of adhesive pads in wet conditions has been noted in other organisms before - geckos pads show a decrease in performance when wet (Stark, Sullivan *et al.* 2012), and the geckos pads themselves utilise a self-drying mechanism to combat this (Stark, Wucinich *et al.* 2014). In the natural world, the poor performance of insects on wet surfaces is utilised by pitcher plants, which use highly wettable surfaces to cause insects to aquaplane and fall into their trap (Bohn and Federle 2004). In this study, it was thought that the pads of torrent frogs would be able to cope with the excess water and still produce high friction and adhesive forces, but this was not seen. It is possible that the experimental technique - pipetting fluid onto the pads before bringing into contact with the force plate - is not representative of what happens when the frog is attached to a waterfall. The frogs could have greater control over the squeezing out of fluid from beneath the pad, which could help bring the pad in closer contact with the surface. The circumferal groove which is found around the edge of the pad could also play a role in directing fluid away from the pad whilst the frog is attached - TEM samples have shown that this groove is deep (Drotlef, Appel *et al.* 2015), but as yet its precise role is unclear.

One disparity of the above experiments is the differences between the experiments - the force measurements showed a smaller difference in forces between tree and torrent frogs than the tilting experiments (which showed large differences). This may be explained by the differences in contact areas which were seen from the illuminating boards, with the two species showing differing

amounts of skin contact when tilted. So despite the small difference in force per unit area, the behaviours of the frogs on the surfaces could explain the difference in performance.

4.4.4. Linking force measurements with contact area

By having both the force per unit areas for various body parts of the frogs, and the contact areas of the two species when tilted, the two sets of data can be combined to estimate what sort of forces the frogs are producing when sticking. This can only be done with contact area from a smooth, dry surface, so this analysis assumes that the contact area remains the same when a surface is wet. The results of this amalgamation of data are shown in *Table 4.1*.

Contact areas for friction were taken at 90° , as this is the angle where the greatest frictional forces are acting on the frog due to gravity; similarly, areas for adhesive force analysis were taken at 180° , as that is the angle with the highest force acting normally to the frog. The total forces for each body part (median values are used, to eliminate the effects of a few rogue extreme values) are multiplied by the area of that part in contact, to calculate the frictional and adhesive forces. These results are then compared with the hypothetical force required to keep the frog attached - calculated as the mass of the frogs multiplied by the force of gravity.

In dry conditions, both species can produce enough overall force necessary to stay attached. *R.pardalis* can produce a total of 225.8 mN of frictional force and 103.5 mN of adhesive force to stay attached, when 45.1 mN is required to stay attached. *S. guttatus* show similar results - producing 1165 mN frictional force and 373 mN of adhesive force when only 24.5 mN is required. In fact, both species show safety factors by producing more adhesive force than is necessary to stay attached; this is seen in other climbing organisms, such as geckos (Autumn, Liang *et al.* 2000). Under wet conditions, the forces produced by the frogs' falls significantly; but this drop affects the two species differently. While torrent frogs can still produce enough force to stay attached (41.8 mN of overall

friction force, and 88.9 mN of adhesive force), the tree frogs are not producing sufficient adhesive force (17.7 mN when 45.1 mN is needed), and therefore should be falling off before 180° (which was seen in the tilting experiments). Torrent frogs show behaviours of increasing contact area during tilting (see illumination tilting experiment), which will aid attachment forces. Torrent frogs also have a lower average mass than the tree frogs, meaning that the frogs will have a lower force acting against their adhesive forces.

Table 4.1: Force measurements for body parts combined with whole animal contact areas to estimate overall forces produced by tree and torrent frogs. The data is a combination of experimental work from the 2010 and 2012 studies. Reproduced from Endlein et al. (Endlein, Barnes et al. 2013)

	<i>R. pardalis</i>			<i>S. guttatus</i>		
	pads	belly	thigh	pads	belly	thigh
<i>Friction (dry)</i>						
Area at 90° (mm ²)	65.1	72.4	108.1	20.1	38.8	119.1
Force per area (mN mm ⁻²)	1.5	1.0	0.5	3.0	7.3	6.9
Force (Area × Force per area)	98.3	74.5	53.0	60.9	284.1	820.3
Total force (mN)		225.8			1165	
Force required (at 90°)		45.1			24.5	
<i>Friction (wet)</i>						
	pads	belly	thigh	pads	belly	thigh
Area at 90° (mm ²)	65.1	72.4	108.1	20.1	38.8	119.1
Force per area (mN mm ⁻²)	0.2	0.3	0.3	0.1	0.1	0.3
Force (Area × Force per area)	11.1	23.9	28.1	2.2	3.9	35.7
Total force (mN)		63.1			41.8	
Force required (at 90°)		45.1			24.5	
<i>Adhesion (dry)</i>						
	pads	belly	thigh	pads	belly	thigh
Area at 180° (mm ²)	77.2	0	0	22.4	136.2	155.1
Force per area (mN mm ⁻²)	1.3	1.0	0.5	2.4	1.5	0.7
Force (Area × Force per area)	103.5	0	0	54.5	208.3	110.1
Total force (mN)		103.5			373.0	
Force required (at 180°)		45.1			24.5	
<i>Adhesion (wet)</i>						
	pads	belly	thigh	pads	belly	thigh
Area at 180° (mm ²)	77.2	0	0	22.4	136.2	155.1
Force per area (mN mm ⁻²)	0.2	0.7	0.3	0.1	0.3	0.3
Force (Area × Force per area)	17.8	0	0	2.9	39.5	46.5
Total force (mN)		17.8			88.9	
Force required (at 180°)		45.1			24.5	

Values are medians, as mean values were sometimes distorted by the occasional rogue value. All calculations were performed before reduction to a single decimal place.

doi:10.1371/journal.pone.0073810.t002

The numbers in *Table 4.1* are purely estimations, and are likely to be overestimates, as both species will often fall before 180° . Overestimation of adhesive ability is seen in gecko studies as well, where feet were estimated to carry 130 kg of weight, but in reality would not because individual setae are unlikely to be in contact simultaneously due to surface roughness or particle on the surface. The excess adhesive forces could also be a safety measure against sudden falls or gusts of wind (Autumn and Peattie 2002). What is of interest is the higher safety factors seen in torrent frogs compared to the tree frogs, implying that the frogs are better adapted at dealing with the forces they will come across. The torrent frogs utilise their belly and thigh skin more, and this is reflected in their climbing technique of hopping up a surface instead of walking one foot at a time (personal observation). In this way they assure immediate contact of a large area of skin, and most likely successful attachment. It is unclear how fluid would be drained from the belly skin contact area, it may be that the sudden increase in contact area by the frog helps to squeeze out fluid, or that the loose wrinkled skin will allow parts of the skin to come into contact while fluid drains from other parts.

4.4.5. Pad and skin morphology

The SEM images display a similar morphology adaptation first noticed in some torrent and stream frogs, where cells possess pointed ends which indicate a directionality not seen in tree frog pads (Ohler 1995). In *S.guttatus*, these cells were only found around the periphery of the toe pad, whilst in other species, such as *O.hosii*, it is more frequent throughout the pad. The tree frog in this study (*R.pardalis*) showed no such characteristics, and possessed cellular structure typical of other tree frogs (Smith, Barnes *et al.* 2006). At this point, there is only speculation towards the role (if any) of this directionality of the channels, but it is conceivable that excess fluid can be quickly removed by these specialised pads when in contact and produce decent attachment forces (although this was not seen in the force measurement experiments). Experiments of structured surfaces during wet adhesion in bio-inspired surfaces have shown that the shape and size of structures can significantly affect adhesion (Drotlef, Stepien *et al.* 2012). The specialised structures seen in torrent frogs could help in keeping the pad close to the surface in flooded

conditions, as a close proximity of the pad will play a role in controlling hydrodynamic forces, which will aid in adhesion when the usual fluid-air meniscus of the pad is potentially missing. The clear difference in morphology of the belly and thigh skins, and the subsequent differences in frictional forces, could be an indication that having smooth but loose skin on the underside of the frog helps produce added frictional force that would greatly aid staying attached on a waterfall.

4.4.6. The role of body mass

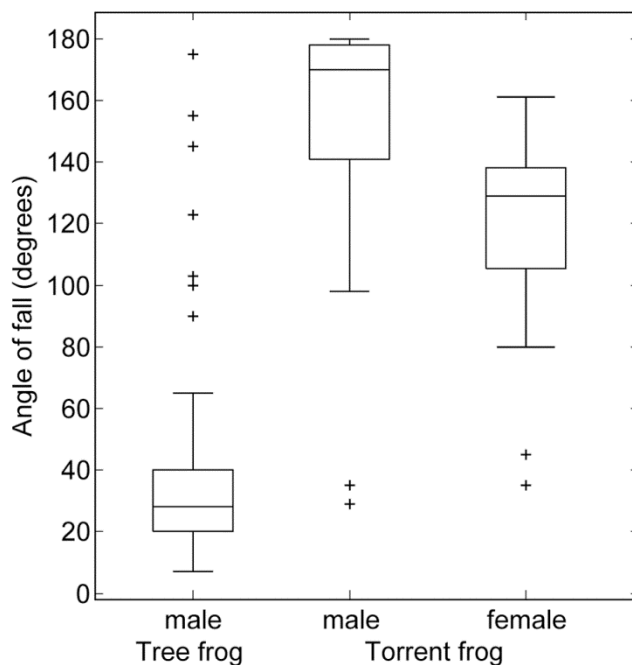


Figure 4.10: Attachment performance on the tilting apparatus of male *R.pardalis*, male *S.guttatus* and female *S.guttatus*; tested on the roughest surface with the highest flow rate. The data from the male frogs is from Figure 4.8. Reproduced from Endlein et al. (Endlein, Barnes et al. 2013)

As the mass of the tree frog is higher than that of the torrent frog, a simple answer for the difference in performance in the tilting experiment is the mass difference - the tree frogs have to deal with a larger mass and therefore cannot hold on as well. Despite being chosen due their closeness in size and mass, there is still a difference between the two species. Previous studies have correlated size to performance in tree frogs, and it has been noted that despite larger frogs having bigger and more efficient pads they still cannot perform as well as

smaller frogs (Smith, Barnes *et al.* 2006). Indeed, one of the large torrent frog species *O.hosii* (mean mass of 12.0 g) performed poorly when tested on the tilting apparatus (data not shown). One method of testing this in this study was to look at the performance of female *S.guttatus* torrent frogs. In general female frogs are larger than male frogs, and in this case the female torrent frogs (mean mass 8.1 g) were larger than the tree frogs (4.0 g), as well as the male torrent frogs (2.7 g). Despite the significantly larger masses, the females could still perform better than the tree frogs on the roughest and highest flow rates in the tilting experiment (see *Figure 4.10*). Whilst the female torrent frog couldn't perform as well as the male torrent frogs ($n = 50$, $z = 4.68$, $p < 0.001$), they still did significantly better than the male tree frogs under the same conditions ($n = 14$, $z = -4.19$, $p < 0.001$). This implies that while mass must have some effect on the frogs' abilities, it may not be the sole reason for torrent frogs' abilities.

4.5. Conclusion

This study shows that torrent frogs can perform better than tree frogs in conditions which mimic their natural habitat, i.e. a waterfall. This means that they are highly adapted for their environment, due to a number of physiological and behavioural differences. Firstly, the torrent frogs are generally smaller than other frog species, and therefore have a lower mass to compensate for during attachment. This gives them a big advantage when adhering in waterfalls, as the fluid under the pads can significantly diminish the forces produced by them. Torrent frogs can also compensate for this by bring a large area of its body into contact with the surface. Despite the low levels of adhesive force when wet, the large area coupled with the smaller mass means that torrent frogs have enough overall adhesive forces to stay attached. The loose skin of the belly and thighs will produce high levels of friction, and the frogs show a behavioural strategy of keeping a large contact area by jumping and landing with large areas of skin in contact. Compare this to the tree frog, which show a decrease of contact area with increased steepness, and therefore struggle to stay attached. The pads of the torrent frog also appear to have some sort of specialisation with directionality to the channels, although the exact role of this adaptation is still not known. Although it is premature to draw too many conclusions from a simple two species comparison, the abilities of torrent frogs to stick and climb in a

challenging environment appear to show a remarkable specialisation. As noted by biomimetic researchers (Wang, He *et al.* 2012), they provide a good model for a wet adhesive system which is highly adaptive.

5. Analysis of tree frog attachment performance on rough surfaces

This chapter includes experiments which are in the process of being written up for a paper entitled “When the going gets rough - studying the effect of surface roughness on the adhesive abilities of tree frogs”.

Summary

The adhesive pads of tree frogs are required to adhere to surfaces of various roughnesses in their natural habitats, such as leaves or rocks. Rough surfaces can affect the effectiveness of their toe pads, due to various problems such as loss of real contact area, loss of fluid and abrasion of the pad surface. Here, we tested the effect of surface roughness on the adhesive abilities of the tree frog *Litoria caerulea*. This was done by testing shear and adhesive forces on various rough surfaces, both on a single toe pad and whole animal scale. It was shown that frogs can stick better on small scale roughness, but perform poorly on larger roughnesses tested. Follow-up studies revealed that the pads lose fluid to the surface when adhering to larger roughnesses, but have a highly deformable pad to aid conformity and therefore sticking ability.

5.1. Introduction

All surfaces possess a degree of roughness to them (Scherge and Gorb 2001); rocks and stone surfaces feature roughnesses on several length scales, while plant cuticle can exhibit directional ridges (Voigt, Schweikart *et al.* 2012), or complex hierarchical folds and bumps (Prum, Seidel *et al.* 2011, Prum, Bohn *et al.* 2013). Plant surface roughness can have an ecological function, such as the superhydrophobic surfaces of Lotus leaves (which aid in self-cleaning) (Barthlott and Neinhuis 1997, Neinhuis and Barthlott 1997), to protect leaves (from water loss or UV light) through wax crystals (Koch, Bhushan *et al.* 2008) or to discourage the climbing of insects and other organisms (Prum, Bohn *et al.* 2013). Rough surfaces can potentially reduce adhesive ability of climbing organisms as they reduce the real contact area of the adhesive pad (Zhou, Robinson *et al.* 2014), and could drain adhesive fluid from the adhesive interface (therefore reducing the ability of the pad to produce the capillary and viscous forces required) (Persson 2007). Rough surfaces can also be abrasive and therefore potentially damaging to adhesive surfaces.

Despite extensive research on the adhesive abilities of tree frogs (Hanna and Barnes 1991, Barnes, Oines *et al.* 2006, Smith, Barnes *et al.* 2006), most studies

have involved testing their climbing capabilities on smooth surfaces. On a smooth surface the fluid on the pad creates an ultra-thin layer, whilst the cells of the pad can come into very close (potentially direct) contact with the surface to create frictional forces (Federle, Barnes *et al.* 2006); therefore the presence of surface asperities is likely to have some effect on adhesive ability. Many climbing organisms possess claws which can interlock or indent on soft surfaces, but tree frogs are not known to possess claws. Emerson and Diehl (Emerson and Diehl 1980) tested tree frogs clinging abilities on wood (without measuring the roughness of the wood), and found that frogs performed poorly when compared to glass. Unpublished data by Barnes has shown that tree frogs displayed minimum adhesive ability on an intermediate roughness which was larger than their cell morphology but smaller than the pad itself. The study on torrent frogs in the previous chapter included varying surface roughness to mimic the rocks found in and around waterfalls - both torrent frogs and tree frogs showed a decrease in performance as asperity size increased under dry conditions (Endlein, Barnes *et al.* 2013). The pads of tree frogs are very soft, and so should deform to mould around rough surfaces, as is seen in smooth padded insects (Zhou, Robinson *et al.* 2014). The Young's modulus of the toe pads have been measured in several studies, with an elastic modulus of 33.5 kPa being the most recent estimate (Barnes, Baum *et al.* 2013). Barnes *et al.* (Barnes, Goodwyn *et al.* 2011) carried out indentations at different depths and measured different degrees of stiffness at different depths. This is partially explained by the stiff keratinous outer layer of the pad, which was measured as a stiffer material (5-15 MPa) in AFM measurements by Scholz *et al.* (Scholz, Barnes *et al.* 2009). The pad also has extensive blood vessels beneath the toe pads which will contribute to the soft nature of the whole pad. It is however unknown to what extent these soft pads can deform and adapt to certain scales of roughness.

An important aspect when using rough surfaces for testing is the quantification of roughness. Roughness can be a regular pattern, or can consist of irregular peaks and troughs on a surface. Roughness can be measured using R_a or R_{RMS} values, which quantify the variance of the profile from a mean hypothetical centre point (considered the halfway point between the peaks and troughs, based on the measurements). The R_a of a surface is defined as the arithmetic

average of the values measured, while the R_{RMS} (sometimes named the R_q) is the square root of the arithmetic average of the squares of the values. When testing pad performance on a rough surface it can be difficult to visualise pad contact on a rough surface, as added roughness scatters the light passing through a surface which can make it difficult to see clear images (the principle behind frosted glass). To compensate, surfaces with controlled heights, diameters and spaces between asperities can be made, so that specific parameters can be changed and tested (Zhou, Robinson *et al.* 2014). Alternatively, the random roughness of a polishing disc or sandpaper is likely to be more representative of a natural surface that a climbing organism would encounter. Thus, studying adhesive ability under both conditions could provide a greater understanding of how frogs can deal with roughness when climbing.

This chapter is a study of the performance of tree frogs on rough surfaces. The aim is to use a variety of techniques to test adhesive ability, both at the toe pad level and in free climbing tree frogs, using different rough surfaces. I tested the hypothesis that rough surfaces with larger asperities (i.e. larger than the pad cells size of 10 μm) will cause fluid to be drained from the pad contact area, which would be reflected in poorer performance (a reduction in adhesive forces), as proposed by Persson (Persson 2007). To gain further insight into this, interference reflection microscopy will be used to view the pad around rough asperities. This can give indications on the extent to which tree frogs can cope with rough surfaces when climbing.

5.2. Materials and methods

5.2.1. Experimental animals

The tree frog *Litoria caerulea* ($n = 8$) were used for all experiments; their housing and care are extensively detailed in the methods chapter (chapter 2). All experiments were carried out with live animals, with frogs not being anaesthetised at any stage. During the experimental period the frogs were regularly weighed using digital scales (mean weight = 16.7 g \pm 6.5 g), and their snout-vent length was measured using callipers (SVL = 57.6 mm \pm 5.5 mm). Frogs were cleaned prior to experiment (rinsed with chlorine free water and lightly

dabbed dry with a paper towel), to remove loose dead skin or dirt particulate from the pads.

5.2.2. Climbing performance in free-climbing frogs

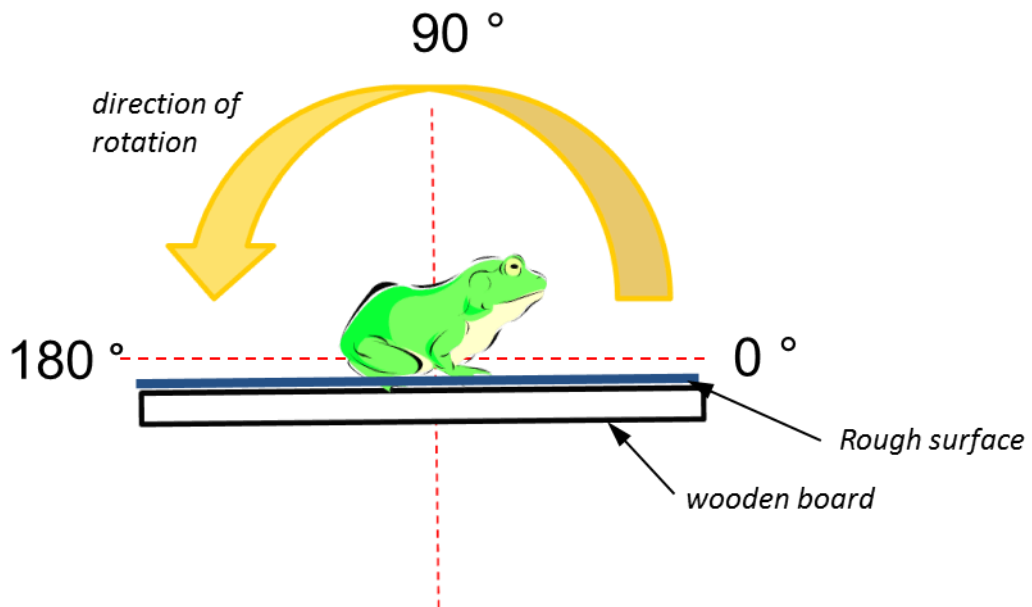


Figure 5.1: Diagram of the frog on the tilting platform, with changeable surface shown in blue.

Testing of the tree frogs' climbing performance on varying rough surface was done using the tilting platform experiment described in the methods chapter (Figure 5.1). Frogs adhesive and frictional forces were tested by placing them on a tilting board to see at what angles the frogs would slip and fall from the board. In this study, frogs were tested on the rough sandpapers and polishing discs to see their effect on performance. The surfaces were attached to the wooden rotating board using large binder clips. In this way surfaces could quickly be changed to minimise time and effort changing surface while testing the same frog. The original polishing discs and sandpapers were used for this experiment, due to them being of a suitable size to cover the area of a clinging frog. As a control, a glass plate was used as a smooth surface. The slip and fall angles for frogs on all of the surfaces were then compared to the control performance. Surface testing was continuously randomised to reduce any potential effect that tiredness could have on results.

5.2.3. Measuring forces of single toe pads

The forces produced by the adhesive pads of the tree frogs were also tested individually, with the use of the setup described in the methods chapter. Frogs were restrained so that a single toe pad could be brought into contact with the force transducer, and adhesive and frictional forces could be measured. The plate attached to the bending beam of the transducer was interchangeable (*Figure 5.2*); therefore surfaces of differing roughness (both surface types are described below) could be attached (both the resin replicas and the PDMS structured surfaces). The resin surfaces could be glued directly onto the bending beam, whilst the PDMS surfaces were attached to a ~1 mm thick piece of flat polyethylene (15 x 15 mm), which had a small opening where the PDMS was situated, therefore avoiding any impeding of the visualisation of contact area. The combination of the PDMS surface being relatively thick and the hole in the polyethylene being small meant that bending of the PDMS material whilst measuring forces was kept to a minimum.

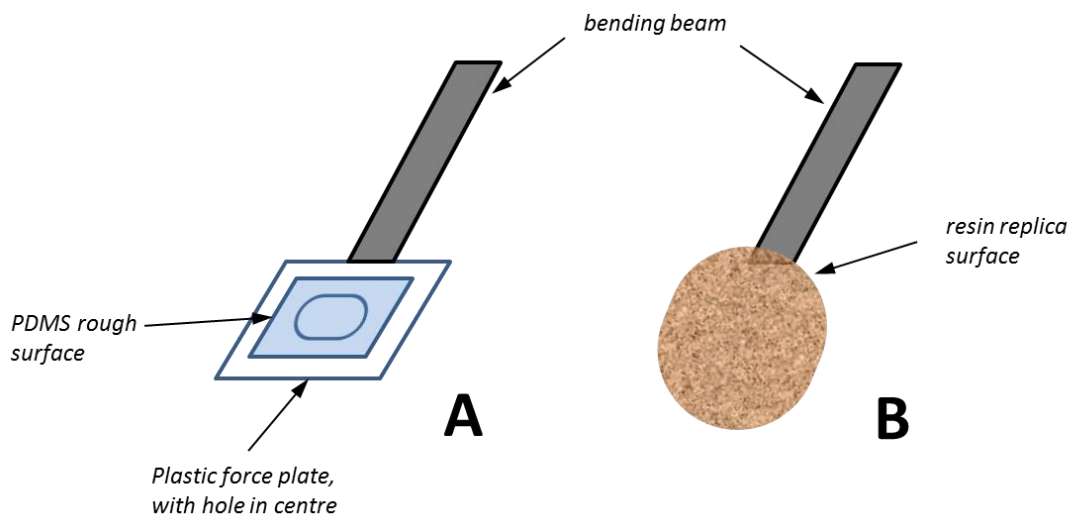


Figure 5.2: diagram illustrating the setup for the two rough surfaces used in the single toe pad force measurements. Image A shows the PDMS surfaces attached to a plastic plate with a hole drilled in it; B shows the resin replica surfaces glued directly to the bending beam.

Using a force feedback system implemented in LabView, the pad was brought into contact and kept with a preload of 2 mN. This preload was maintained throughout a lateral movement (proximally, representing pulling the pad towards the body) in order to measure the friction forces (a 5 mm drag at 1 mm s⁻¹). Finally, the pad was pulled away vertically from the surface, which

produced measurable adhesive forces. This set of movements, controlled by a manipulating stage, was used for both surfaces and for all frogs tested. Contact area was extracted in conjunction with the force measurements to give force per unit area, also termed stress (mN/mm^2 , or kPa). A digital video camera was used to record the contact area with help of a stereo microscope. Illumination was given by coaxial illumination (light travelling through the optical path). For some samples (particularly the resin surfaces) an additional external source of illumination was required to see the pad contact area with more clarity.

5.2.4. Rough surfaces

Two different kinds of rough surfaces were used in this study, which display different topographic features.

The first kind of rough surfaces used consisted of various grades of polishing discs and sandpaper (made from Aluminium oxide) from multiple sources (3M, USA; Norton abrasives, France; Ultratec, USA). For the whole animal tilting experiments in this study (described in the methods chapter, and above), the original surfaces were used; this provided a large area of rough surface required for tests on the scale of whole animals. In these experiments, the control surface was a glass plate, whilst all the other surfaces were aluminium oxide polishing discs or sandpapers, with the exception of the roughest surface, which was a monolayer of glass beads (glass beads of $1125\ \mu\text{m}$ diameter were laid on top of a glue covered surface, and rolled out to create a monolayer of the beads on the surface. Distribution of the beads was judged by eye). Thus the middle 8 of these surfaces had identical chemistry, whilst the roughest surface differed in both chemistry and the nature of the roughness, since glass beads are spherical, whilst the particles on sandpaper will, by their very nature, feel sharp to the frog.

For individual toe pad force measurements (also described in detail above and in the methods chapter), inverse replicas were made of the original surfaces using a low viscosity resin (TAAB laboratories equipment Ltd, UK). For each sample,

liquid resin was poured into a sample dish, and a small sample of the sandpaper/polishing disc was then put on top of this. The samples were placed in a vacuum to remove any potential bubbles, and the samples were then set by leaving them in an oven for 4 hours. The use of resin provided a hard yet transparent material which could mimic the sandpapers structure by accurately conforming before setting. The R_a values (a commonly used measure of roughness parameter, where average distance from a hypothetical centre line on the surface is taken to measure the average heights of the peaks and troughs of the surface) for both the originals and the copies were measured using a Dektak stylus surface profiler (Veeco Dektak 6M Height Profiler, USA. Vertical resolution 0.1 nm at 6.5 k(nm) horizontal range, Stylus force from 7 mg, Stylus tip radius of 2.5 μm . Scan length 1 mm, 9000 data points per scan.) - the R_a values are shown in *Table 5.1*. A control "smooth" surface (glass slide used as the original) was tested on (measurements are the first column from the left), along with 8 polishing disc/sandpapers and 7 of the replicas using the profiler. Although the replicas were not an exact match, they were close to the originals in terms of the roughness values recorded.

*Table 5.1: List of average roughness values (R_a , in μm) for surfaces used in experiments (polishing discs/sandpaper and their resin copies). * R_a value calculated using the formula in Appendix 3. The wavelength (width of the asperities) was measured by eye by viewing the surfaces under the microscope (except for the beaded surface). Replica resin surfaces were not created or used for the two largest surfaces tested (425 and 562.5 μm) due to difficulties in successfully replicating and visibility through the surfaces. R_a for the largest tested surface have been calculated using equations in the appendix*

Surface	Original surface R_a (μm)	Resin surface R_a (μm)	Wavelength (μm)
glass cover slip	0.01	0.02	-
0.3 μm	0.21	0.33	1.2
3 μm	1.4	1.6	8.3
6 μm	3.7	2.9	16
16 μm	4.6	5.4	29
30 μm	6.8	6.6	57
58.5 μm	15.5	14.1	100
100 μm	21.5	22	250
425 μm	33.3	-	833.3
562.5 μm (beaded surface)	127*	-	1125

The largest roughness tested on (the 562.5 μm surface) is the same surface used for the tilting experiments from the study on torrent frogs in Brunei in Chapter 4 (Endlein, Barnes *et al.* 2013). The surface consisted of a monolayer of closely packed Ballotini glass beads which have an average diameter of 1125 μm (see Appendix 3). This provided a test surface with large asperities with the difference of exhibiting round asperities rather than jagged ones like in the sandpaper surfaces.

The other surface type was used exclusively for single toe pad force measurements, due to the fact that the surfaces could only be reproduced on a small scale, and therefore could not be used for any whole animal experiments which would require a larger surface area. These surfaces were designed to provide a transparent surface that would allow contact area to be visible through it, and to provide a standardised topography which has specific dimensions (as opposed to a surface made of peaks and valleys of a random

height and distribution). With these considerations, polydimethylsiloxane (PDMS) was the readily available material used for these surfaces. Although PDMS is a relatively soft material (a Young's modulus of approximately 360-870 kPa), the toe pads are made from a material which is overall softer, and therefore the softness of the PDMS should not affect the contact area, and so long as the PDMS is thick enough then the material would not bend whilst being used to visualise contact area. The PDMS surfaces are fabricated using moulds kindly made by Dirk Drotlef of the Max Planck Institute for polymer research in Mainz. Moulds were created from thin silicon wafers, with micro-patterns etched onto the surface using microlithographic processing. This involves cleaning the silicon wafers in piranha solution overnight before rinsing with deionised water and acetone and blow drying using nitrogen. The desired pattern was produced by laying down a layer of SU-8 photoresist, then applying a mask to remove specific areas of resistance, and then developing the exposed areas using photolithography to give the desired patterns. The moulds were negatives of the PDMS patterned surfaces, which produced surfaces consisting of rounded dimples (looking like circular pillars from above) which had fixed measurements for the height ($3\ \mu\text{m}$) and diameter ($2\ \mu\text{m}$) for all surfaces used (see *Figure 5.3*).

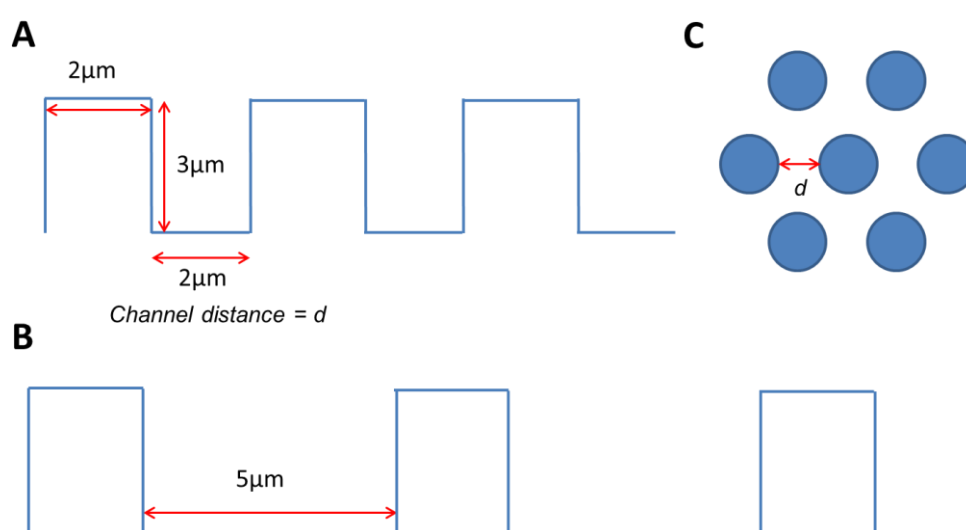


Figure 5.3: Diagram illustrating the topography of the PDMS structured surfaces. Each pillar on the surface has the same height and diameter, but varies in the minimum channel size (the smallest gap present between the asperities - each asperity will be surrounded by six asperities which are this distance away) or gap between each pillar (d). Images A and B display gaps of 2 and 5 μm respectively, and image C shows the layout of pillars from above.

Variation between surfaces came in the gap between each asperity - gap sizes tested on were 2, 5, 10 and 30 μm , as well as a smooth PDMS surface acting as a control. SEM imaging confirmed that the surfaces were successfully made (Figure 5.4). Gap width was selected as the experimental variable, as this was considered the simplest single parameter to change to view the effects on real contact area - dimples that are further apart are likely to have little effect on performance, whilst close together asperities could have a significant effect on forces, as they could potentially interact with the pad by interlocking or could change the contact area of the pad.

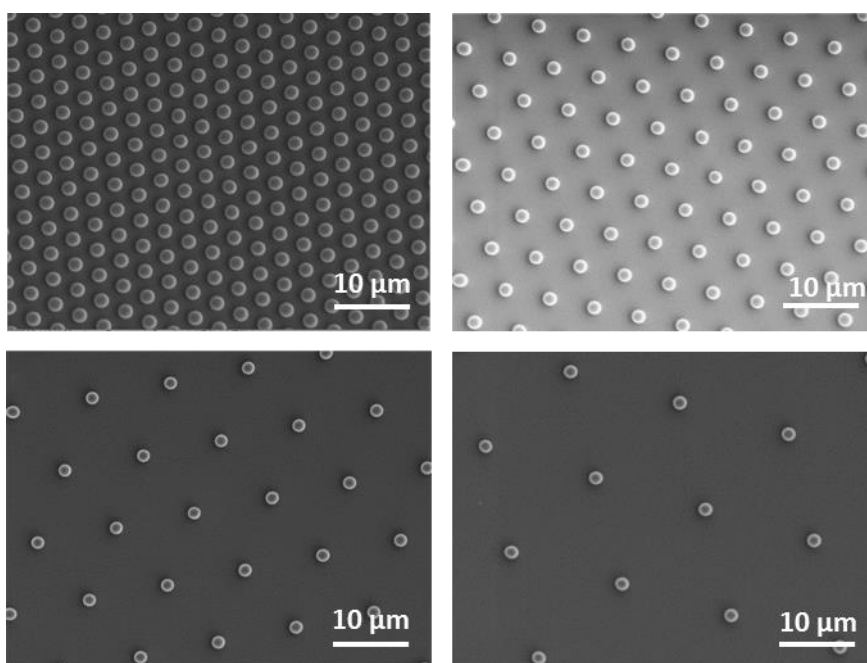


Figure 5.4: SEM imaging of examples of the PDMS structured surfaces used for single toe pad experiments. Structures (or dimples) are 3 μm in height, 2 μm in diameter, with varying gaps between the structures. Top left: 2 μm gaps, top right: 5 μm gaps, bottom left: 10 μm gaps and bottom right: 15 μm gaps. Scale bars = 10 μm .

PDMS is hydrophobic by nature (water forms contact angles greater than 90° on it), and so to cancel out any possible effect that surface energy can have on adhesive forces on rough surfaces, the surfaces were plasma treated before use each time. Plasma treatment involves placing the PDMS sample into a plasma cleaner (Harrick plasma, NY, USA), where on the surface of the sample Si-OH bonds were formed which changed the properties of the surface to a hydrophilic

state. Once surfaces were plasma treated, they were used immediately for experiments (all tests carried out within an hour of treatment), as plasma treated surfaces are unstable and lose their hydrophilic properties over time.

5.2.5. Visualising pad contact using IRM

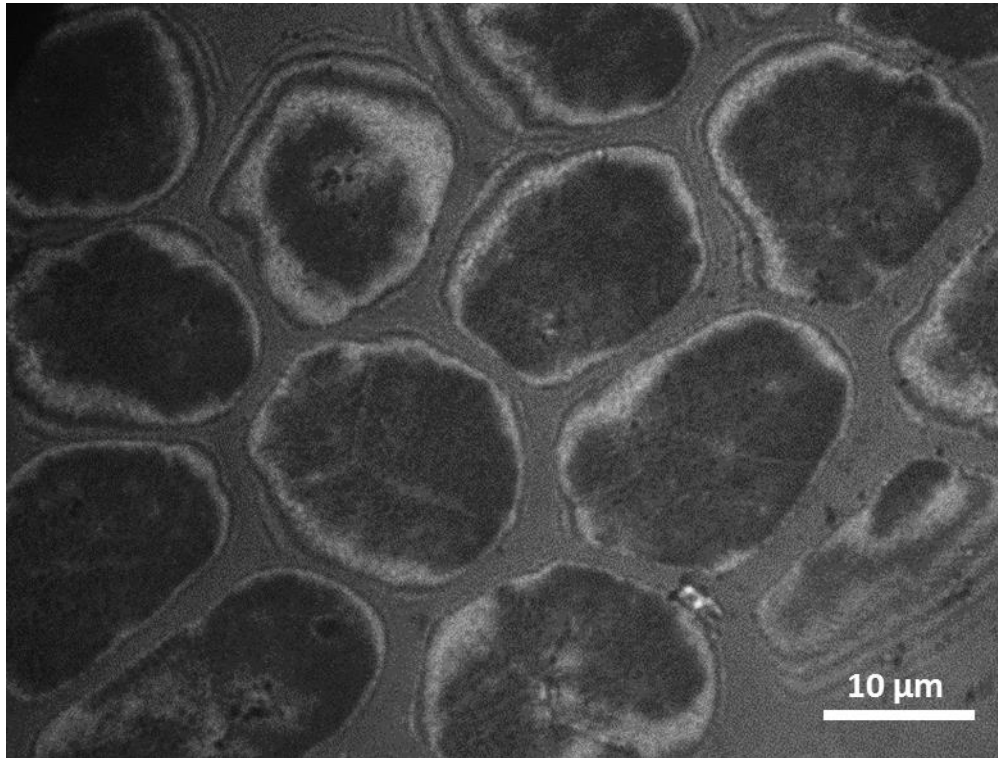


Figure 5.5: IRM image of the toe pad cells, with fluid-filled channels between them. The dark areas in the centre of the cells are the closest parts in contact with the glass, and around the edges of the cells interference fringes can be seen.

In order to gain further understanding of pad contact on rough surfaces, the contact area of the pad around an asperity was visualised using interference reflection microscopy (IRM). IRM is a technique that has been used previously to view the contact of the pad onto a smooth surface; the polygonal cells of the pad come into close contact with the surface, whilst the channels are filled with fluid (Federle, Barnes *et al.* 2006). The paper explains in great detail the technique and calculations required for analysis of the distance of the pad to the surface, but the following is a summation of the technique.

IRM involves the interference of monochromatic light rays depending on their phase shift, which results in light and dark bands. When the pad is in contact, a dark patch is seen. As the pad slopes away from the glass surface (and no longer being in contact), this produces darker and lighter alternate bands (interference fringes) as the distance from the surface increases. This creates an image where close contact is shown as a dark patch (typically seen in the centre of each pad) and at the edge of each cell there are black and white interference fringes as the distance of the cell from the surface increases (*Figure 5.5*). The interference fringes are due to the interference of light reflected from the glass cover slip (to which the frog is adhering) and the surface of the toe pad. Each band then represents a change in the height of the pad at that point, and so in knowing this, the slope of the pad (which will vary if the fringes become wider or narrower) can be visualised. The zero-order maximum is assumed to be the central part of the cell where it is in contact with the surface (based on the work by Federle *et al.* (Federle, Barnes *et al.* 2006)), and so using one wavelength of light the slope is calculated by the sequence of maxima and minima values on a sinusoidal wave formed by the dark and light fringes. IRM on the pad is limited by distance (depending on the illuminating aperture) - fringes will vary less and less as the surface slopes away, therefore this technique will only show the initial slope of the pad away from the surface. Using this technique the conformity of the pad around an asperity could be seen. This would help in understanding whether the soft nature of the toe pad would help when encountering a rough surface made up of asperities.

Individual frogs were kept in a stationary position by holding them in a petri dish, with a single foot and toe pad held in position (as in the single toe pad force measuring setup, see Methods chapter for details). This meant that the frog would not be able to move excessively, therefore allowing contact of the pad to be seen at a cellular level. An Axiovert 200M microscope (Zeiss, Oberkochen, Germany) was used for IRM, with bandpass filters within the illumination path (to form monochromatic light and reduce stray light) and a custom built pinhole slider (which defines the illumination aperture (illuminating numerical aperture = 1.001)) for this technique. A camera attached to the microscope (Evolution EX1, Princeton instruments, New Jersey, USA. Image

dimensions: 1390 x 1040 pixels) could record images of pad contact at cellular level - this meant that pad conformity around an asperity could be visualised.

The glass surface was randomly covered with glass beads (Ballotini beads, Jencons, VWR International, UK) of various sizes, which ranged in size from 4.48 μm to 130.51 μm (3 grades of categorised Ballotini beads were used on separate occasions), by tapping a coated cotton bud over the surface to scatter the beads. The pad was then brought into contact with the surface and the beads, to see how well it could conform to the beads present. Using Matlab scripts written specifically for this technique, the distance between the point where the pad is in close contact (seen as the dark patch in the centre of each cell) and the centre of the bead could be measured (*Figure 5.6*). This allows the effect of bead size on the gap size to be investigated. The spacing of the interference fringes coming away from the point of close contact allows the angle the pad is creating to be calculated (a function of the Matlab script), and so the initial slope of the pad coming away from the surface can then be calculated. For each particular point of detachment, the slope to the bead top is calculated from the light and dark fringes. The gap between the pad and the bead can also have fluid either present or absent from it - this area is seen as grey when fluid is present and bright when no fluid (i.e. air) is present. With each bead studied, it was noted whether fluid was present or not (seen as a bright light of the air interface, but small amounts of fluid at the pad contact still allowed the slope of the pad to be seen).

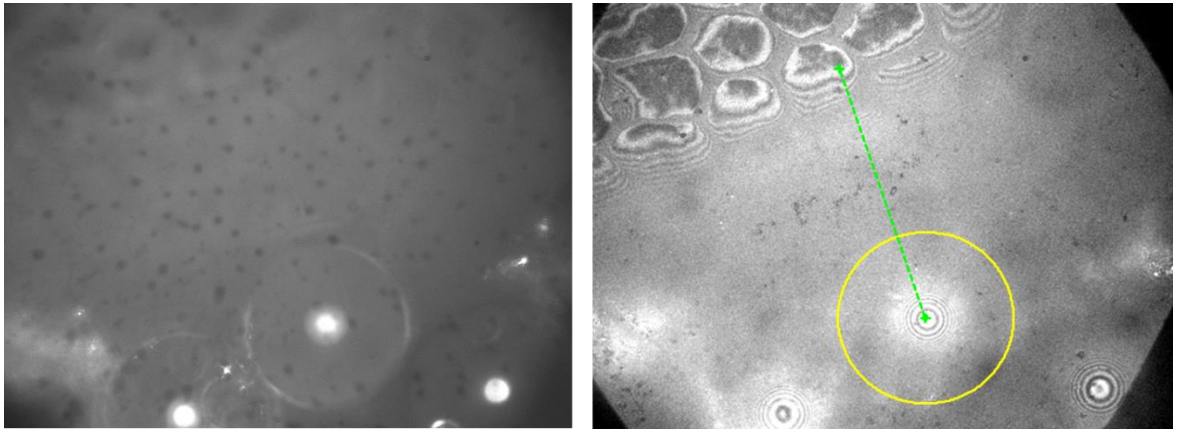


Figure 5.6: IRM images of the toe pad in contact with the glass surrounding an asperity bead. The two images are taken at different focal planes; the left image allows the circumference of the bead to be seen, which can then be recorded and superimposed on the second focal plane (on the right). The distance from the centre of the bead to the closest cell in close contact with the glass can be seen (the dark central part of the cell). Interference fringes as the pad surface slopes away from the glass can be seen along the edges nearest the bead.

5.2.6. Statistics

All individual data sets were tested for normality using Lilliefors tests (based on the Kolmogorov-Smirnov test). Depending on the normality of the data sets, either Student's *t*-tests or Wilcoxon rank sum tests (also known as a Mann-Whitney *U* test) were used for comparisons between two sets of data in the whole animal and single toe pad experiments. For the IRM experiments, linear rank correlation tests were conducted on the data. Data which has been used for multiple tests have been corrected for using the Bonferroni correction. Value ranges are written as means \pm standard deviation. All statistical analysis was done using the statistical toolbox in Matlab (r2011a). Boxes on boxplots denote 25th and 75th percentiles, the whiskers display 99% of the data, the middle line shows the median and outliers (data points located far outside the range of the majority of the data) are shown as +.

5.3. Results

5.3.1. Attachment abilities of free climbing tree frogs

The climbing abilities of freely moving tree frogs were tested on varying rough surfaces using the tilting board described previously ($n = 60$ for all surfaces tested). At the beginning of the test, frogs usually exhibited a relaxed and

crouched posture with all legs tucked into the body. However, as the angle of the board increased and it became more difficult for the frog to stay attached, frogs would typically spread their limbs in order to help stay attached. This behaviour (which has been described in previous studies and is not unique to this experiment) helps in producing friction forces whilst keeping the peel angle of the pads low (Endlein, Ji *et al.* 2013). A 'smooth' glass surface was tested on as a control for rough surface tests. Boxplots are shown below, comparing the performances (angles of slip and fall) of the frogs' frictional (*Figure 5.7*) and adhesive forces; Mann-Whitney *U* tests were conducted on comparative sets of data ($n = 60$), with a Bonferroni correction implemented for multiple data usage (95% confidence interval $p = 0.0055$, 99% $p = 0.0011$, 99.9% $p = 0.00011$). Comparisons of purely slip and fall angles (without converting to force values) allows for patterns of climbing ability to be seen between the different surfaces.

Slipping behaviour, an indication that frictional forces have reached their maximum, was generally not seen on the smooth surface until 90° had been reached, and occurred at $92.89 \pm 5.05^\circ$ (mean angles \pm standard deviation, as with all angles cited). All tests were compared to the smooth surface performance, which was the control surface. The frogs performed best on the smaller scale roughnesses, not slipping until a higher angle of $99.5 \pm 7.44^\circ$ on the $3 \mu\text{m}$; this was significantly higher than the performance on the smooth ($z = -4.9915$, $p < 0.0001$), also seen on the $6 \mu\text{m}$ surface ($z = -5.7368$, $p < 0.0001$). As the roughness of the surfaces increased, this resulted in a decreasing of the angle of slips. Slipping occurred before vertical (to 89.4°) on the $30 \mu\text{m}$ surface, therefore lower than the smooth surface performance ($z = 3.6554$, $p < 0.0001$). The largest roughnesses tested on showed poor performances by the frogs, with the frogs failing to produce much friction and slipping at comparatively low angles.

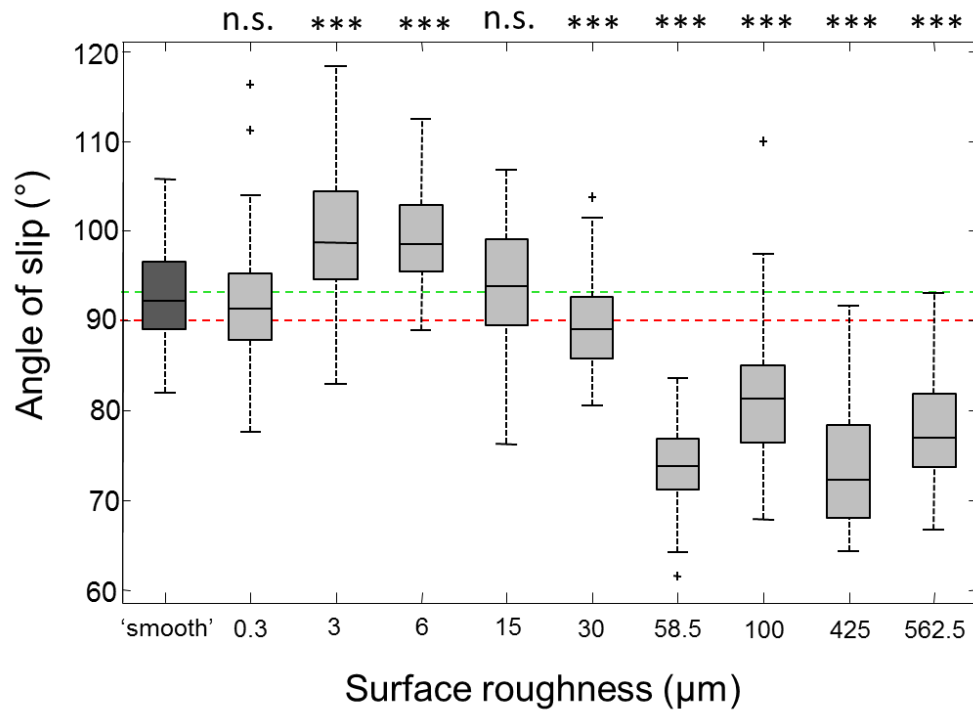


*Figure 5.7: Comparison of slip angles of free climbing tree frogs on varying rough surfaces. Smooth glass is on the left, with increasing roughness (larger asperities) moving right across the x axis. The red dashed line through 90° on the plot shows the angle where friction forces would have their maximum effect on an inanimate object on a slope. The green dashed line shows the mean smooth measurements, to aid comparisons. Statistical tests which compare each surface with the smooth surface performance are shown above each box - n.s. if not significant, * if $p < 0.0055$, ** if $p < 0.0011$ and *** if $p < 0.00011$.*

The angles at which the frog fell off the surface correspond to the adhesive forces failing, and can thus be linked to the maximum adhesive force produced by the frog (*Figure 5.8*). Frog performance again showed good performance on the smaller scale roughness, and performing poorly on surfaces with larger roughnesses. On the smooth surface the frogs could stay attached until $108.7 \pm 10.9^\circ$, staying attached beyond vertical as the surface becomes an overhang. The frogs stuck best on the 3 μm ($z = -3.388$, $p < 0.0007$), staying attached until $115.2 \pm 7.2^\circ$. On the 58.5 μm surface the frogs failed to reach 90°, and therefore did not test their adhesive ability. This also occurred for the 100 μm and the 425 μm surfaces, with frogs generally failing to stay attached to an angle beyond 90°. For the final surface, the 562.5 μm , there appeared to be some recovery, with frogs managing to stay attached until $94.9 \pm 7.5^\circ$ and showing some adhesive ability.

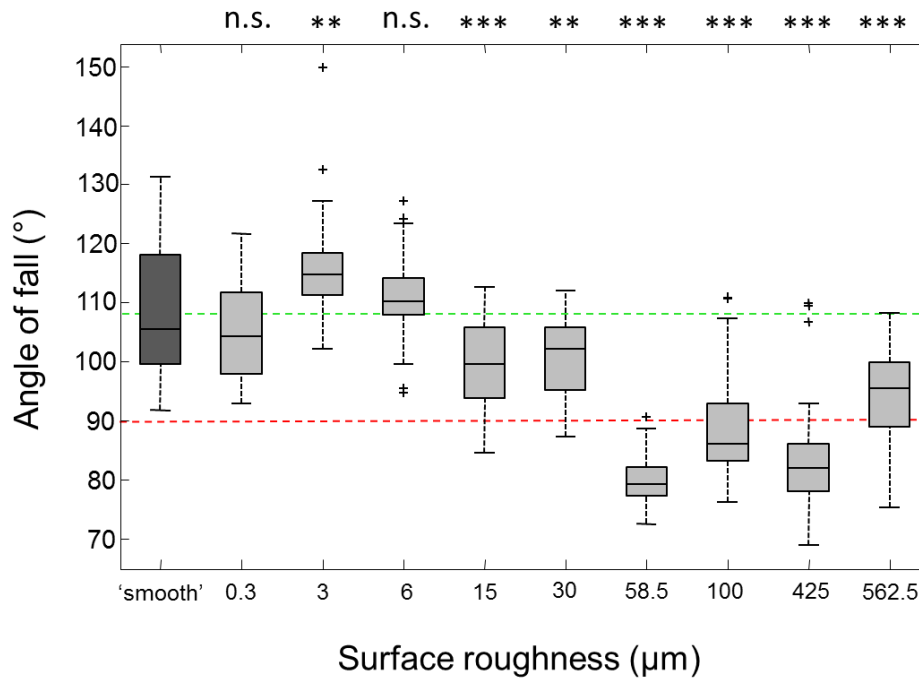


Figure 5.8: Fall angles of climbing tree frogs on varying rough surfaces. The glass surface ('smooth') is on the left, with increasing roughness (increasing R_a values) going right along the x axis. The red dashed line indicates the angle where adhesive forces begin to play a role in an inanimate object staying attached to the surface. The green dashed line shows the mean smooth measurements, to aid comparisons. Other details are as in Figure 5.7.

In order to help relate each surface to another in terms of size, the data for both sets of angles were plotted on log scale together (Figure 5.9) as opposed to the categorical x-axes seen on the previous graphs. This helps in summarising what was seen in the tilting experiment - the tree frogs show significantly better performance on the smaller scale roughness (3 - 6 μm) compared to the smooth glass surface (for both slip and fall angles). However, on larger roughnesses (58.5 - 562.5 μm) the frogs performed worse, with frogs slipping and falling at significantly lower angles than on the glass.

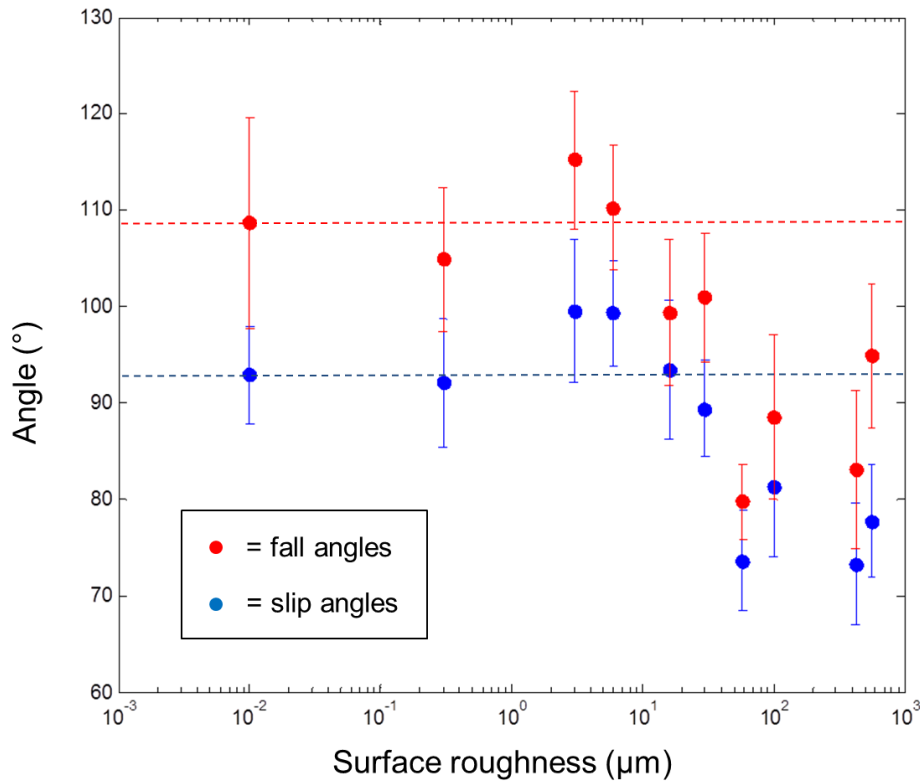


Figure 5.9: Mean slip (blue) and fall (red) angles plotted on a log axis for different surface roughnesses. Standard deviation whiskers are shown. The dashed lines indicate the mean angles for the glass surface (the first values on the left), to aid visual comparison.

5.3.2. Individual toe pad force measurements

In order to understand the performance of unrestrained frogs described before, I measured the friction and adhesion of individual toe pads under controlled conditions where I could 1) record contact area and 2) use defined surface geometries. Single toe pads were tested on different rough surfaces for frictional and adhesive forces produced ($n = 30$ for each surface tested), and the extracted force per unit area measurements for adhesion and friction were plotted (*Figure 5.10*) and analysed. Contact area was visualised using the microscope described in the setup in the methods chapter. The contact area was seen as a dark patch where the pad was in contact; however it was not possible to determine whether full contact or partial contact had been made, and so contact area was simply measured by the outer perimeter of the pad surface in contact.

On smooth resin surfaces, the pads produced a mean maximum of 7.76 ± 12.9 kPa of frictional shear stress (Figure 5.10A). Forces initially increased with roughness, with the largest shear stresses measured on the 6 μm surface by reaching a higher value of 30.1 ± 13.8 kPa ($z = -5.1672$, $p < 0.00014$). Shear stress values on the 15 μm surfaces were 18.48 ± 6.1 kPa - still higher than the smooth values ($z = -5.5663$, $p < 0.00014$), but lower than the forces on the 6 μm surface. The shear stress measured on the largest roughnesses tested were at a consistent level of approx. 16 kPa, which were still higher than those measured on the smooth surface (e.g. comparing smooth to 100 μm , $z = -5.5072$, $p < 0.00014$).

Adhesive forces (Figure 5.10B) on the smooth surface were measured as 1.74 ± 1.9 kPa, with peak adhesive forces measured on the 6 μm surface (3.72 ± 1.5 kPa; $z = -4.4871$, $p < 0.00014$). On the two largest roughnesses tested on (58.5 and 100 μm), the adhesive forces were significantly lower than the smooth surface forces, with 0.9 ± 0.8 kPa ($z = 3.0382$, $p = 0.0024$) and 0.66 ± 0.6 kPa ($z = 4.7828$, $p < 0.00014$) respectively being measured.

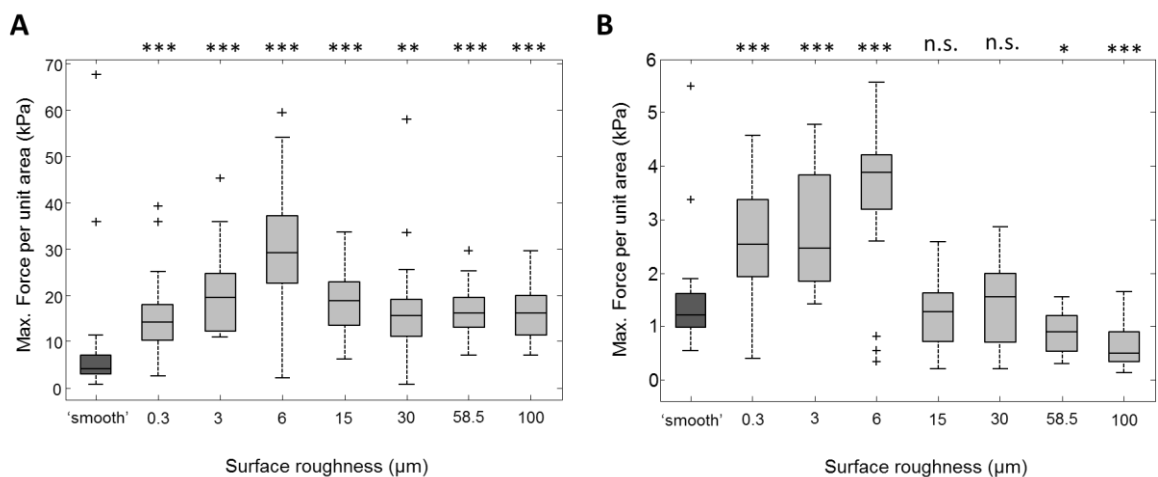


Figure 5.10: Single toe pad forces on rough surface replicates. Force per unit area (mN/mm^2 , or kPa) has been calculated for friction (graph A) and for adhesion (graph B). Performances on surface of varying roughness (R_a values) are compared with 'smooth' surface ($R_a = 0.02 \mu\text{m}$) performance (dark grey box, left). Statistical tests are denoted above each box - n.s. if not significant, * if $p < 0.0071$, ** if $p < 0.0014$ and *** if $p < 0.00014$.

Using the same movements on the force plate, a different variation of rough surfaces made from PDMS were used, where the only parameter changed between surfaces is the gap between the asperities on the surface. Forces measured on these rough surfaces were compared to forces measured on a smooth PDMS surface. The forces per unit area (kPa) measurements were plotted for comparison (Figure 5.11).

Shear stress values ($n = 30$) measured on a smooth PDMS surface were of a similar range as those measured on the resin smooth surfaces, measured at 5.94 ± 2.6 kPa. The highest friction forces were measured on the $2 \mu\text{m}$ gapped surface (13.7 ± 4.9 kPa, significantly higher than the smooth surface forces - $t = -7.6879$, $p < 0.00025$), and an increase in the gap size resulted in shear stress gradually returning the levels seen on a smooth surface. Adhesive forces on the PDMS surfaces ($n = 30$) followed the same pattern as the shear stresses, with a peak of adhesive forces seen on the $2 \mu\text{m}$ gapped surface. Forces reached 3.49 ± 1.5 kPa, which was higher than the smooth values of 1.43 ± 0.6 kPa ($p < 0.00025$). An increase in the gap between pillars resulted in adhesive stress returning to smooth surface values.

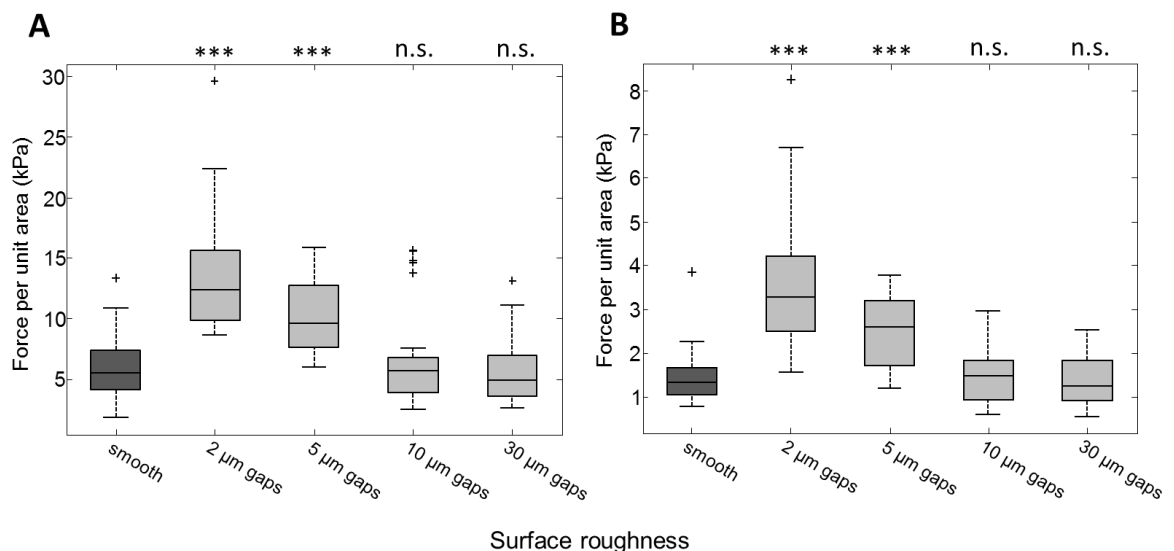


Figure 5.11: Force measurements of single toe pads on PDMS rough surfaces. The pads force per unit area (kPa) is shown for friction (graph A) and for adhesion (graph B), with different rough surfaces (varying in the size of the gap between the asperities) are compared to the forces produced on a smooth surface (dark grey) - n.s. if not significant, * if $p < 0.0125$, ** if $p < 0.0025$ and * if $p < 0.00025$.**

To sum up the force measurements on individual toe pads, the adhesive and frictional forces of the pads appear to be increased when roughness occurs on the small scale (on the 3 and 6 μm surfaces). The resin replicates displayed a levelling out of shear stress on larger roughnesses, while adhesive force showed a lower performance than on a smooth surface. On the PDMS surfaces, as the gap between asperities increased, the adhesive and frictional forces returned to the values seen on a smooth surface after producing increased stress on surfaces with tighter packed asperities.

5.3.3. Using IRM to visualise pad contact

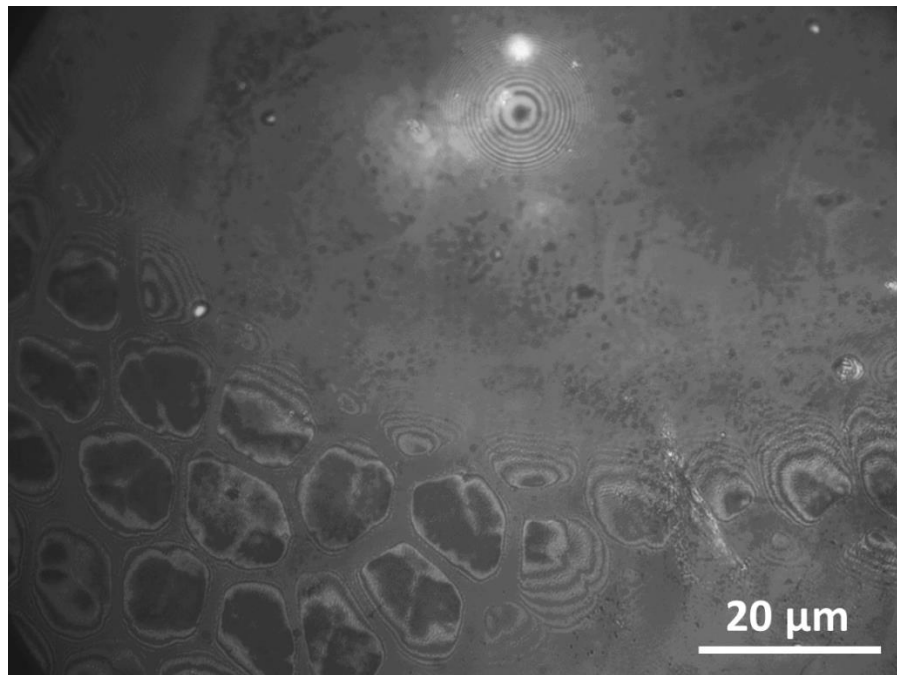


Figure 5.12: Toe pad in contact around a glass bead. Interference fringes indicate the pad sloping away from the glass surface, due to the presence of a bead nearby (top centre).

Using IRM allowed for pad contact to be visualised, where the polygonal cells of the pad can be seen to be in direct contact with the surface, with channels between the cells to allow the flow of pad fluid throughout the contact area (Figure 5.12). This corresponds with toe pad studies previously conducted by Federle *et al* (Federle, Barnes *et al.* 2006), and the technique allows pad contact to be closely examined (and measured) on a cellular level. For this

experiment, glass beads of different sizes were used to act as asperities on the surface, which the pad would potentially have to conform around to achieve proper contact with the surface (*Figure 5.12*). The distances between each asperity (of varying size) and the toe pad in contact with the surface are shown in *Figure 5.13*. The data has also been labelled depending on whether fluid filled the gap between the pad, the asperity and the glass surface, or if an air pocket could be seen.

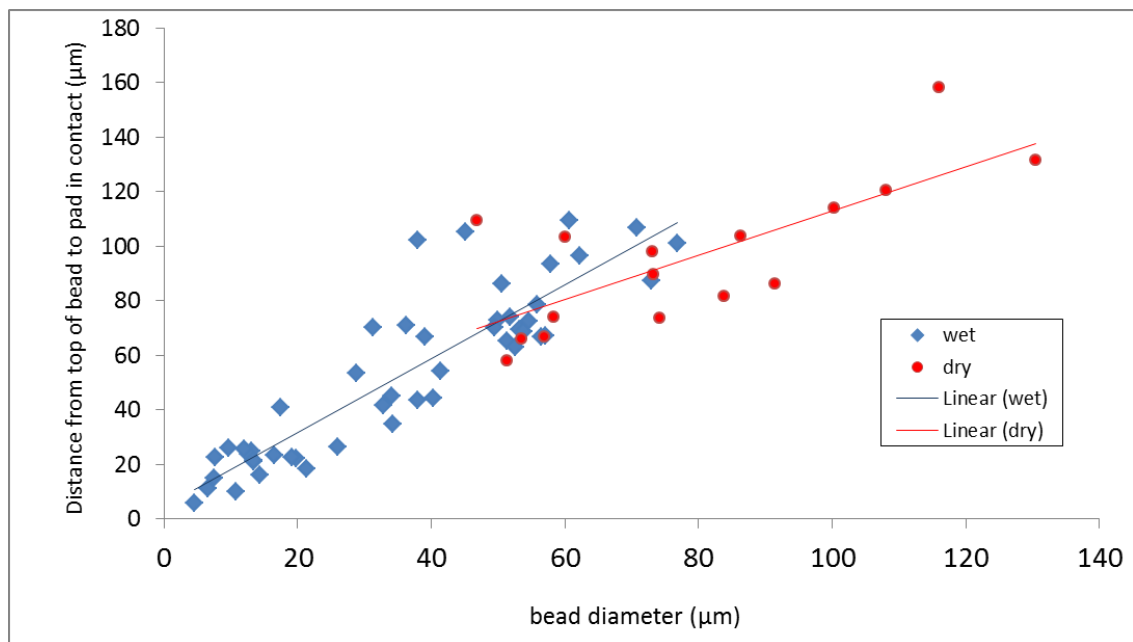


Figure 5.13: Scatterplot showing correlation between asperity size and pad contact (distance from bead edge to pad in contact with the surface). Data are differently coloured depending on whether fluid was present (blue) or absent (red) in the gap created between the pad, bead and surface.

Generally, a linear trend that can be seen in the data: as the bead size increases, so too does the gap between the bead and pad contact with the surface (Spearman correlation test; $Rho = 0.7307$, $n = 64$, $p < 0.001$). A transition from $\sim 50 \mu\text{m}$ until $\sim 75 \mu\text{m}$ in the bead size is apparent, where the pad fluid goes from being present in the gap to no longer fully filling the space. The lack of fluid only appears to occur around the larger beads that were used, which indicates that the size of the asperity affects whether fluid can fill the gap created by the asperity (comparison of gap distances from fluid filled and non-fluid filled gaps: Mann-Whitney U test, $n = 48$, $z = 3.0466$, $p < 0.001$). Interestingly, linear tests on the separated data - fluid filled ('wet') or fluid

being absent ('dry') show a significant linear correlation for the 'wet' measurements (Spearman correlation test; $Rho = 0.7866$, $n = 48$, $p < 0.001$), but not for the data points where fluid did not fully fill the gaps (although a slight trend is visible - Spearman correlation test; $Rho = 0.3947$, $n = 16$, $p = 0.1303$). The concentric lines seen at the edge of the pads for the first few μm give an indication of the initial slope (and therefore the conformity) of the pad away from the surface. For all beads tested, a similar slope of the pad was seen (mean slope = 0.21 ± 0.09), which indicates that the pad is a highly soft material as it consistently moulds to the surface rather than varying with bead size. When compared to a sine wave (where the wavelength coincides with first contact of the pad on the glass and pad contact on the top of the bead), the pad forms a similar shape when conforming (*Figure 5.14*), which is again an indication of the pad being a soft material.

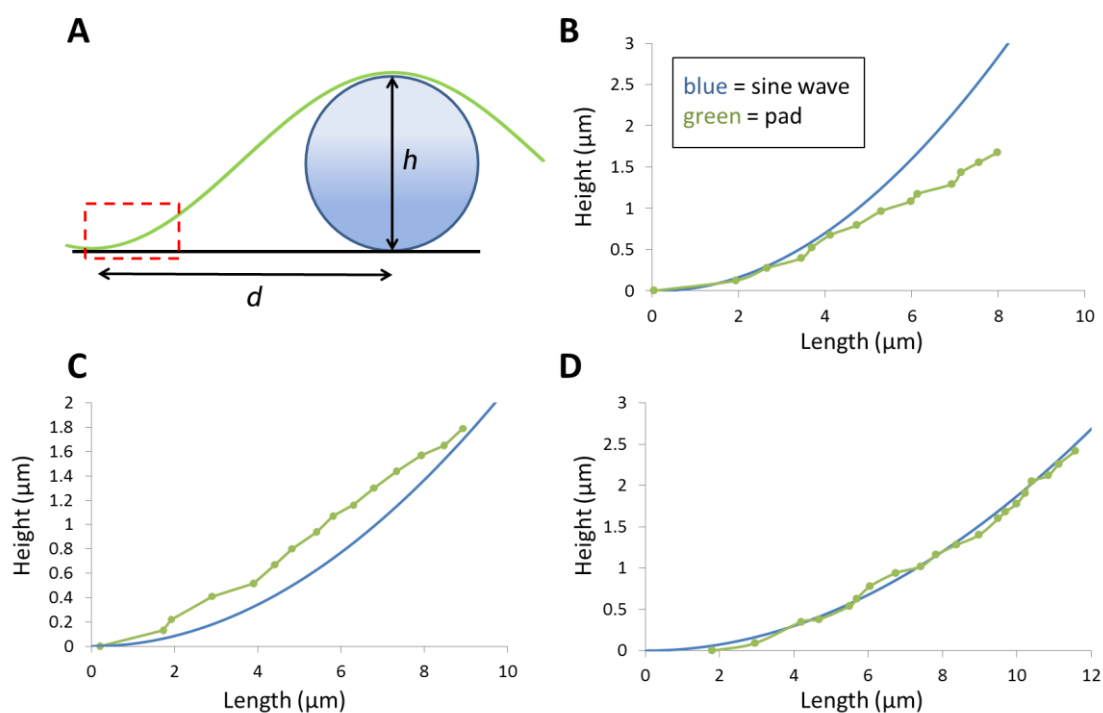


Figure 5.14: Comparing pad contact around an asperity to a sine wave (image A). The slopes of the pad separating from the surface can be seen using IRM (the red dashed box). When compared to a sine wave which matches the wavelength of varying bead sizes (B = $32.79 \mu\text{m}$, C = $39.09 \mu\text{m}$ bead, D = $57.92 \mu\text{m}$ bead), the pad generally follows a similar shape.

5.3.4. Climbing performance on a rough and wet surface

The previous experiments involving IRM indicated that frogs may be unable to produce sufficient pad fluid to fill gaps between asperities on the roughest surfaces. This would mean a loss of adhesive ability such as those seen on the larger roughnesses in the tilting experiment. Therefore, an additional test was done to see whether the addition of fluid to a rough surface increases the frictional and adhesive abilities of tree frogs (4 frogs used for experiments, $n = 40$). This was done using the tilting board experiment used earlier in this study, testing the efforts of a frog on smooth glass surface and on a rough sandpaper surface (the 58.5 μm surface was used, as the frogs had performed poorly on this surface in the previous tilting experiment). Performance on these surfaces when they were dry were conducted, and also when the surface was wet - water was sprayed onto the surface (using a water spraying mister) prior to each run of the test. As before, the frogs were observed for the angles they slipped and fell, which are related to the frictional and adhesive abilities respectively. Results for this are shown in *Figure 5.15*.

The angles of slip and fall on the dry smooth surface - $97.6 \pm 6.2^\circ$ for the slip and $121.2 \pm 6.1^\circ$ - were within a similar range to the results from the previous experiments. Likewise, the frogs also showed poor performance on the dry rough surfaces (slip angle: $73.4 \pm 4.98^\circ$, fall angle: $82.8 \pm 3.7^\circ$). When water was introduced to the smooth surface, it caused a loss of friction in the frogs' pads. This led to the frogs sliding at relatively low angles ($66.1 \pm 9.2^\circ$), which is a poorer performance than on the dry surface ($z = 7.6739$, $p < 0.001$). However, when extra fluid is introduced to the rough surface, the frictional performance significantly improved from when the same surface was dry ($t = -18.3666$, $p < 0.001$), so much so that the slip angle performances on a rough wet surface (mean $95.6 \pm 5.8^\circ$) did not significantly differ from the slip angles on a dry smooth surface ($z = 1.5348$, $p = 0.1248$).

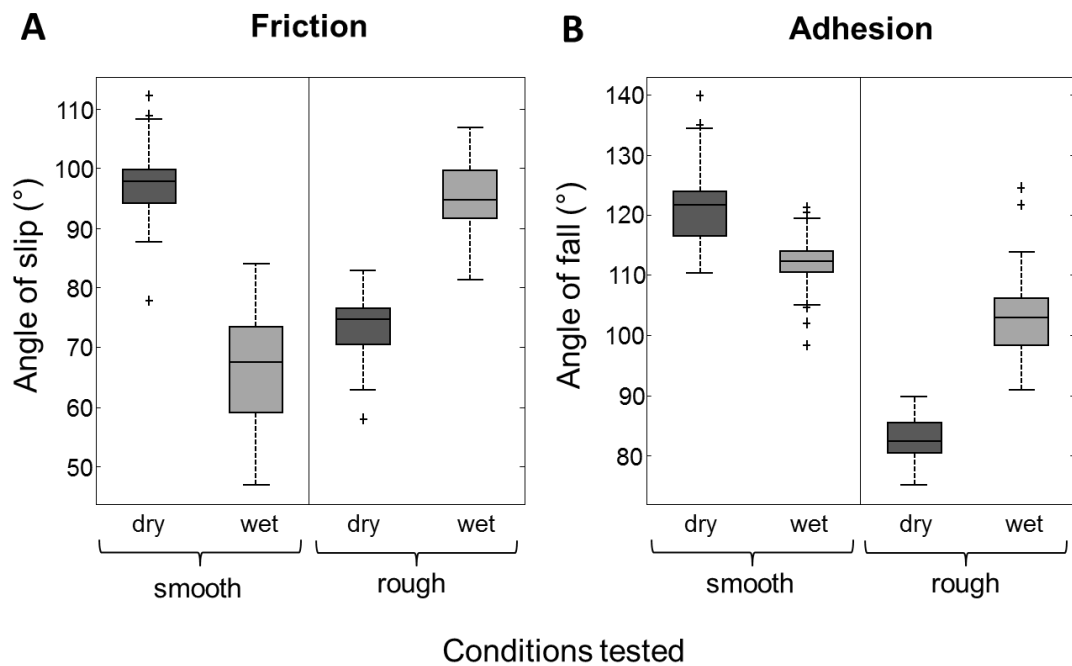


Figure 5.15: Boxplots displaying attachment performance of tree frogs in varying conditions. The angles of slip (graph A) and fall (graph B) of the frogs are shown for dry and wet surfaces, which could also be either rough or smooth.

For the angles of falling (representing maximum adhesive performance), the performance on a smooth, wet surface was lower than on a smooth dry surface, meaning that the frogs were still able to stay attached past 90° (therefore retaining some adhesive ability). The frogs were able to stay attached (even though the pads were continually slipping due to low friction) until $111.9 \pm 4.6^\circ$. On the wetted rough surfaces, the frogs were able to perform better than when the same surface was dry; they stayed attached until $103.1 \pm 7.1^\circ$ when it was wet, compared to $82.8 \pm 3.7^\circ$ when the surface was dry ($t = 16.198$, $p < 0.001$).

These experiments show that poor performance of frogs on the roughest surfaces can be significantly improved when the surface is wetted. However, on a smooth surface the presence of water leads to a drop in their climbing abilities, particularly in frictional forces.

5.4. Discussion

5.4.1. Rough surface effects on adhesion and friction

Most evidence supports the hypothesis that tree frogs adhere by capillary forces (Hanna and Barnes 1991, Barnes, Oines *et al.* 2006), but roles for other adhesive mechanisms (such as hydrodynamic forces, referred to as Stefan adhesion - see introduction for full equation) cannot be excluded. However, Stefan's equation refers to fluid movement between rigid plates, and so the equation does not apply in respect of the softer material of a tree frog's toe pad. Additionally, with close surfaces a role for van der Waals forces cannot be excluded (Federle, Barnes *et al.* 2006). For good capillary forces, the volume of fluid should be kept to a minimum, particularly at the air-water interface around the edge of the pad, for it is the curvature of the meniscus that provides the adhesive force, either directly through tensile forces that depend on length (circumference of pad) or on pressure forces (Laplace pressure) that depend on the area under the pad (Zhu 1999). On rough surfaces, the contact area would be expected to decrease, while the circumference could increase or decrease depending on the overall contact area and whether it forms a single area of contact.

Since tree frog adhesion depends upon a fluid joint and fluids tend to act as lubricants if they form a continuous film, it is surprising that tree frogs can generate high friction forces. Such forces are due to close contact between the tips of the nanopillars that cover the pad surface and the substrate (friction forces are much larger than would be predicted by any system involving a continuous fluid layer under the pad)(Federle, Barnes *et al.* 2006). Micro-rough surfaces will interdigitate with the polygonal epithelial cells using the channels if the rough surface has a similar wavelength providing further increases in friction. Rougher surfaces, on the other hand, are likely to reduce friction, since there will be a reduction in the area of close contact of the two surfaces. Also, the frog may be unable to produce enough fluid to fill all these gaps, which will reduce capillary forces as well.

5.4.2. Whole animal experiments

The whole animal experiments conducted provide direct data about the tree frog's capabilities on rough surface, as the slip and fall angles reflect friction and adhesive forces of the frogs. With slip angles, an angle of 90° represents the maximum friction force that this technique can measure. One might expect that, if a frog did not slip by 90° then it should not slip at all, and simply falls from the platform when the angle for maximum adhesion was reached. This occurred in some cases, but most of the frogs did actually slip before they fell. How then do we explain slip angles of greater than 90° ? The most likely explanation is that, at these high angles when the frog's mass is pulling the animal away from the platform, there is a decrease in actual toe pad contact area. This would mean that even though the shear stress remains the same or may even increase, the total force will decline and the frog would slip. It is important to note that this analysis makes the assumption that the shear forces in tree frog toe pads are directly proportional to the contact area, which is not fully understood. There could also be a dependence of shear stress on the normal adhesive forces, especially on rough surfaces. If the frog is coming away from the surface due to gravity, then adhesive forces will be reduced by the frog being pulled away from the surface, and so friction could also decrease.

With reference to fall angles in these experiments, no frogs stayed attached at 180° , but some fell below 90° . This will have been due to poor friction, the frogs simply sliding off the platform before adhesion can be tested. Therefore, friction and adhesion can affect each other. Indeed, the maximum adhesive capabilities of frogs can depend hugely on friction, for friction forces keep the pad/ground angle low, maximising the resultant force and preventing peeling of the pad from the surface (Endlein, Ji *et al.* 2013). Similar interactions in geckos have led to the coining of the term 'frictional adhesion' (Autumn, Dittmore *et al.* 2006). This means is that it is not possible to separate adhesion and friction unambiguously from whole animal tilting experiments, but the data remain useful in showing how surface roughness affects a tree frog's climbing performance.

Slip angles increased as the roughness increases from very low values (a 'smooth' glass plate), reaching a peak for wavelengths in the range of 6 - 12 μm (spacing of asperities is approximately twice their height, see *Table 5.1*). This is approximately the diameter of the toe pad epithelial cells, which are separated from each other by deep channels. This strongly suggests interlocking of the epithelial cells with the asperities on the surface. For larger roughnesses (particle sizes greater than 100 μm), slip angles are well below the values obtained on the smooth surface. Even though the pad material is very soft (see later for calculations of the effective elastic modulus), the area of close contact is likely to be reduced with particle sizes as large as this, inevitably leading to reductions in the friction forces that the frogs can generate. Even though it is unknown whether the pad makes full contact on the smaller scale roughness, it is conceivable that the comparatively large valleys on the larger rough surfaces will result in large areas where direct (or close to direct) contact will not occur, and therefore less frictional force.

For fall angles, the pattern of response shows many similarities with slip angle values. Fall angles were significantly higher on the 3 μm (wavelength of 6 μm) surface compared to the smooth surface, but were significantly lower for the larger particle sizes (esp. wavelengths in the 120-850 μm range). These reductions may be due to loss of close contact and the presence of gaps in the fluid (seen with larger beads in the IRM experiments), as well as a reduction in friction forces. As described above, the last of these possibilities would lead to sliding, which would cause an increase in the pad/surface angle with a concomitant reduction in adhesion (Kendall 1975). Interestingly on the largest asperities tested (the 562.5 μm beads surface) the frogs began to recover adhesive ability. This could be due to the beads being within the range of entire pad size; therefore close contact could be made by the whole toe pad on the bead. This was seen in geckos, where adhesive forces on larger roughnesses were high, due to contact area of spatulae being restored on each asperity (Huber, Gorb *et al.* 2007). The geometry of the beaded surface was also different from the sandpaper surfaces, with the beads providing a smooth surface (on each bead) for the pads to stick effectively, while other surfaces are likely to have roughness on several different length scales.

As well as these tilting experiments on a dry board, experiments were also carried out with water present on the glass surface and the 58.5 μm surface (on which both slip and fall angles were low). This resulted in a dramatic change in the frog's abilities. Compared to the dry surface, slip angles and to a lesser extent fall angles were reduced on the glass surface, but greatly increased on the rough surface. The extra fluid led to reduced friction on the smooth surface, since the extra fluid would have reduced the ability of the pad to make contact with the glass plate. Conversely, on the rough surface the extra fluid played a positive role, since now there was enough fluid between the pad and the surface for contact without any air pockets. This supports the conclusion that the presence of air pockets was one of the causes of low adhesion on rougher surfaces.

5.4.3. Single pad force measurements

On the resin replicas, increasing roughness increased friction by a factor of at least 3 on all rough surfaces tested, with a peak (approx. 6-fold increase in friction) at 12 μm (assuming spacing of asperities is approximately twice their height). This is in the range of the diameter of the toe pad epithelial cells (approx. 10 μm) and strongly suggests that the large friction increase was due to interlocking of the tips of the asperities with the channels (~1 - 2 μm wide) that separate the epithelial cells. In fact, in the IRM experiments, often the smallest beads used (< 3 μm diameter) would get stuck within the channels which separate the cells (*Figure 5.16*). This provides evidence that small asperities can interdigitate with the pad. With the larger roughnesses tested, interlocking effects are lower, but still higher than on a smooth surface. Though toe pads being very soft (Barnes, Goodwyn *et al.* 2011) use area-based 'rubber' friction, it does appear that friction can still be increased when rough surfaces are present. On the PDMS surfaces where the only variable is the spacing of the pillars, the increase in friction force occurred where gaps between asperities was in range 2 - 5 μm . This is at a lower spacing than the peak increase seen for the resin surfaces. Although smaller than the diameter of the epithelial cells (~10 μm), it is an appropriate size for interdigitation of the surface pillars (2 μm

diameter) and the channels between the cells. Although interdigitation is unlikely to be the sole explanation for the increase in forces (see further on in the discussion), it could be that it plays an important role in production of frictional forces on surfaces. Interlocking has also been seen in the euplantulae of stick insects, which consist of frictional ridges (Clemente, Dirks *et al.* 2009).

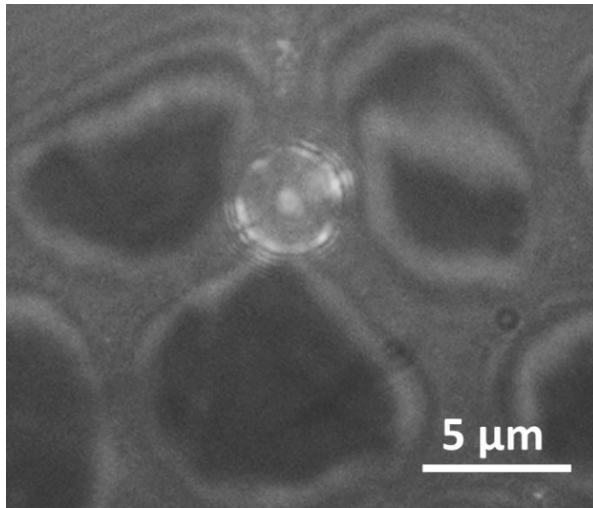


Figure 5.16: IRM image of a small glass bead (diameter 2.6 μm) getting stuck within the channels found between the cells.

As with the tilting experiment, the adhesive forces decreased on the larger roughnesses (58.5 and 100 μm), which is likely due to the large asperities meaning that close conformity of the pad could not occur, and the relatively large valleys on the surface draining away fluid from the contact zone or be too big to be filled by the volume of fluid available (and without the fluid layer adhesive forces would be negligible). There was an increase in adhesion for the fine resin surfaces at low roughnesses. On the PDMS surfaces, gaps in the range 2 - 5 μm again increased adhesion. These results are surprising, and require further investigation. Capillary forces should not increase on a rough surface, and a reduction in close contact should significantly reduce any adhesion component from van der Waals forces. The improved adhesive performance of the pad on smaller roughnesses could be attributed to the viscoelastic nature of the pads (although viscoelasticity is time dependent, which was not tested here but could play a role), which would allow them to conform to the rough surfaces (Persson 2007). This would result in an increase of the contact area (not the

perceived contact area, but the actual contact area on a micro-scale), and the increase in contact area should result in increased adhesive forces. Another explanation for the increase in adhesive forces could be the hydrodynamic forces. Although toe pad fluid is not very viscous (Federle, Barnes *et al.* 2006), the amount of fluid can be small and channel pathways can be long. It is possible that the presence of small-scale asperities increases still further the resistance to fluid flow. A test of whether this is a factor would be to test the effect of pull-off velocity on adhesion. Effects on capillary forces should be negligible, but the effect on time-dependant hydrodynamic forces much greater. Future work will hopefully provide useful insights into the different components of tree frog adhesion. Interestingly, Tulchinsky and Gat (2015, currently under consideration) proposes that interactions between viscosity and elasticity may play an important role in tree frog adhesion, but the predictions remain to be tested.

The results showed some variation between the whole animal and the single toe pad experiments. Varying the separation speed of two surfaces would affect how the fluid flows between them, which would affect the adhesive forces (Persson 2007), so it could be possible that the separation speed in the force measurement experiments differed from the separation in a climbing frog, and therefore could be increasing the adhesive forces seen in the force measuring experiments. However, this has not been tested here, and would need further experimentation to improve our understanding of this.

5.4.4. The role of fluid

As the frogs' sticking ability is reliant on wet adhesive forces such as capillary forces, the fluid layer beneath the pad in contact with the surface is key to how effectively tree frogs can climb. On rough surfaces, we see poor performance on the larger asperities tested ($> 50 \mu\text{m}$), while on smaller roughnesses ($< 10 \mu\text{m}$) the adhesive and friction forces actually show higher levels compared to the adhesion on smooth surfaces. IRM showed that within the proximity of a large asperity, the pad fluid failed to fill the gap between the pad and the surface. It appears that poor climbing performance of the frogs on rough surfaces is due to pad fluid either being lost to the surface, or not being a sufficient volume to fill

the gaps and adhere (Figure 5.17). This is reinforced by the tilting experiment where water was added to the rough surface, and the frogs showed a much improved performance than when the surface was dry. This would also explain why on PDMS surfaces there is no drop in performance, as gaps between the bumps are likely not to be big enough in volume to drain fluid from the contact area (though from the images from this experiment the difference between full and partial contact could not be seen).

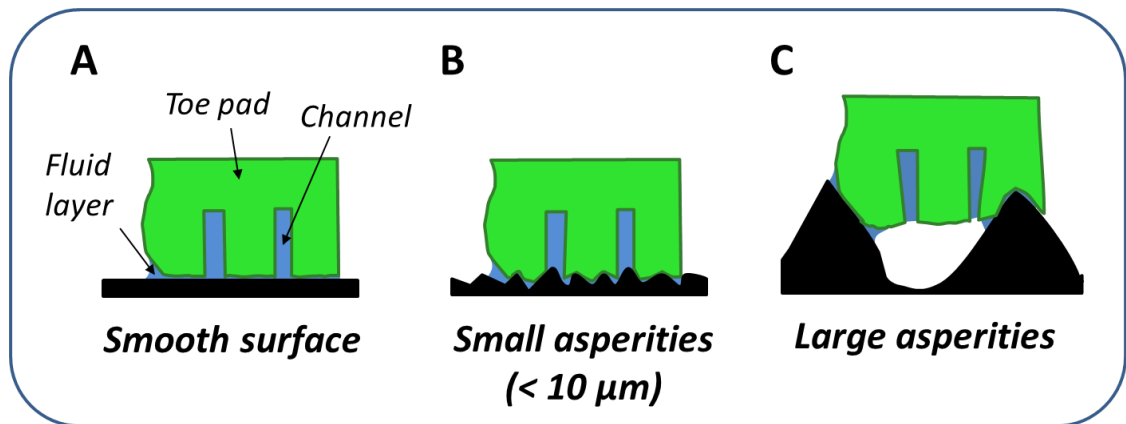


Figure 5.17: simplified diagram predicting toe pad contact on different rough surfaces. Contact on a smooth surface (A) is shown, along with the pads conformity to smaller roughnesses (B) and larger asperities (C).

The tilting experiments from the torrent frog study (see previous chapter (Endlein, Barnes *et al.* 2013)) revealed a similar result, with the increase in roughness leading to less adhesive force under dry conditions. The addition of water (at a low flow rate) led to an improved adhesive performance by the frogs in those experiments. Despite pad fluid probably having a slightly higher viscosity to water (Federle, Barnes *et al.* 2006), it seems that excess water on a rough surface can help the frogs to stick by fulfilling the role the pad fluid has in wet adhesion by providing additional to fluid to fill the gaps in the pad area which would normally not have enough fluid to form a continuous fluid layer. The pad sporadically produces its secretions from pores located on the pad surface. The strongest forces will be produced when this fluid layer is kept ultra-thin; however, there will still be significant forces being produced even if close contact is not maintained while fluid is present. However, excess fluid on a smooth surface results in frogs producing no friction and slipping easily from a surface. There must therefore be a fine balance for frogs with the volume of pad

fluid they produce which will work effectively on a consistent level whilst climbing on all varieties of surfaces. It is unclear how the fluid productions by the pores is controlled in frogs, but as fluid is often left behind in steps (Crawford, Endlein *et al.* 2012) it must have to be replenished frequently. The fluid level within the contact area could also be controlled by changing the channel size and width (which is perceivable due to the soft nature of the pad), but is not fully understood at the moment.

5.4.5. Surface contact on a rough surface

Previous studies have shown that the pad acts as a highly soft material, even if the different layers of the pad are varying in stiffness (Barnes, Baum *et al.* 2013). The IRM studies shown here have also indicated that the pads are highly deformable. The pads were able to conform well to the asperities on the surface, by curving down to fill the gap between the pad and the surface by moulding to the surface. If the pad was stiffer, then direct contact of the pad on the surface would occur further away from the asperity, which would mean less overall close contact. The strongest adhesive forces will occur when the fluid layer between the pads is ultra-thin, and a conforming pad helps this to occur. Federle *et al.* (Federle, Barnes *et al.* 2006) showed that the top of the cells come into close (possibly direct) contact with the surface, and creating high friction forces - a soft pad aids in achieving this contact. The presence of the channels and grooves will also help in making the pad a highly conforming surface (Persson 2007). As the asperity size increased, the pad is less able to conform to the surface, which could result in a poorer adhesive performance (as was indeed seen for the larger roughnesses in the tilting experiment). With the pad acting in such a way, this allows it to form “full” contact with the surface (coming into direct contact between asperities) - with larger asperities leading to greater distances until the pad is in contact (and is similar to what was shown by Zhou *et al.* (Zhou, Robinson *et al.* 2014)).

5.4.6. Comparing performance with other climbing organisms

Several other studies have looked at the effect of surface roughness on the climbing capabilities of other adhesive pad bearing organisms. Variations between species, size and adhesive systems mean that it is useful to compare the performances seen.

Many climbing organisms utilise claws to climb on rough surfaces, which can interlock with asperities on vertical surfaces - this is seen in geckos (Zani 2000), spiders (Kesel, Martin *et al.* 2003) and many insects (Dai, Gorb *et al.* 2002, Bullock and Federle 2011). However the effectiveness of a claw is usually dependent on the asperity size being larger than the claw tip diameter (Labonte and Federle 2015). When the claws fail to interlock on the surface, staying attached relies on the adhesive pads of the organism (Endlein and Federle 2008). The setae hairs of geckos are built so that they can adapt (acting like a soft material) and conform on rough surfaces of different length scales. Their setae work least effectively on surfaces where spatula tip contact area is split (100 to 300 nm roughness) and therefore the geckos cannot climb as effectively (Huber, Gorb *et al.* 2007). Traction experiments in spiders yielded a similar result, with their adhesive hairs performing poorly when asperity sizes were 0.3 and 1 μm (Wolff and Gorb 2012). In these studies, it is unclear whether the larger roughness surfaces also exhibited a smaller scale roughness too, but this was not seen in the results. Several insect studies relate their abilities to an interaction with a specific plant (such as a pitcher plant (Bauer, Scharmann *et al.* 2012), while others are testing on surfaces mimicking the ridges (Voigt, Schweikart *et al.* 2012) or bumps found on plant surfaces in general (Prum, Seidel *et al.* 2011, Prum, Bohn *et al.* 2013). Zhou *et al.* (Zhou, Robinson *et al.* 2014) tested insect pads on surfaces with controlled roughness parameters (the height diameter and space between asperities), and found that the density of asperities affect whether the pads made full or partial contact with the surface (which could not be determined in the tree frog studies above). Many studies tested the combined abilities of claws and adhesive pads (Endlein and Federle 2008, Bullock and Federle 2011, Busshardt and Gorb 2014) on rough surfaces, with pads playing a role when claws fail to attach (Endlein and Federle 2008). Insect pads are either made from hairy fibres or soft smooth cuticle (Beutel and Gorb 2001), and so

both can deform on rough surfaces. The pads also produce a fluid, which will help to fill gaps on the surface as with frogs. Kovalev *et al.* found in flies a decrease in friction forces on rough surfaces, and hypothesised that this was due to fluid being lost to the surface (Kovalev, Filippov *et al.* 2013).

5.5. Conclusions

This study has shown a complex relationship between the efficiency of tree frogs' toe pads and the roughness of a surface, with fluid loss and the pads' softness both playing a role in how well the frogs can stick. Despite the limitations of the frogs seen in this study, their adhesive system is still highly adaptable, as the pads abilities are combined with additional climbing behaviours which will aid the climbing of rough surfaces in the wild (these include grasping (Herrel, Perrenoud *et al.* 2013) and readjusting (Endlein, Ji *et al.* 2013) behaviours). Surfaces mimicking toe pads show similar performances on rough surfaces (Wang, He *et al.* 2012). The specialised polygonal structures and the soft nature of the toe pad produce friction on rough surfaces, which can provide inspiration for adhesives which would maintain adhesive and/or frictional force on rough surfaces which could inhibit traditional adhesives. As most surfaces exhibit some degree of roughness, the continued study of how animals with adhesive pads can climb these surfaces can only aid the development of adaptable adhesive surfaces.

6. The effect of 'wettability' of surfaces on the adhesive abilities of tree frog toe pads

This chapter comprises of some experiments conducted solely by the author, and experiments done in conjunction with Thomas Endlein, Eraqi Khannoon and Jon Barnes.

Summary

Hydrophobic surfaces (such as waxy leaves) are commonly found where tree frogs can be found resting - but it is unclear how their pads adhere to such surfaces when their adhesion is based on capillary forces coming from a watery fluid. Here, the adhesive abilities of single toe pads were tested using force measurements. I could show that tree frogs pads can stick just as effectively on hydrophobic and hydrophilic surfaces, as adhesive and friction forces measured on both surfaces were similar. The properties of the toe pad fluid were also studied, where contact angles of the fluid on hydrophobic surfaces were measured using a standard goniometer but also by reconstructing the shape of the fluid droplets left behind on the surface after a step using Interference Reflection Microscopy. These techniques revealed that the fluid maintained low contact angles on hydrophobic surfaces (unlike water which exhibits high contact angles), which indicates the presence of molecules which aid in wetting low energy surfaces.

6.1. Introduction

Natural surfaces display a wide range of surface energies. The surface energy of a material is defined as the excess energy that exists at the surface of the material compared to the bulk. As the molecules on the periphery of a material are not surrounded on all sides by molecules, there is a net inward cohesive force, known as the surface tension. A surface is termed 'hydrophilic' if the contact angle of a water droplet is $<90^\circ$ and wetting. Surfaces which are non-wetting have a contact angle that is $>90^\circ$ are labelled 'hydrophobic'. Surfaces with a low surface energy tend to show hydrophobic properties, while high surface energies exhibit hydrophilic properties. Whether a surface is wettable or not is largely dependent not only on the surface energy of the surface material, but also the micro- or nano-topography of the surface (Guo and Liu 2007). A well-documented example of this in nature is the surface of the leaves of the lotus plant, which possesses a micro-scale roughness combined with an epicuticular waxy surface. This gives the surface 'superhydrophobic' properties, causing water to 'bead up' and roll off the surface, thus aiding in cleaning the leaf surface (Neinhuis and Barthlott 1997). AFM studies on superhydrophobic

surfaces have shown that adhesive and friction forces are reduced due to this state (Burton and Bhushan 2006). Many plants also possess waxy cuticles to reduce water loss from the leaf surface (Schönherr 1982). Conversely, most other surfaces in a tree frog's habitat (e.g. rock surfaces) are probably hydrophilic. In rare cases, some plant surfaces can exhibit a highly hydrophilic state, for example used by pitcher plants to create a slippery surface to trap insects (Bauer, Scharmann *et al.* 2012). This huge variation in surface properties presents a significant challenge to the functioning of the adhesive systems of climbing animals.

Studies on geckos have shown that they cannot adhere to Polytetrafluoroethylene (PTFE) (Autumn and Peattie 2002). These surfaces have few/no polar groups (i.e. no electric charges on their surface, polarity is caused by the pull of electrons to one part of the surface), and gecko adhesion (thought to be caused by van der Waal forces) is reliant on some degree of polarity in order for van der Waals forces to form with the nanoscopic setae of their feet (Autumn and Peattie 2002). However, geckos have been shown to be able to stick to some hydrophobic surfaces - which could be an indicator for other adhesive forces such as capillarity playing a role (Autumn, Sitti *et al.* 2002). A recent study combining the effects of fluid presence and wettability of surfaces found that geckos can stick better to a hydrophobic surface if water is present, while water on a hydrophilic surface led to decreased adhesive ability (Stark, Badge *et al.* 2013). The adhesive pads of dock beetles show a reduction in forces on hydrophobic surfaces, and when combined with a micro-rough pattern the beetles showed a fourfold reduction in forces (Gorb and Gorb 2009). Low energy surfaces can also affect the self-cleaning properties of insect pads, where for some ant and beetle species self-cleaning of the pads takes longer on low energy surfaces, meaning that the pads would not stick as effectively (Orchard, Kohonen *et al.* 2012). Plants such as *Macaranga* utilise loose waxy particulates which also exhibit hydrophobic properties to create slippery surfaces that prevent all insects (with the exception of one ant species of the genus *Crematogaster* and *Camponotus*) to climb their stems (Whitney and Federle 2013). Therefore it seems that in general lower energy surfaces have a negative effect on climbing organisms, which cannot climb as effectively.

For tree frogs, which use a wet adhesive system akin to some insects for climbing, there is to date no published data on their performance on hydrophobic/hydrophilic surfaces (although there has been some initial tests of tree frogs' performance on different plant leaves with unpublished data by Casey and Barnes, 2004). As the frogs use wet adhesion to stick to surfaces, in theory one would assume that frogs would not be able to stick effectively. Wet adhesion relies on the fluid being able to wet a surface (via surface tension, see *Equation 1*) to produce adhesive force, and if the fluid was to be repelled by the surface then capillary forces caused by surface tension could not occur. This then depends on the composition of the pad secretions, as fluids which contain other components from water may aid the spread of the fluid on a surface and therefore the adhesive ability of the pad. Although the varying skin secretions of different species of frog have been studied in many individual cases (Clarke 1997), it is unknown how much toe pad secretions differ between species. Initial studies of the secretions of tree frogs (unpublished data from Eraqi Khannoon) indicate that they contain amphipathic lipid components which would behave as surfactants; the presence of a hydrophilic head and a hydrophobic tail in the toe pad fluid could change the fluid properties by lowering the contact angle, thus potentially aiding adhesion on surfaces which usually would not exhibit the spread of fluids by displaying high contact angles. The fluid produced by insects' pads contains both an oil and aqueous solution (Dirks, Clemente *et al.* 2010), which help to produce frictional force on smooth surfaces, but it is unknown if it plays a role in the 'wetting' of hydrophobic surfaces. The continuous oily phase is likely to wet both hydrophilic and hydrophobic surfaces effectively.

The aim of this study was to test the effect that surface energy has on tree frog adhesion. This was done by testing the forces produced by individual toe pads on and hydrophilic and hydrophobic surfaces, and measuring the wetting properties (i.e. the contact angles) of the toe pad fluid on these same surfaces. As tree frogs use wet adhesion as their principal mechanism for climbing, the assumption would be that tree frogs should struggle to produce adhesive forces on hydrophobic surfaces if the fluid they use is on the whole a watery solution (Federle, Barnes *et al.* 2006); water forms a high contact angle on hydrophobic

surfaces, which would cause the meniscus around the edge of the pad contact area to change from being convex to concave. This would mean that internal forces would pull inward rather than outward, and the pad is likely to lose surface tension and therefore capillary forces necessary for wet adhesion to be effective (although Stefan adhesion could still play a role). However, the fluid could be comprised of chemicals which could aid wet adhesion by reducing the contact angle on surfaces of low surface energies; this would allow frogs to be able to stick.

6.2. Materials and methods

6.2.1. Frog species used for experiments

Two species of tree frogs were used for this study; the Cuban tree frog, *Osteopilus septentrionalis* ($n = 4$; mass \pm S.D. = 12.5 ± 8.6 g, snout-vent length = 54.5 ± 8.4 mm) and the Whites tree frog *Litoria caerulea* which has been used in the studies in previous chapters ($n = 6$; mass \pm S.D. = 18.3 ± 8.6 g, snout-vent length = 57.5 ± 8.1 mm). Tree frog secretions may vary greatly between species, and so studying two different species meant that potential variations in toe pad secretions and performance between these two species could be viewed. The frogs were weighed and measured prior to experiment, and before each trial the frogs were cleaned; the pads were cleaned in water, but frogs were not experimented on immediately - they were contained in a plastic container for a short period of time. This way any excess water shouldn't dilute or affect the pad secretions.

6.2.2. Surfaces tested

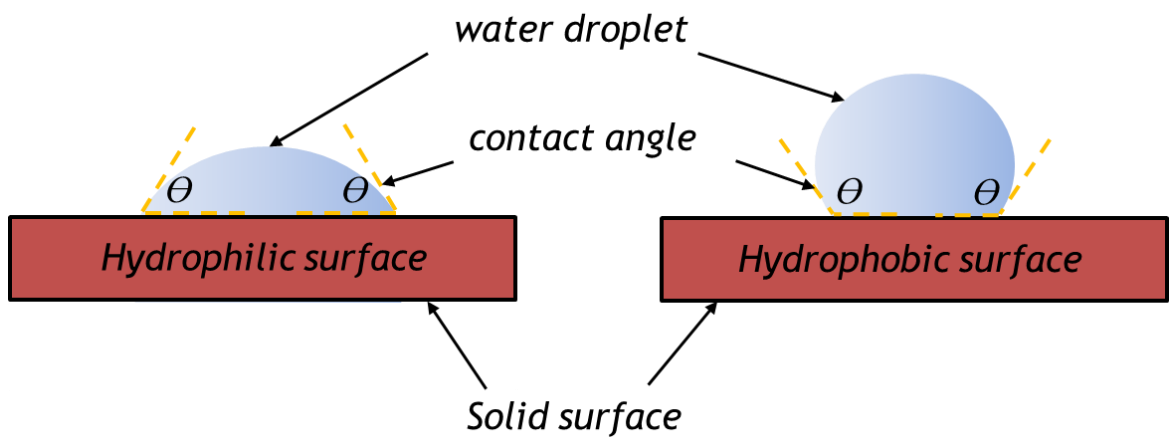


Figure 6.1: Examples of contact angles of water on different solid surfaces. On a hydrophilic surface (left), the water forms low contact angles ($<90^\circ$). On a hydrophobic surface (right), water has a high angle of contact ($>90^\circ$), and so the water balls up on the surface.

In order to test how well frogs can adhere to hydrophilic and hydrophobic surfaces, experiments were conducted on surfaces which exhibited those properties. On hydrophilic surfaces (in air), water will form a layer of fluid where the contact angle at the edge of the fluid will be less than 90° , which indicates that the surface is ‘wetable’ by water (Figure 6.1). Conversely, on a hydrophobic surface the angle of contact will be greater than 90° , as the fluid attempts to make less contact with the surface by beading up.

All of the following experiments involved testing on hydrophilic and hydrophobic surfaces for comparison - the contact angles of water on each surface are shown in Figure 6.2. In this study, glass was used as the hydrophilic surfaces (either as glass cover slips or glass slides). Glass is naturally hydrophilic, and the contact angle of water was measured as $55.8 \pm 4.1^\circ$ ($n = 6$ different droplets) when tested using a goniometer (CAM100, KSV Instruments, Helsinki, Finland). As an opposing hydrophobic surface, specially manufactured surfaces were kindly provided by David Labonte (Dept. of Zoology, Cambridge University). These surfaces consisted of a self-assembled monolayer (SAM), on top of a glass cover slip (20 x 60 mm). The SAM used in this study is Octadecyltrichlorosilane (OTS), which is made up of 3 connected groups - $\text{CH}_3 - (\text{CH}_2)_{17} - \text{SiCl}_3$. The methyl $-\text{CH}_3$ tail group provides the desired hydrophobic nature, the $-\text{SiCl}_3$ end binds with

the surface of the glass and the middle $-CH_2$ section connects the two other groups and is important for alignment; this allows a monolayer of the OTS to be formed across the cover slip. Once the molecule is bound to the glass surface, the silanized surface is highly stable which means it can retain its hydrophobic properties against abrasion and most cleaning solvents, and over time when stored in air. The surfaces are formed by exposing cleaned glass cover slips to oxygen plasma treatment, before being submerged in a solution of 1 mM OTS in Toluene. This provided the hydrophobic surface used in this study; contact angles of water on the OTS surface were measured as $111.2 \pm 10.2^\circ$ ($n = 6$) with the goniometer in these preliminary trials.

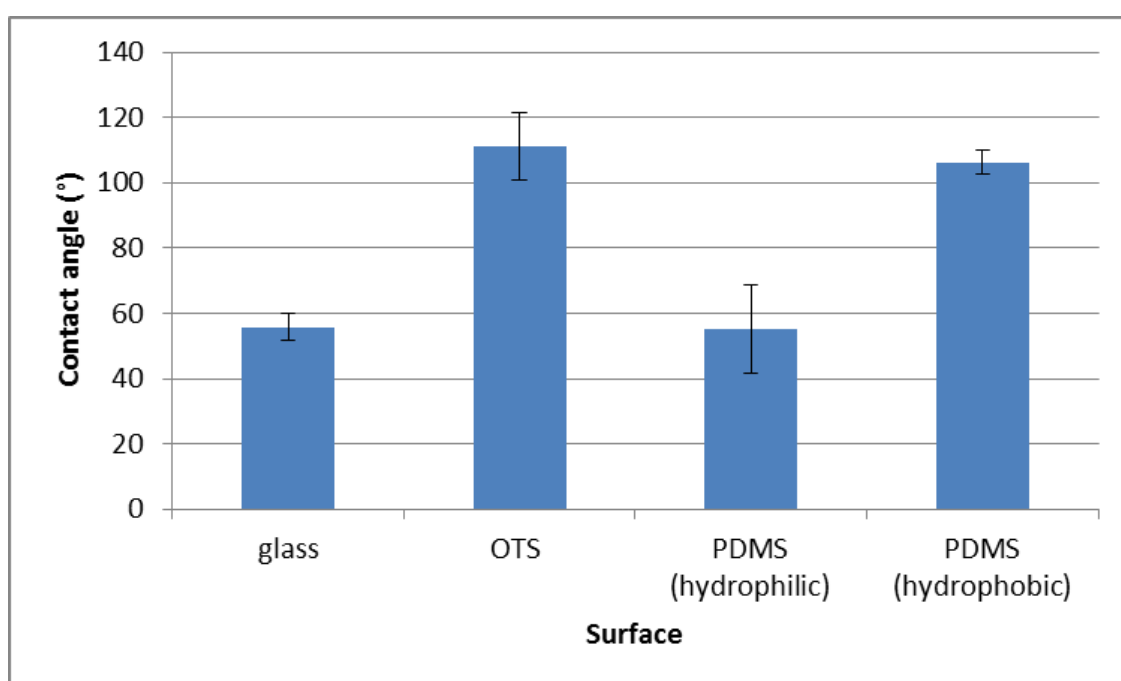


Figure 6.2: Contact angle measurements of water on varying surfaces ($n = 6$), measured using a goniometer. Bars show mean values, and whiskers represent the standard deviation.

For the force measurements described below, a further pair of surfaces was tested. These surfaces were made from PDMS, which in its natural state is hydrophobic (using water in the goniometer, it produced contact angles of $106.3 \pm 3.7^\circ$). PDMS can be temporarily changed (for roughly 2 hours) into a hydrophilic surface by plasma cleaning; the PDMS was placed in a plasma cleaner (Harrick plasma, NY, USA), which formed Si-OH bonds on the surface of the PDMS and therefore turned the surface hydrophilic (mean contact angle of

water, $55.1 \pm 13.5^\circ$, within an hour after plasma treatment). PDMS surfaces were tested due to the material being used in studies in previous chapters (meaning force measurements are comparable), and using PDMS also allows the exact same surface to be tested in a hydrophobic and hydrophilic state (whereas with the OTS and glass tests, they are two separate surfaces). Using both sets of surfaces helped to confirm the effects of hydrophobic surfaces on adhesive and friction forces.

6.2.3. Force per unit area measurements

Force measurements (for adhesive and frictional forces) for the individual toe pads of both frog species were collected using the force plate setup used previously and described in the methods chapter. The OTS and glass surfaces could be attached by simply gluing them to the bending beam (as the usual glass or plastic surfaces are attached). For testing the PDMS surfaces, they were attached to the beam as described in the rough surface tests (using a polyethylene surface with a small hole drilled in the middle to view contact area). The PDMS is formed by thoroughly mixing the elastomer (Sylgard 184 Elastomer, Dow Corning, UK) and hardener (to a 10:1 ratio) before putting the mix into a depressurisation chamber to remove any bubbles. The mix is then poured onto a flat glass surface (within a petri dish), and cured in an oven at 60°C for 1 hour. The sample can then be cut out using a scalpel (1cm x 1 cm, 3 mm in thickness), and used for experimenting.

As described before in the general methods chapter, the frogs were contained within a petri-dish while one leg protruded from an opening in the petri dish lid - this allowed for one single toe pad to be in contact with the plate at a time. Using a LabView program which utilises force feedback, a set of movements were controlled by the motorised stage and the computer. The pad was initially brought into contact with the attached surface (with the force plate keeping a constant load of 2 mN), and was then dragged along the surface (in a proximal to distal direction for the pad) in order to measure the frictional forces produced (drag speed was 1 mm s^{-1} for 5 mm). The pad was then pulled perpendicularly from the surface (at a constant speed of 0.4 mm s^{-1}) to measure the adhesive

forces of the pad. This program of movements (the same as the one used in the rough surface experiments in chapter 5) were used for all surfaces tested and for both species of frog. The area of pad in contact was also measured using a camera attached to a microscope with built-in illumination. This allowed for the force per unit area (or stress) to be calculated (mN/mm^2 or kPa) for each surface for comparison.

6.2.4. Contact angle measurements using goniometer

A goniometer (CAM100, KSV Instruments, Helsinki, Finland) was used to conduct a series of contact angle measurements (*Figure 6.3*), incorporating the footprints of both tree frogs on the hydrophobic OTS surfaces. Firstly, the contact angle of a distilled water droplet (as a control) on a clean OTS surface was measured. A single toe pad of a frog is then brought into contact with the surface (by holding the frog and repeatedly placing the toe pad onto the surface by hand until a well-established footprint is seen), so that some of the toe pad secretions are left behind in footprints on the OTS surface. The contact angle measurement is then repeated in the same location as the footprints (which has quickly evaporated from the surface), again using water. The contact angles measured before and after the footprints could then be compared.

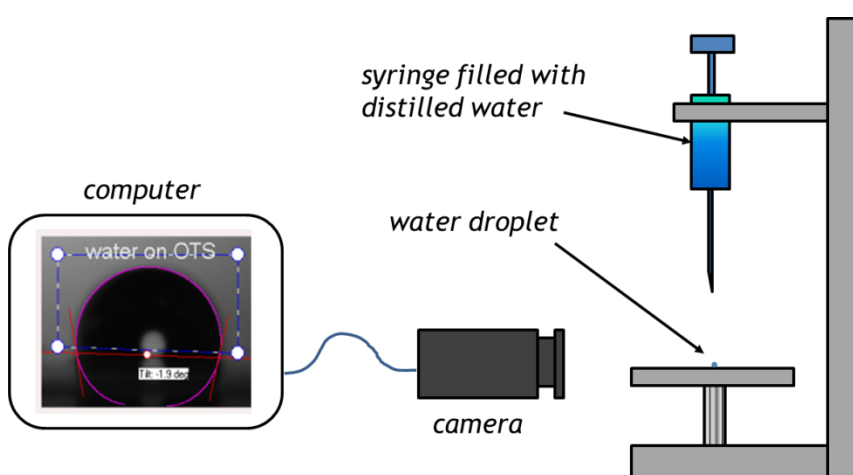


Figure 6.3: diagram showing the setup for the goniometer. A fixed volume of fluid (usually distilled water) is deposited onto the surface using the mounted syringe. The camera will take a photo immediately after the fluid is on the surface. The contact angles on each side of the fluid are calculated using the built-in program (CAM100 optical contact angle measurer version 2 1.1, KSV Instruments, Helsinki, Finland), and a mean contact angle is given.

A slight variation on this experimental procedure was also conducted, to help determine if the secretions simply coat the surface or whether they can dissolve into the fluid. In this variation, after the frog has had its toe pad dabbed on the OTS surface, water is then dropped onto the surface. The water is then mixed with the footprints (using a dissecting needle), before being drawn into the syringe. This water/secretion mix is then deposited in a new location on the OTS surface (away from the site of the footprint), and the contact angle was measured. These experiments would help to determine whether there were chemicals present in the pad secretions which could dissolve in water and aid wet adhesion by reducing the contact angle. Such substances would be acting as surfactants.

6.2.5. Contact angle measurements of 'footprint' fluid droplets

Having previously been used to visualise the contact of the toe pad cells on surfaces (Federle, Barnes *et al.* 2006) (see also chapter 5), IRM was used to reconstruct the shape of the droplets left behind after the frog has taken a step in order to measure the contact angle. As the fluid left behind by the toe pad is in very low quantities as small droplets, measurement of the contact angle using the goniometer was not possible. IRM was an alternative method to see the contact angle of the fluid as the pad was removed from the surface. The fluid evaporated from the surface very quickly after the frog had taken a step, therefore using IRM with a high-speed camera allowed the receding contact angle of the fluid to be measured as the fluid evaporated (in contrast, measurements using the goniometer are usually close to the advancing angle). A more detailed description of the principles of IRM can be found in the methods section of chapter 5. For this study, an inverted compound microscope was used (Zeiss Axiovert 25, Zeiss Instruments, Jena, Austria; x 100 magnification); monochromatic light interference and a customised pinhole slider were used to produce the characteristic interference fringes. As the fluid slopes away from the surface in contact, black and white fringes are formed, showing an increase in the distance of the fluid surface from the substrate surface (approximately 0.1 μm for each band). When fluids are in contact with a surface, it forms a

contact angle with the surface which depends on the surface energy. If the surface shows hydrophilic tendencies, then the contact angle of water will be low and therefore the fringes can be seen by IRM from below. Narrow and closely packed light and dark fringes indicate a steep angle, while wide fringes indicate a low contact angle of the fluid on the surface. On hydrophobic surfaces water will produce high contact angles, and therefore the contact angle and slope of the water would not be visible by IRM (i.e. the IRM method is limited to small contact angles less than 40°). This principle can then be applied to the toe pad secretion on the hydrophobic OTS surface. The frogs took a step on the OTS surface, and the footprint left behind tiny volumes of secretion, which evaporated very quickly (usually within a few seconds; it varies depending on how much fluid is left). Using a high speed camera (Basler, Ahrensburg, Germany), the contact angles of the secretion as it evaporates from the OTS surface can be measured by measuring the distance between the fringes of the fluid as it slopes away from the surface. This can then be compared to the contact angles of a) the toe pad secretion on glass, and b) distilled water on glass (which should exhibit a hydrophilic behaviour). Ideally, it would be useful to also measure the contact angles of water on the OTS surface, but as this produces a contact angle above 90° , this is not measurable by IRM. Videos of the fluid were recorded at a high speed of 30 frames per second, and the contact angles were calculated using a customised Matlab script (Mathworks, Natick, USA).

6.2.6. Statistics

All collected data was tested for normality using the Lilliefors test, which is based on the Kolmogorov-Smirnov test. The force data for both species on both surfaces were tested using either a student's *t*-test or a Wilcoxon rank sum test (also known as a Mann-Whitney *U* test), depending on normality. The same tests were also used for the IRM experiments. For the goniometer contact angle experiments, paired *t*-tests and the Wilcoxon signed rank test were used for comparing contact angles measured immediately after each other on the same surface. Value ranges are written as means \pm standard deviation. All statistical analysis was done using the statistical toolbox in Matlab (r2011a).

6.3. Results

6.3.1. Force measurements of single toe pads

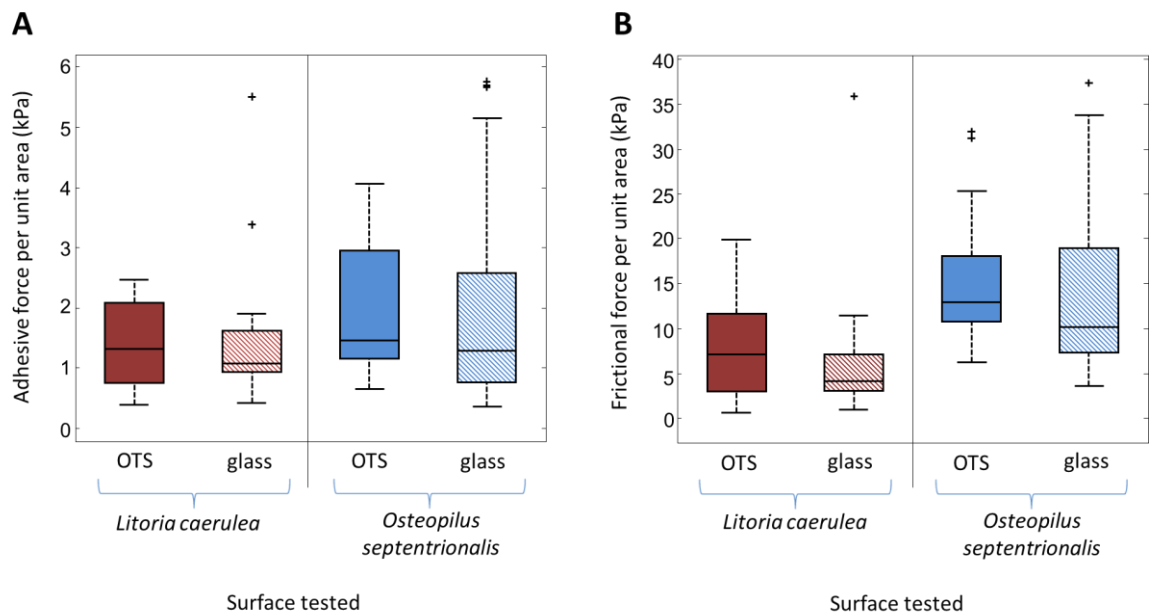


Figure 6.4: Boxplots showing the force per unit area generated by single toe pads on OTS (solid boxes) and glass (striped boxes). Graph A shows the adhesive force per unit area (kPa), and graph B shows the frictional force per unit area. Data for *Litoria caerulea* is shown in red, and *Osteopilus septentrionalis* in blue. The two surfaces tested (OTS and glass) are labelled beneath the appropriate data set. Boxes denote 25th and 75th percentiles, the whiskers display 99% of the data, the middle line shows the median and outliers are shown as +.

The force per unit area (adhesive and frictional) produced by a tree frogs toe pad in contact with surfaces of varying surface energies were measured and analysed ($n = 30$). A comparison between forces measured on OTS and glass for both species is shown in Figure 6.4. For adhesive forces (Figure 6.4A), both the *Litoria* and the *Osteopilus* showed highly equivalent stress measurements between the OTS and the glass surfaces. Due to this, statistical comparison failed to show any difference between the two, for both the *Litoria* ($z = 0.5544$, $p = 0.5793$) and the *Osteopilus* ($z = -1.4415$, $p = 0.1494$).

For frictional force per unit areas measured on OTS and glass (Figure 6.4B), the values are very similar within each species. Statistical tests failed to find significant difference between the two surfaces for either species (*Litoria*: $z = 1.5598$, $p = 0.1188$. *Osteopilus*: $z = -1.0571$, $p = 0.2905$). Thus, the forces

produced by both species on glass are comparable with those measured on a hydrophobic OTS surface.

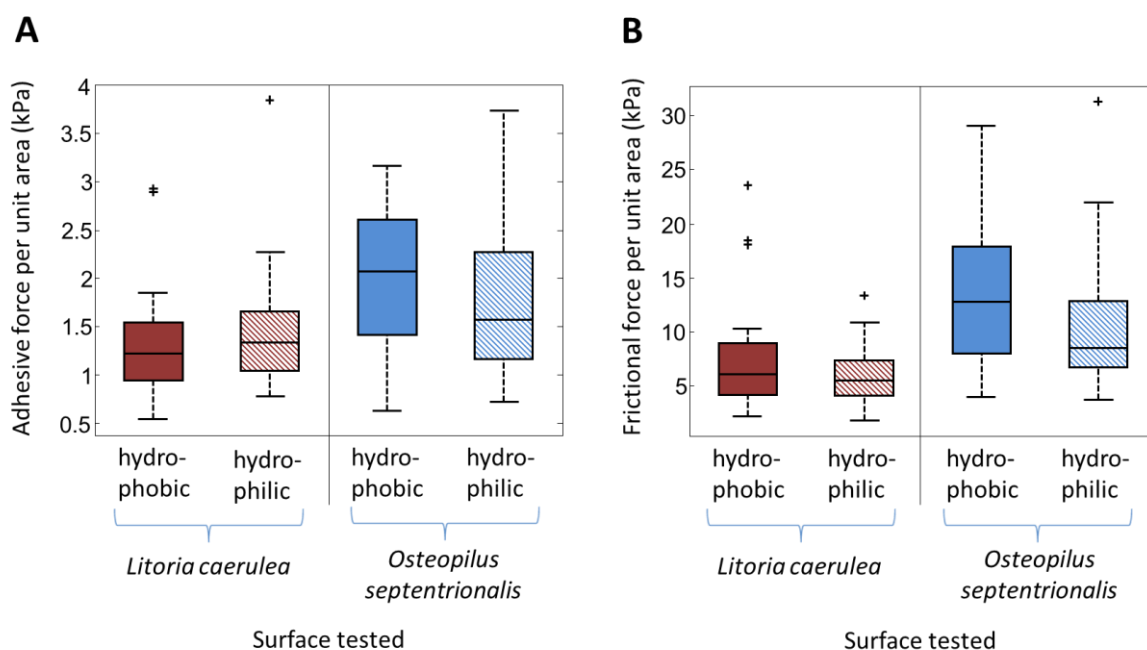


Figure 6.5: Boxplots showing the forces generated by single toe pads on PDMS with differing surface energies. Graph A shows the adhesive force per unit area (kPa), and graph B shows the frictional force per unit area. Data for *Litoria caerulea* is shown in red, and *Osteopilus septentrionalis* in blue. The two surfaces tested (hydrophobic and hydrophilic PDMS) are labelled beneath the appropriate data set. Other details are as in Figure 6.4.

The same protocol was used for surfaces made from PDMS, which is hydrophobic in nature but can be made hydrophilic using plasma cleaning (see Figure 6.2). The results for the adhesive and frictional stresses on both surfaces and for both species are plotted together in Figure 6.5 ($n = 30$). Forces per unit area measurements were highly similar to the values in the OTS/glass experiments. There was no significant difference in adhesive forces (for either species) between the two surfaces, as seen in Figure 6.5A (*Litoria*: $z = 0.9979$, $p = 0.3183$; *Osteopilus*: $z = -1.1458$, $p = 0.2519$). The same was true for the frictional force per unit areas tested (Figure 6.5B), with no significant difference seen in the *Litoria* measurements ($z = -0.5248$, $p = 0.5997$) and the *Osteopilus* measurements ($z = -1.7224$, $p = 0.085$).

For all of the force measurements, there was no significant difference between the performances on the hydrophobic surface and on the hydrophilic surfaces; the only pair which come close to testable variance is the friction values from *Osteopilus* on the PDMS surfaces. Although one cannot make full conclusions from the lack of statistical significance (all that can be said is that there has been a failure to show any significant difference), the data indicates that tree frogs can stick just as effectively on a hydrophobic surface as on a hydrophilic surface.

6.3.2. Contact angles using the goniometer

Analysis of the contact angles of pad secretions was conducted using water droplets from a goniometer. Droplets of water were syringed onto the OTS surface, and onto dried footprints on the OTS surface (see *Figure 6.6*).

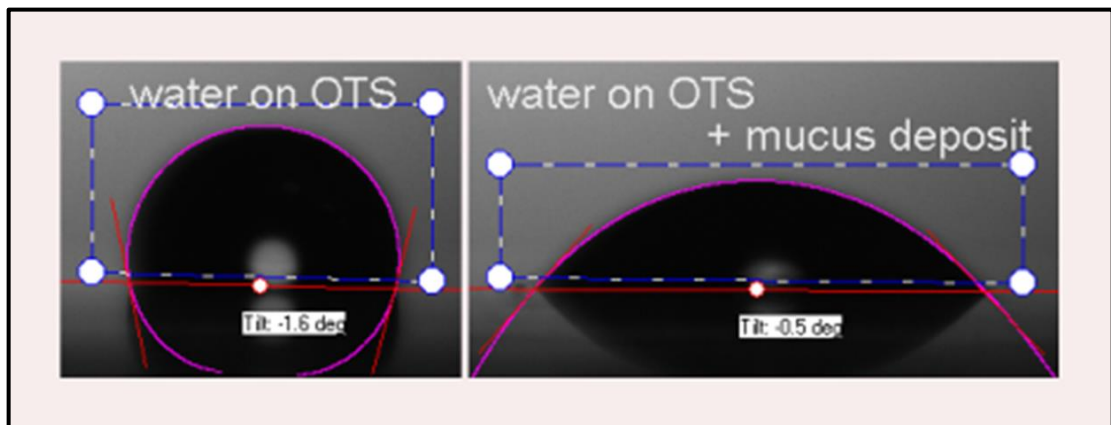


Figure 6.6: Images displaying droplets of water on different surfaces - on the left, the droplets are on clean OTS surface; on the right, the droplets are placed on the same location as toe pad 'footprints' (dried secretions). The computer program analyses the droplet image to calculate the contact angles at either side of the fluid.

The contact angles of the water for these experimental procedures were analysed and plotted for both species in this study (*Figure 6.7*). As expected, the contact angles of water on a clean OTS surface were high (means of 103.75° and 105.38° for the separate species trials), which indicates that the surface in its natural state is hydrophobic. After the frogs had placed their toe pads on the surface, there was a significant change in the contact angles produced when

comparing the angles before and after the footprints were placed; this was true in *Litoria* ($t = -10.9566$, $p < 0.001$) and *Osteopilus* ($z = -3.823$, $p = 0.0001$). There was no statistical difference between the contact angles seen in the two species footprints ($t = -0.9585$, $p = 0.3498$). The difference in contact angles indicate that the frogs leave behind something in their pad secretions which displays hydrophilic properties, despite the surface being naturally hydrophobic previously.

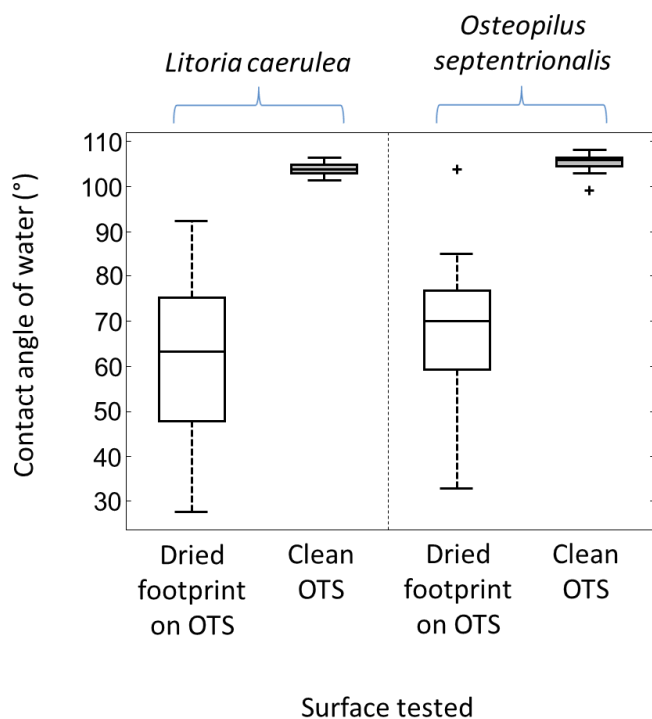


Figure 6.7: Boxplot showing the contact angles of distilled water on clean OTS (grey boxes) and on dried footprints (white boxes) on OTS, for both species. For other details regarding the boxplot, refer to Figure 6.4.

A further experiment using the goniometer setup was conducted, where water was stirred with the dried footprint, before being deposited back onto the OTS surface in a new location. The contact angles of the resulting droplets on OTS could then be measured as before by the program (see Figure 6.8).

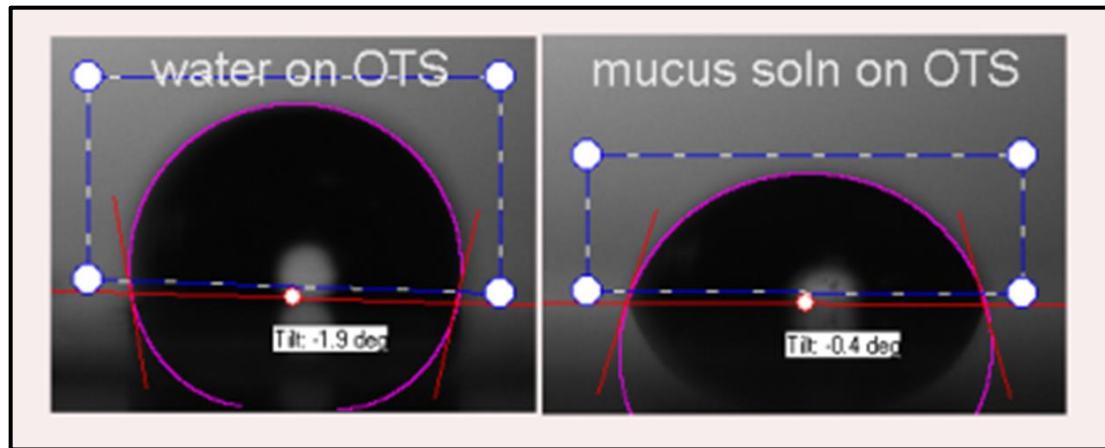


Figure 6.8: Images showing the contact angles of fluid on OTS - on the left a droplet of water, and on the right is a droplet of water which had been mixed with the footprint of the tree frog. The contact angles are calculated by the program automatically from the side on images of the fluid.

The contact angles of the differing fluids were then analysed for both species, and plotted together in *Figure 6.9*. For both species, a reduction in the effect of the pad secretions compared to the previous experiment was seen. The secretion mix will be highly diluted, and therefore it is expected that the contact angles are closer to those seen in water. Nevertheless, for both species there is a significant reduction in the contact angles measured (*Litoria*: $t = -7.4805$, $p < 0.0001$. *Osteopilus*: $z = -3.9199$, $p < 0.0001$), with the secretion mix forming lower contact angles. This indicates that there is a soluble part to the pad secretion, which would contribute to helping the fluid to wet whatever surface it is in contact with. The angles which were obtained from water on the dried footprint were significantly lower than the angles obtained by mixing and redepositing the fluid in a new location, for both species (*Litoria*: $z = -4.3417$, $p < 0.0001$. *Osteopilus*: $z = -4.4227$, $p < 0.0001$). This may indicate that secretions deposited onto the surface have a stronger effect on wettability than dissolved secretions.

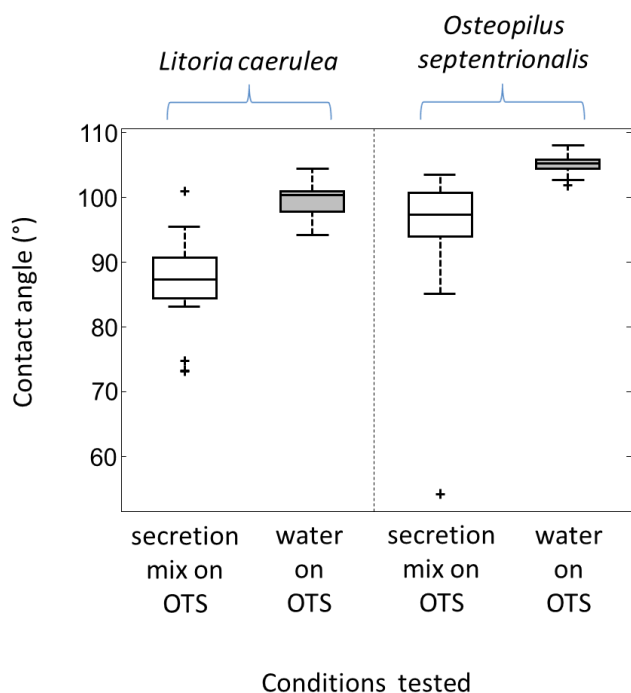


Figure 6.9: Boxplot displaying the contact angles of differing fluids on a clean OTS surface. Distilled water droplets (grey boxes) were compared to a water/secretion mix (white boxes), for both species tested in this study. For other details regarding the boxplot, refer to Figure 6.4.

6.3.3. Contact angles using IRM

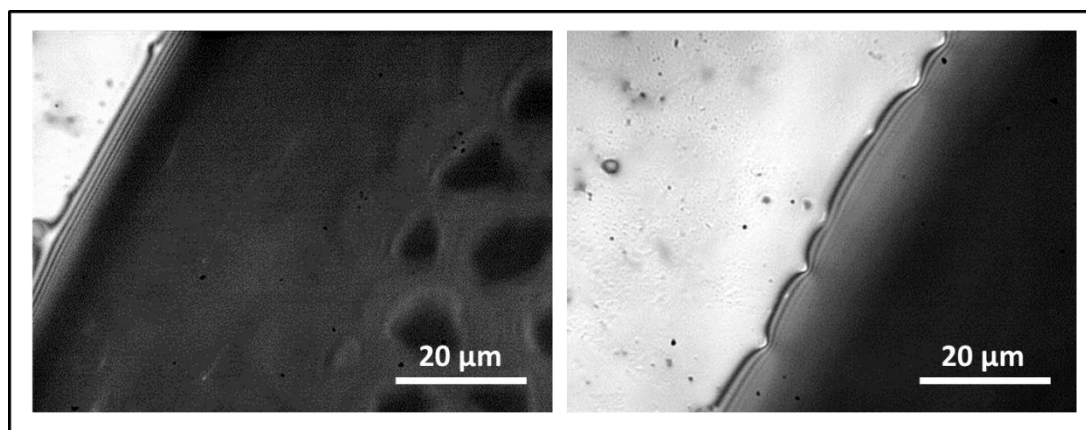


Figure 6.10: Examples of pad fluid on an OTS surface, with interference fringes seen at the periphery of the fluid (black and white bands). These two images were taken 0.5 seconds apart, with the pad in contact with the surface on the left (pad cells can be seen in contact in the image), and the pad has been removed in the image on the right.

The contact angles that the residual pad fluid formed in footprints were measured using IRM to view them from beneath (INA = 1.001; refractive index (RI) of the glass = 1.5, RI of the pad = 1.7 and RI of the mucus = 1.335. Blue wavelength light was used - approx. 475 nm). Once the pad is pulled away from

the surface, the secretions quickly evaporate (often within a few seconds). High-speed cameras can capture images of the fluid before this happens (see example in *Figure 6.10*). The interference fringes at the droplet edge are used to calculate the contact angle the droplet makes with the surface as illustrated in *Figure 6.11*.

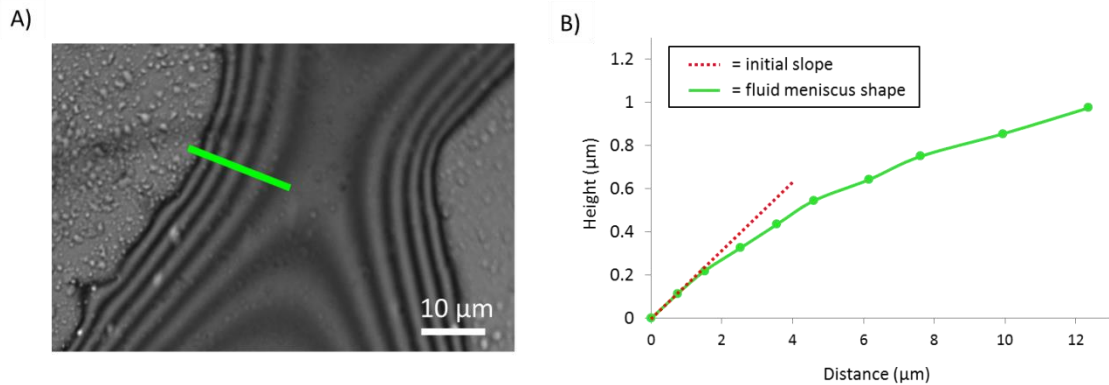


Figure 6.11: Reconstruction of the shape of pad fluid droplets (from *O.septentrionalis*) on an OTS surface. Using IRM the evaporating fluid shows the interference fringes of the receding droplet (A), and the distance between the fringes can be used to reconstruct the slope of the fluid from the surface (B). In the graph, the green line indicates the slope of the fluid meniscus away from the OTS surface, and the red line shows the initial slope which gives the contact angle. See text for details on IRM parameters.

In the example in *Figure 6.11*, the height was measured for each of the visible light and dark fringes, and the horizontal distance being plotted against the calculated height change between each fringe (approximately $0.11 \mu\text{m}$). Contact angles of the pad fluid on varying surfaces were compared with each other, as well as the contact angle of water on glass by the same method. The results are shown in *Figure 6.12*. The contact angles of all of the fluids tested were very low; water droplets on glass had shown a mean contact angle of 55.8° using the goniometer, but using this technique showed a contact angle of $18.5 \pm 6.6^\circ$. This is due to the differing techniques in measuring the contact angle, as the goniometer measures a static fluid angle whilst the IRM is measuring the angle on a receding fluid which is rapidly evaporating. For both species, the contact angles measured on the two surfaces were compared; for *Litoria* there was no difference between the contact angles ($n = 14$, $z = -0.4095$, $p = 0.6822$), and the same was found for the *Osteopilus* contact angles ($n = 14$, $z = 0.2068$, $p = 0.8362$). Comparing with the contact angles of water on glass ($n = 14$), there was

a lower contact angle measured for both species on the glass (*Litoria*, $z = 3.5233$, $p = 0.00043$; *Osteopilus*, $z = 3.8833$, $p = 0.0004$), and indeed on the OTS surface (*Litoria*, $z = -2.8782$, $p = 0.004$; *Osteopilus*, $z = 4.1919$, $p = 0.00003$). These results show that pad fluid shows a lower contact angle than water on all surfaces, and in particular exhibits hydrophilic characteristics by showing lower contact angles on the OTS than water does on glass. Although not shown (as it cannot be measured), water on the same OTS surface exhibited hydrophobic tendencies; i.e. the fluid had contact angles greater than 90° . The fluid behaves as if it contains surfactant, molecules known to reduce surface tension. However, this technique can only measure receding contact angles in this situation. There is also the possibility of some degree of a selection bias with this experiment, as only visible fringes would be available to measure and analyse. Fortunately, the goniometer experiments described above did not suffer from this problem (as will be discussed later).

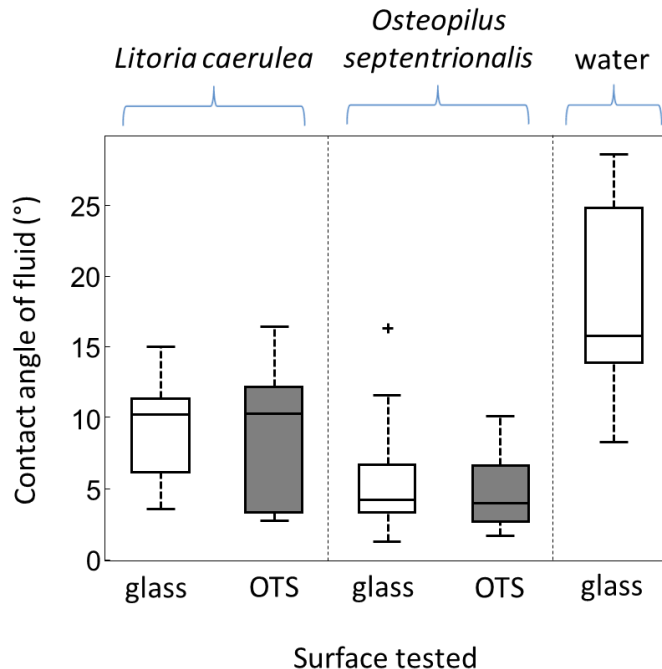


Figure 6.12: Contact angles of pad fluid on glass (white boxes) and OTS (grey boxes), representing hydrophilic and hydrophobic surfaces respectively. This was tested for two species, *Litoria caerulea* and *Osteopilus septentrionalis*, as well as testing water on glass too (denoted above the corresponding boxes). For other details regarding the boxplot, refer to Figure 6.4.

To summarise these experiments, a change in surface energy appears to have no detrimental effects on the adhesive and friction forces that tree frogs produce. Coupled with that are the interesting properties of the pad fluid, which show wetting ability on hydrophobic surfaces.

6.4. Discussion

6.4.1. Wet adhesion and fluid properties

Tree frogs will have to climb many surfaces in the wild, and will therefore need an adhesive system which will work effectively on a variety of surfaces. The common consensus on tree frog adhesion is that they use wet adhesion in their toe pads to stick (*Figure 6.13*). The pad is kept consistently wet by a fluid produced by the pad, which forms a thin layer between the pad and the surface (though the pad may be in direct contact via the tops of the nanopillars). Around the edge of the pad the fluid forms a meniscus with the air, where surface tension keeps the fluid in place and produces forces which help the pad to stick. This creates a pressure difference (according to Laplace's law) which is one of the main components of the adhesive force in the pad, the other being the tensile force of the meniscus. This capillary bridge relies on the pad fluid needing to be able to 'wet' the surface (Persson 2007) - by which it needs to form low contact angles to create an effective meniscus and to spread on the surface. Maintaining the surface tension (and therefore the forces produced by the pad) also relies on the cohesive properties of the fluid between the two surfaces in contact.

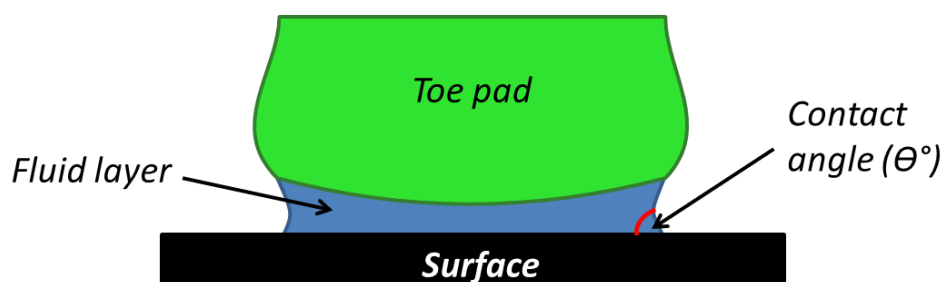


Figure 6.13: simplified diagram showing a cross section of the toe pad in contact with the surface. A thin fluid layer is spread beneath the pad, forming a capillary bridge which has a continuous meniscus round the edge. The fluid forms a low contact angle with the surface as it bridges the gap between the pad and the surface.

If the fluid produced by the frogs was entirely water, then it would be effective on 'wetable' hydrophilic surfaces (where it can form a low contact angle with the surface and spread) but should not be able to stick well on a low energy hydrophobic surface. This is because the fluid would form a high contact angle with the surface with a consequent reduction in the capillary force. However, in the force measurement experiments conducted for this study, the toe pads of tree frogs produced adhesive and frictional forces which were equivalent on hydrophilic and hydrophobic surfaces (for both glass/OTS comparison and the PDMS surfaces - forces produced on both pairs were within a similar range). Although purely a test of single toe pad forces per unit area, the results show that the wet adhesive system that the frogs implement will allow them to stick on hydrophobic surfaces. From the IRM experiments it can be seen that the fluid left behind by a climbing frog has a low contact angle on a hydrophobic surface, and therefore can wet the surface more effectively than water can. This must mean that the pad fluid possesses some component which allows wetting of low energy surfaces.

Had it been possible to collect large droplets of frog mucus where contact angles could have been measured using the goniometer, the results of these experiments would have been clear-cut. However, when only tiny droplets could be tested, it was inevitable that we could only study receding contact angles. The question then arises as to whether any possible differences in contact angle were not seen simply because, in very tiny droplets, all contact angles are very small. Properties of receding contact angles have been examined by Bourges-Monnier and Shanahan (Bourges-Monnier and Shanahan 1995). Although this study shows that, indeed, contact angles do decline as the droplet evaporates, it does appear that differences in contact angle remain until moments before complete evaporation (personal observation, data not shown). However, a small degree of uncertainty still remains as to how the IRM data should be interpreted. This makes the goniometer experiments that much more important, for they demonstrate that the presence of *both* dried secretions on the glass surface *and* a diluted form of the secretions in water result in significant reductions in contact angle.

6.4.2. Fluid composition

Some insects which also use wet adhesion to stick whilst climbing, have a two phasic emulsion for the fluid they adhere with. This is made up of water droplets in an oily layer; this gives the pad fluid non-Newtonian properties (with viscosity being dependent on flow rate). In a Newtonian fluid, a smooth pad in contact with a surface with a fluid layer between would result in a lubricating effect. However, the smooth pads of some insects (such as ants, stick insects and bees) can still produce significant frictional forces. The two phasic fluid of the pad is described as behaving as a Bingham plastic, whereby a finite shear stress is required before the pad can begin to flow. This means that the pads can produce velocity dependent shear stress for the pad which prevents the insects from slipping (Dirks, Clemente *et al.* 2010), and the fluid could also act as a non-Newtonian emulsion (Vötsch, Nicholson *et al.* 2002). Analysis of pad fluid in several insect species revealed the presence of a variety of molecules, including: saturated and unsaturated hydrocarbons, amino acids, fatty acids and cholesterols (Vötsch, Nicholson *et al.* 2002, Betz 2003).

Although frequently termed as ‘mucus’ throughout the literature (Ernst 1973), and the fluid has been described as ‘watery’ (Endlein, Barnes *et al.* 2013), the composition of the adhesive fluid produced by the toe pads is not precisely known (or indeed if it differs from other skin secretions). The results of this study have shown that there must be natural molecules within the fluid which gives it wetting properties on a hydrophobic surface. If there are specific chemicals present in tree frogs, it appears to stay on the surface when the frogs take a step, and after evaporation of the footprint. This was shown by the goniometer contact angle measurements, where the presence of a frog footprint allowed water to spread and wet a hydrophobic surface. When water droplets were mixed with the footprints, this resulted in a reduction of contact angles (although not as clear cut); this indicates that the surfactant chemicals in the footprint are soluble.

Preliminary studies into the chemistry of the secretions of tree frogs have been conducted using gas chromatography mass spectroscopy (GC-MS) techniques

(experiments were carried out by Eraqi Khannoon). These have indicated the presence of several molecules, with many molecules seen in both species (Table 6.1).

Table 6.1: Some of the chemicals found present in the secretions of tree frogs using GC-MS. Chemicals present in each specie's secretions are marked with a tick.

<u>Retention time (RT)</u>	<u>compound</u>	<u><i>Litoria caerulea</i></u>	<u><i>Osteopilus septentrionalis</i></u>
19.62	Octanoic acid	-	✓
20.26	Glycerol	✓	✓
22.23	Nonanoic acid	-	✓
24.71	Decanoic acid	-	✓
29.32	Dodecanoic acid	✓	✓
33.49	Tetradecanoic acid	✓	✓
37.34	Hexadecanoic acid	✓	✓
39.12	Heptadecanoic acid	✓	✓
40.30	Octadecadienoc acid	✓	✓
40.40	Octadecenoic acid	-	✓
40.87	Octadecanoic acid	✓	✓
54.26	Cholesterol	✓	✓
56.01	Stigmasterol	✓	✓
56.63	β -Sitosterol	✓	✓

Although the results varied between the samples, the secretions from both species in the study (*Litoria caerulea* and *Osteopilus septentrionalis*) contained similar chemicals. In addition the secretions from the toe pads and belly regions of the frog contained the same chemicals, and so the toe pad fluid does not appear to be significantly different from the fluid produced by the rest of the body. Several long-chained carboxylic acids were detected in the secretions, which are polar fatty acid molecules that comprise of a hydrophilic head and a hydrophobic tail. Sterol compounds were also detected, which are made up of larger lipid molecules, as well as evidence of glycerol molecules in the secretions. As these chemicals are amphiphilic, they will naturally be found at the interface of the pad fluid with air. Chemicals such as these are known to act as surfactants, and lower the surface tension of fluids (Bargeman and Van Voorst

Vader 1973, Megias-Alguacil, Tervoort *et al.* 2011). The surface tension of a fluid is the force preventing the fluid from spreading over a larger area, and so a drop in surface tension results in the contact angle of the fluid decreasing as the fluid spreads on the surface. The difficulties in obtaining samples of toe pad fluid (due to the small quantities of fluid produced) and the variability of the results mean that the results of the GC-MS can only be considered preliminary at this stage. However, it is likely that natural lipids and other polar molecules will play a role in the effective wetting of tree frogs' toe pads on hydrophobic surfaces, which results in the frogs being able to stick using their wet adhesive technique.

Although the lowering of surface tension on a hydrophobic surface is beneficial to the adhesive performance of the frog, the effect on hydrophilic surfaces may be different. Tree frogs are reliant on surface tension to form the meniscus surrounding the pads, subsequently forming the capillary bridges necessary for wet adhesion to occur (Federle, Barnes *et al.* 2006). If surface tension is lowered by the presence of such molecules, this could result in decreased adhesive forces on hydrophilic surfaces (and technically on hydrophobic surfaces too, though the fluid properties will have increased it already). This has not been tested in this study - the effect of fluid composition on the adhesive abilities of toe pad mimics is a potential experiment which would aid our understanding of this. If this is the case, then it would seem tree frogs have sacrificed maximum adhesive forces on one kind of surface to allow an adaptive form of wet adhesion on a variety of surfaces. Previous studies have noted that tree frogs can climb most effectively on vertical surfaces (Hanna and Barnes 1991), where frictional forces will play a predominant role. In smooth padded insects, the two phasic fluid of the pad provides resistance to shear forces as well as adhesive forces (Dirks, Clemente *et al.* 2010). Although significant frictional forces are produced by the nanostructures of the pad coming into direct contact with the substrate, the presence of long chain molecules in the fluid could give the fluid non-Newtonian properties when under shear stress (particularly in the confined space underneath the pads) (Federle, Barnes *et al.* 2006).

6.5. Conclusion

The natural conditions in which tree frogs will need to stick will vary in many other parameters alongside surface energy - roughness and loose particulates which often coincide with extremes in wettability. Whether tree frogs would be able to stick on such surfaces is unknown. Based on the results of this study, it appears that tree frogs are well placed to climb effectively on hydrophobic surfaces. The composition of the pad fluid provides the low contact angles necessary to produce the adhesive forces for frogs to climb, which is ideal for frogs which will regularly encounter hydrophobic surfaces on leaves.

7. General Discussion

7.1. Research summary

Tree frogs display a climbing strategy which is fast, efficient and versatile. There have been several studies on the biomechanics behind their climbing, which have investigated many aspects of their specialised toe pads: how the toe pads produce adhesive force (Emerson and Diehl 1980, Green 1981), the detachment method of the pads (Hanna and Barnes 1991), the effect of scaling on adhesive ability (Barnes, Oines *et al.* 2006, Smith, Barnes *et al.* 2006, Smith, Barnes *et al.* 2006), the role of friction in the toe pads (Federle, Barnes *et al.* 2006), peeling theory in relation to their toe pads (Endlein, Ji *et al.* 2013), as well as several morphological studies of the particular structures found on the toe pad. The overall aim of this thesis was to look at how tree frog adhesion adapts to cope with challenging conditions for sticking: when surfaces have rough topographies, when a surface is covered in contaminant, specialisations to deal with flooded surfaces, and whether tree frogs are able to stick to hydrophobic surfaces. A variety of techniques were deployed to help answer these questions, mainly through the use of whole animal adhesive ability tests and force measurements of single toe pads.

In chapter 3 the self-cleaning abilities of the toe pad were studied. The feet of tree frogs were artificially contaminated using glass beads, and recovery of adhesive force was recorded over repeated steps of the pads. The presence of a contaminant on the pad area lead to a decrease in direct contact of the pad with the surface, which did result in a dramatic drop in adhesive force to below 7 % of clean pad forces. With subsequent steps there was an increase in adhesive forces, with recovery reaching 75 % by the eighth measurement. The recovery of adhesive force was greatly facilitated by a small lateral drag of the pad across the surface (as opposed to simply a vertical push on and off from the surface, which showed very little recovery from a fully contaminated pad). As the pads produce a fluid, this allowed for the contaminant to be clustered together and then left behind with residual fluid on the surface. This recovery of forces compares similarly to those seen in insects, where high levels of recovery of forces were seen within eight steps (Clemente, Bullock *et al.* 2010), and the presence of higher levels of fluid also led to faster cleaning of pads (Clemente and Federle 2012).

The experiments in chapter 4 displayed how effectively the torrent frog species *Staurois guttatus* could adhere on surfaces which replicated their natural waterfall habitat. The toe pads of torrent frogs can produce higher force per unit area than the tree frog used for comparison (*Rhacophorus pardalis*). A closer look at the toe pads of torrent frogs reveals an interesting variance from other tree frogs, where channels appear straighter with directionality away from the centre of the pad (particularly around the edges); this concurs with the study by Ohler, where evidence of a difference between torrent frog and tree frog species was first noted (Ohler 1995). The precise functionality of these channels has not been tested, however they could play a role in helping to drain excess fluid away from the pad (although this was not seen from the single toe pad tests where water was put beneath the pad before contact). The torrent frogs utilise a large contact area compared to their body size and mass to stay attached on overhangs. A correlation in the size of a tree frog and its climbing ability has previously been shown (Smith, Barnes *et al.* 2006, Smith, Barnes *et al.* 2006), and it could be that living in a waterfall environment greatens the need for effective adhesive ability compared to body size. However, female torrent frogs could still outperform tree frogs with a smaller mass, so this may not be the sole reason for success.

Tree frogs' abilities on rough surfaces were dependant on the scale of the roughness, as shown in chapter 5. Tree frogs do not stick well on surfaces with asperities greater than 50 μm in size, but can stick well when the size of the asperity is smaller. Although this study only tested climbing ability on asperities that were up to 562.5 μm in size, it would be logical that tree frogs would begin to show an improvement in sticking ability on surfaces with larger asperities than that, as contact area of the toe pad would then be able to stick onto asperities which were within the size range of the pad. This would follow the pattern seen in geckos, spiders and insects, where minimising contact area reduces the adhesive ability of the organism. Another important aspect of tree frogs adhesion on rough surfaces is retaining fluid in the contact area, which is essential for adhesion to take place. This has been hypothesised previously (Persson 2007), and has been shown to occur in the wet adhesive pads of insects as well (Kovalev, Filippov *et al.* 2013). These two key aspects - loss of fluid and

contact area - appear to play a key role in how well adhesive pads work in nature on rough surfaces.

In chapter 6 we investigated the effect of surface energy on adhesive performance. Through testing toe pad forces on hydrophilic and hydrophobic surfaces using a bending beam, it was found that the surface energy did not affect the sticking ability of the pads. Further analysis of the toe pad secretions showed that the fluid produces low contact angles on hydrophobic surfaces, which would enable the wet adhesion used by the pads to work effectively. Given that waxy leaves are common in nature (Burton and Bhushan 2006), it is perhaps not surprising that tree frogs have adapted an adhesive system which would allow them to stick on these surfaces. However, not all climbing organisms can stick well to such surfaces; the dry adhesion used by geckos does not work well on low surface energies (Autumn and Peattie 2002), while dock beetles show a poorer performance on hydrophobic surfaces (Gorb and Gorb 2009). Some insects are known to produce a fluid composed of lipid content and an aqueous solution part (Dirks, Clemente *et al.* 2010), and it would seem likely that the tree frogs secretion would have components which would produce wettability on many surfaces (although the pads of tree frogs differ in that they are hydrophilic, water based systems while insects have hydrophobic systems, which would not encounter the same wetting problems).

In general, this study has shown how versatile the adhesive pads of tree frogs are. This gives climbing frogs a tremendous advantage for inhabiting many niches. One common feature of these studies is the role of the fluid secretions. Their pads adhere by wet adhesion, but the fluid has also been shown to play a huge role in enabling the frogs sticking ability to continue working in many conditions. The fluid can fill gaps on rough surfaces, it can help to remove contaminants from the pad surface, and its composition allows the pads to work on many surface energies. Although pad fluid and the pores they exude from are seen in most tree frog species studied (Smith, Barnes *et al.* 2006), the ability of the frog to control the amount of fluid is unknown. Fluid production can be sporadic and non-continuous during single toe pad experimentation, and the pad

tends to have more fluid on it when the digit or foot has been flexed by the frog (*personal observation*), which indicates a passive mechanism whilst the pads are in use. Closer observation of the pores on the pad reveals that they are each surrounded by muscle and nerve cells (Ernst 1973), which could play a role in fluid excretion by muscle activation (for example when the digit is flexed). Too much fluid beneath the pad could potentially be detrimental to sticking (by disruption of the meniscus, and the pad would produce less friction), and so intermittent fluid production should suit the tree frog. However when more fluid is needed (on a rough surface or when the pad is contaminated) then more fluid could hypothetically be produced by the pad to aid climbing.

7.2. Future tree frog research

Future work on tree frog adhesion could combine the parameters tested in these studies. Many surfaces in nature exhibit several of the traits that have been studied; many plant species possess surfaces made from loose waxy crystals which form a rough surface. As they are in place to deter climbing organisms (usually insects) then it would be expected that tree frogs should also struggle on such surfaces. This has not been tested, and the behaviours of the frog may show a different result. Kinematic investigations of frogs when climbing in these challenging circumstances could help with the design of robots which show versatile climbing. In addition, models explaining the dynamics of the pads in flooded, rough or contaminated surfaces would help in designing smart adhesive surfaces suitable in these conditions. The experiments carried out in this study were on 'flat' surfaces (no curvature), but most surfaces that tree frogs encounter will have some degree of curvature. Some studies have tested the kinematics of climbing frogs on varying diameters (Herrel, Perrenoud *et al.* 2013), but further studies into the use of the pads and force measurements could be useful in understanding how tree frogs climb, particularly using grasping behaviour.

7.3. Adhesive replicate design

Based on current research, what considerations are there for smart adhesives design, potentially for use in climbing robotics? Firstly, the structural design of a tree frogs toe pad would provide a good gripping surface. The polygonal cells, which possess nanostructures atop each cell and interconnecting channels between them, are seen throughout frog evolution and have cropped up in several unrelated lineages (Green 1979). A hexagonal pattern is also seen in some cricket species (Barnes 2007), therefore this must be an effective structure for an adhesive pad using wet adhesion. Replicated surfaces would have pillars where the tops would remain in direct contact with the surface to produce high levels of friction, as happens in tree frogs pads (Federle, Barnes *et al.* 2006). The channels would also allow the pad to bend and conform better to an undulating surface, for a better overall contact. Channels could be designed to give the pad directionality, drawing excess fluid away from the centre of the pad to outside of the contact area. The channels in torrent frogs display curvature and directionality (which are thought to play a role in the drainage of excess fluid, though this has not been shown to occur in frogs thus far and the detailed function is unclear), which could be applied to a smart surface. This would move fluid away from the centre to the periphery of the pad, which can remove fluid from the pad quicker than the plain hexagonal pattern seen in other frogs. The channels can also act as fluid reservoirs, where excess pad fluid can stay present until in contact with a surface and is squeezed out onto the surface to produce hydrodynamic forces (Persson 2007). The pad fluid tends to evaporate away quickly in the quantities seen in toe pads, so maintaining fluid on the pad may prevent fluid depletion and subsequent poor adhesion.

The second factor in surface design is that the material that the replicate is made of will also be important for its function. Whilst the outermost layer of cells are quite stiff, the pad overall is a highly soft material. This allows the pad to be more resistant to wear, but soft enough so that there is a high degree of conformity by the pad (Barnes, Baum *et al.* 2013). For a replicate adhesive surface, having a soft material would help to match contours of rough surfaces, and this would therefore result in greater adhesive and frictional forces. This was seen in the IRM experiments, where the softness and the elastic nature of

the pads result in high levels of conformity. Conformity of the pad means that the ultra-thin layer of fluid beneath the pad can be maintained for adhesive forces, while direct contact with the surface can still occur to allow frictional forces to exist. Frogs appear to rely heavily on frictional forces; therefore close contact is important in allowing them to climb effectively. Any replicate surface should therefore be made from a soft deformable material which will exhibit these characteristics. Most materials will become stiffer as they are stretched on a surface (although it is unknown whether the toe pads show such behaviour), which should be considered when choosing a material for surface design.

Finally, the sticking ability of tree frogs is wholly reliant on the fluid they produce. The fluid not only produces the forces necessary for adhesion; it also plays a role in removing contaminants, in filling in the gaps on a rough surface, and is composed of chemicals which allow it to spread and form capillary bridges in the presence of any level of surface energy. For the design of a replicate which produces a fluid, this may be more difficult as it would rely on a steady supply of the fluid coming from the surface, like the pores of the toe pad. This is in contrast to a gecko mimic surface, which would use dry adhesion to stick and does not require additional fluid.

Tree frog adhesion is a sophisticated method of sticking and climbing, but this relies on the behaviours of the frog whilst climbing as well as the pads themselves. Frogs frequently pull the pads in towards the body as they climb, and this creates additional friction forces and improves the contact area of the pad. In order to prevent peeling, the pads are repositioned away from the centre of mass to lower the peel angle, before repeating the drag of the pad on the surface (Endlein, Ji *et al.* 2013). Control of sticking on and easy detachment of the pad is also dictated by frog behaviour, and so any a climbing robot aiming to replicate tree frog adhesion would need to do likewise. The studies of torrent frogs in Brunei showed that they quickly increase their contact area when stronger adhesion is required on an overhang or when the surface is flooded. It is important to look at biomimetics as inspiration rather than replication -

however, the climbing abilities and strategies of tree frogs provide several useful qualities for any potential adhesive surface design.

7.4. Biomimicry

Dynamic adhesion in animals has become an intensely investigated field over the past 25 years, and one of the principal drivers for this is for the potential for innovative bio-inspired surfaces that will be multifunctioning and efficient for practical adhesion. There have been several examples of biomimicry being used for novel innovations: Velcro (Velcro USA Inc., Manchester, USA) was inspired by seed burrs from burdock plants which would attach to the fur of animals by tiny hooks for seed dispersal, and a self-cleaning paint which is based on the hydrophobic properties of the lotus leaf (Neinhuis and Barthlott 1997). The dynamic adhesion of climbers in nature can be highly desirable because large adhesive forces can be combined with easy detachment and (in the case of geckos) non-sticking states (Barnes 2007). The dry adhesion used by geckos in particular serves as a big inspiration for smart adhesives, as their adhesive system does not require any additional fluid to function (which could restrict how much repetition of sticking and unsticking the surface could endure). It only took a few years from discovering the mechanism of gecko adhesion (Autumn, Liang *et al.* 2000), to the first prototypes of micro-fabricated surfaces with adhesive abilities (Geim, Dubonos *et al.* 2003). Since then there has been a multitude of gecko-inspired surfaces produced: Das *et al* designing an anisotropic pillared surface (Das, Cadirov *et al.* 2015), Ruffatto *et al* incorporated electrostatic forces to gecko adhesion (Ruffatto, Parness *et al.* 2014), and some level of self-cleaning has been achieved in gecko replicates (Lee and Fearing 2008)(to name a few examples). There are now over a hundred papers which all relate to gecko inspired surfaces (Cutkosky 2015). Despite the huge amount of effort going into making gecko replicates, they are still a long way off both the effectiveness and adaptability shown in geckos (Cutkosky 2015). This is partly due to the complexity of the nano-scale structures of the gecko foot, which thus far appears to be a limiting factor in the development of gecko inspired materials. It is likely then that gecko adhesion can only serve as inspiration for design of surfaces. Even in geckos the maximum adhesive pressures decreases with an increase in size of the adhesive area, and this is

frequently seen in smart surfaces that are manufactured on a larger scale. One way of solving this is to attempt to distribute the load throughout the pad as uniformly as possible (Cutkosky 2015).

Tree frogs adhesive pads (and pads similar to tree frogs) provide an alternative adhesive system which is potentially more reproducible (*Figure 7.1*). Image A in the figure displays a tree frogs' toe pad, while B to F show different inspired surfaces which have a similar design to a tree frog toe pad. Despite the pads being made of a specialised polygonal pattern which intersperse channels and are topped with a nano-pattern, it is still easier to replicate compared the multiple branched setae found on the feet of geckos. However until recently only papers considering the modelling of tree frog adhesion were all that had been done in terms of copying tree frog adhesion - particularly with the potential for application with tyre pattern design (Persson 2007). Certainly the design of tree frogs pads bear large similarities with tyre design, as tyres are designed to remove excess fluid from the contact surface and produce large friction forces (Barnes 2007). The hexagonal pattern has been shown to reduce the hydrodynamic drainage forces necessary to remove fluid from the contact area due to the presence of the channels (and is dependent on the size of the channels as well) (Gupta and Frchette 2012). As a consequence fluid is likely to reside within the channels on contact, but is removed from the non-channel areas to allow direct contact, which will improve the adhesive and frictional forces of the pad.

Microstructures similar to tree frog hexagonal patterns have been shown to dramatically increase friction forces and maintain them, even at high sliding speeds where in smooth surfaces friction forces are reduced (Huang and Wang 2013). An increase in the density of pillars on the surface led to a decrease of frictional forces at low speeds (likely due to the lower real contact area), but with high sliding speeds there is little decrease on the structured surfaces compared to the smooth surfaces. This is due to a continuous fluid film forming on the smooth surface, which leads to a hydroplaning effect. The benefit of the pillared surface is that the channels can act as a reservoir for the fluid to be

reused when necessary (Huang and Wang 2013); a phenomenon which is seen in the pads of tree frogs as well (Federle, Barnes *et al.* 2006).

Many other applications for a tree frog inspired adhesive have been speculated: Effective gripping shoes, non-slip flooring or surfaces (for example on boat decking or on life buoys used when people are drowning), reusable plasters or surgical bandages, or surgical instruments which will minimise tissue damage as they hold sensitive tissues (Drotlef, Appel *et al.* 2015). Drotlef *et al* looked at force measurements on designed surfaces, testing varying pillar forms and surface energies. T-shaped pillars combine wide channels and large surface area which results in large adhesive forces. The study showed that tree frog design is designed to maximise for frictional forces, which could be the main application for such surfaces (Drotlef, Stepien *et al.* 2012). The high friction capabilities of such surfaces in wet conditions have led to another potential application for these inspired surfaces; modern razors can utilise high friction with drainage to help with shaving, as the skin will be lubricated with foam but will also need to be stretched so that the hairs are cut effectively (Tsipenyuk and Varenberg 2014). Recent research has been into mushroom-shaped pillars (a variation on T-shaped profiles), which show high levels of adhesion on a variety of surface energies and wetting conditions (Heepe and Gorb 2014). Iturri *et al* take inspiration from torrent frogs by mimicking the elongated cells seen in their pads, which are shown to increase friction forces and can incorporate directionality into the pads functioning (Iturri, Xue *et al.* 2015).

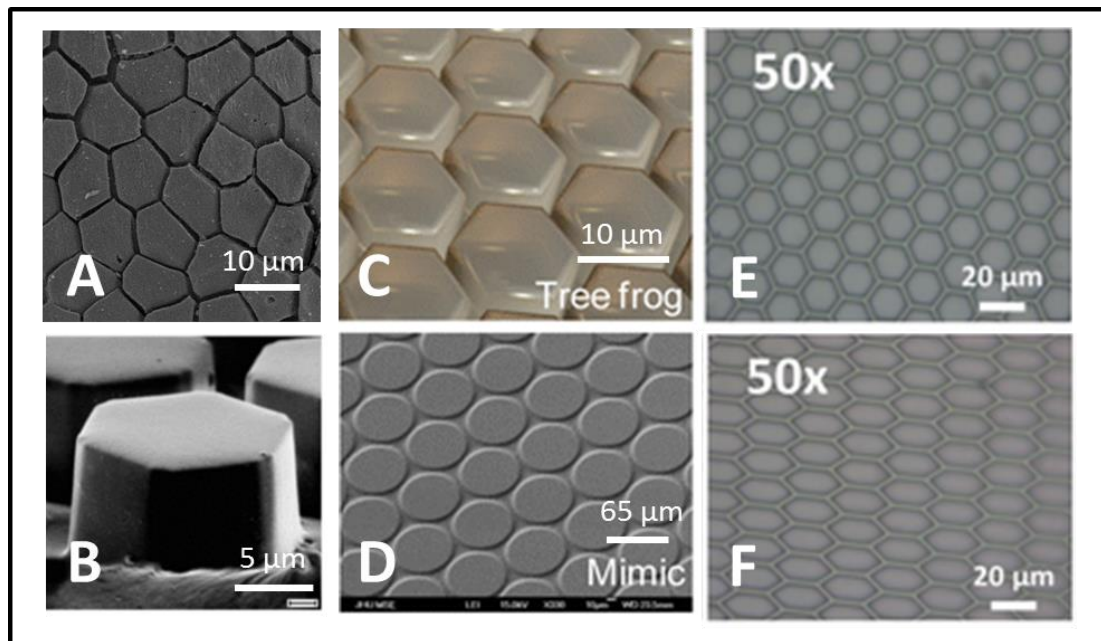


Figure 7.1: Images of tree frogs toe pads and some examples of bioinspired surfaces. Image A shows a tree frogs toe pads, and images B through F show various manufactured surfaces with a similar patterning. Image B is adapted with permission from Drotlef *et al.* 2012, Copyright (2012), *Advanced Functional Materials* (Drotlef, Stepien *et al.* 2012). Images C and D are adapted with permission from Gupta *et al.* 2012, Copyright (2012), *American Chemical Society* (Gupta and Frachette 2012). Images E and F are adapted with permission from Iturri *et al.* 2015, Copyright (2015), *Advanced Functional Materials* (Iturri, Xue *et al.* 2015).

As well as the surface topography, the internal structuring of toe pads has been considered in adhesive design. Overall the pad acts as a very soft material, with a few outer layers of cells which act as a stiffer material (Barnes, Baum *et al.* 2013). This provides an adhesive surface which will be soft enough to conform, but will be somewhat wear resistant. The interior part of the pad possesses fibrils which run along the pad, and to some degree are similar to a gecko's adhesive setae (but inside the pad). Shahsavan and Zhao used this configuration as inspiration for a surface which consists of micropillars, topped with thin elastic and viscoelastic layers; the surfaces were then tested and found to have strong frictional and pull-off forces (Shahsavan and Zhao 2014). The fibrils are also thought to contribute to directionality of the pad, meaning that the pads detach easily by peeling from one direction but produce high frictional forces when pulled in the other direction (Endlein, Ji *et al.* 2013). This was incorporated into adhesive pads made by He *et al.*, where pads which are semielliptic in cross section have internal inclined fibres which provide the pad with directionality, softness and robustness. This is coupled with an outer layer diamond patterning which is a simplified variant on tree frogs pads. These pads

can produce high levels of friction when pulled in one direction, but detach easily when pulled in the other direction. This makes them ideal for use in robots designed to climb steep inclines (i.e. when friction is the principal force used in attachment) (He, Wang *et al.* 2014). It would seem likely that any smart surfaces used in the future will incorporate the material and structure beneath the surface of the pad as well as the patterning of the adhesive surface.

7.5. Concluding remarks

It appears then that modern smart adhesives are getting more sophisticated as novel techniques and designs are conjured up. Their inspiration is several small species of tree frogs which are highly evolved to inhabit the environments they live in. Their pads have been shown to allow them to stick to a variety of surfaces or conditions; although these conditions will be commonly present, the fact that tree and torrent frogs can overcome them and successfully climb is no less remarkable. I look forward to seeing what the future holds in the ingenious design of smart surfaces, which are inspired by climbers like tree frogs.

Appendices

A1. Protocols for fixation of SEM samples

Euthanasia

(1) Stock solution: 1 g Benzocaine (Sigma-Aldrich), dissolved in 20 ml 95% ethanol

(2) Dose solution: 5 ml stock solution, diluted in 500 ml distilled water.

Fixative

The quantities given in the following fixation protocol made up 100 ml of fixative, 0.1 M phosphate buffer and buffer rinse. Dry chemicals were weighed using a digital balance; aqueous chemicals were measured using either measuring cylinders (for larger volumes) or syringes (for smaller volumes).

(1) Stock solutions A and B:

A - Potassium dihydrogen phosphate (KH_2PO_4): 6.8 g dissolved in 250 ml of distilled water

B - Disodium hydrogen phosphate (Na_2HPO_4): 14.2 g dissolved in 500 ml of distilled water

(2) 0.1 M phosphate buffer stock:

19 ml of stock solution A and 81 ml of stock solution B; the resulting solution has a pH value of 7.4.

50 ml of 0.1 M phosphate buffer, 40 ml of distilled water, and 10 ml of 25% gluteraldehyde.

Buffer rinse

50 ml of 0.1 M phosphate buffer, 50 ml of distilled water, and 2 g of sucrose.

SEM protocol

(1) A single toe pad was transferred to a clean glass vial

(2) The sample was treated with 3 x 5 minute washes in buffer rinse

- (3) The vial was filled with 1% osmium tetroxide (50:50, osmium tetroxide:buffer rinse), and left for 1 hour (after which the solution was removed)
- (4) The sample was treated with 3 x 10 minute rinses in distilled water
- (5) The vial was filled with 0.5% aqueous uranyl acetate, and placed inside a sealed opaque container (due to the light-sensitivity of uranyl acetate) for 1 hour (after which the solution was removed)
- (6) The sample was rinsed in distilled water until the water ran clear
- (7) The sample was then dehydrated in an acetone series (30% to dried absolute):
 - 30% acetone -> 2 x 10 minute washes
 - 50% acetone -> 2 x 10 minute washes
 - 70% acetone -> 2 x 10 minute washes
 - 90% acetone -> 2 x 10 minute washes
 - Absolute acetone -> 4 x 10 minute washes
 - Dried absolute acetone -> 2 x 10 minute washes (using a molecular sieve)
- (8) The sample was critical point dried (Polaron CPD)
- (9) The sample was then mounted onto an aluminium pin stub (ventral surface facing up), stuck down using double-sided copper-conductive tape. This was carried out under a dissection microscope
- (10) A streak of silver paint (quick-drying silver DAG paint) was applied from the cut end of the sample to the end of the stub

A2. Profiles of Rough surfaces using the Dektak profiler

To calculate the roughness of the sandpaper surfaces and their replicates made from resin, their profiles were measured using a Dektak stylus surface profiler (Veeco Dektak 6M Height Profiler, USA. Vertical resolution 0.1 nm at 6.5 k(nm) range, Stylus force from 7 mg, Stylus tip radius of 2.5 μm . Scan length 1 mm, 9000 data points per scan). The following graphs (*Figure A.1*) are the recorded profiles for the original surface and their replicates (except for the 425 μm surface which did not have a replicate surface made). The surface profiler also calculated roughness values for each surface; the R_a value, which is a measurement of average distance from a mean line of the peaks and troughs of the surface. The profiles and the R_a values indicate how well the resin replicas have copied the surfaces of the sandpapers.

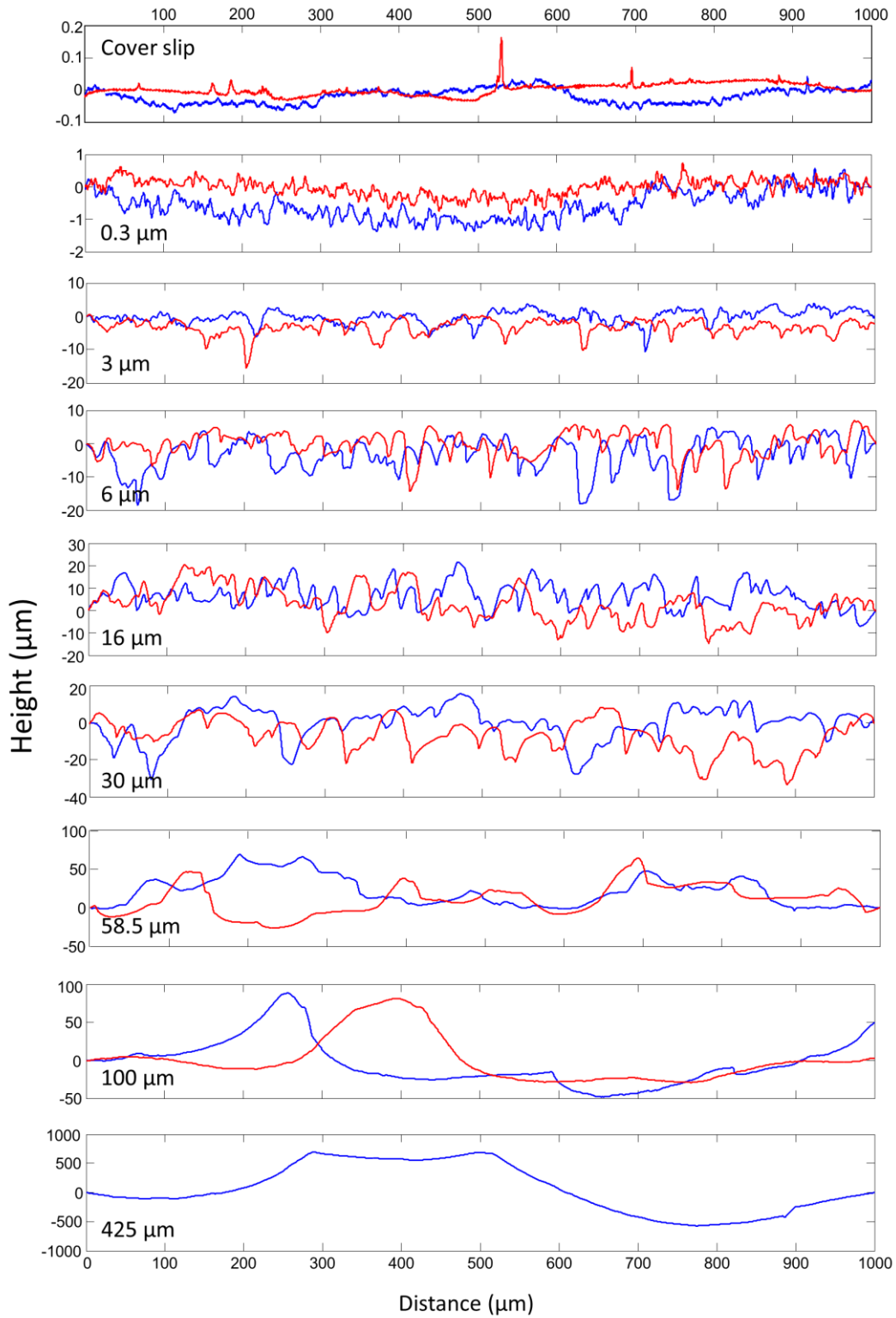


Figure A.1: Profiles of various surfaces over a length of 1000 μm . The original sandpaper surfaces are shown in blue, and replicates made from embedding resin are shown in red where appropriate.

A3. Calculating the R_a of a uniform bead monolayer surface

In order to calculate the average roughness (R_a) of a surface covered with a monolayer of beads, a formula was required to calculate the height of the surface throughout a specified area of the surface. The surface used for testing was made from gluing Ballotini glass spheres (Jencons, VWR International, Leicestershire, UK), with the average diameter of $1125\ \mu\text{m}$, to a board. The beads were arranged as a tightly-packed monolayer on the surface; this gave the beads a hexagonal configuration, with each bead surrounded by 6 adjacent beads (*Figure A.2*). This configuration leaves small areas between each of the beads where another bead is not present. The adhesive used to keep the beads in place is a relatively thick layer, which for much of the surface has partially filled the gaps between beads. Given this, the size of asperity is recorded as the radius (r), with the highest points being the top of the beads ($562.5\ \mu\text{m}$), and the lowest points are at the edges where the beads touch or in the gaps between the beads (measured as $0\ \mu\text{m}$).

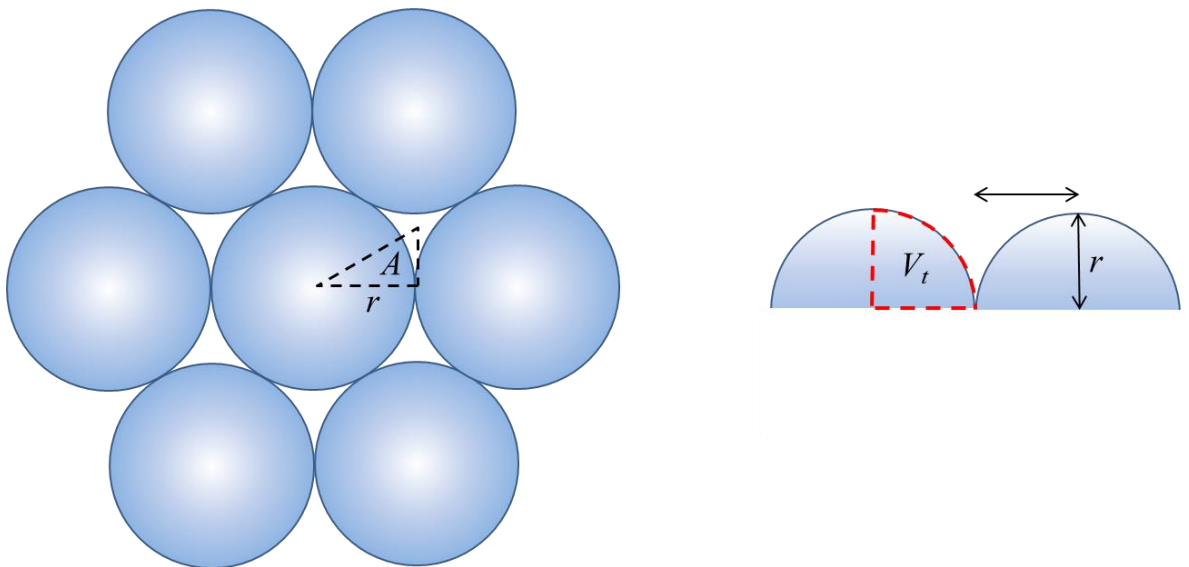


Figure A.2: Diagram of the configuration of the monolayer of beads on the surface. The area of interest (A) is $1/12$ of a hemisphere, which incorporates the radius (r) and the volume within the bead (V_t).

The volume of a bead can be calculated using the following equation:

$$V = \frac{4}{3} \pi r_0^3 \quad (8)$$

As we assume the beads to be tightly packed and for the gaps to be filled with the glue, the volume for a hemisphere is more appropriate:

$$V_{hemi} = \frac{2}{3} \pi r_0^3 \quad (9)$$

To simplify down the calculation, the volume of interest can be decreased to 1/12 of the circumference of each hemisphere; given as:

$$V_t = \frac{1}{18} \pi r_0^3 \quad (10)$$

From above, the area of interest is represented by the triangle A in the figure. This triangle can be mirrored round each bead and throughout the entire area so that the entire surface is correctly measured. The area of the triangle that the 1/12 of the sphere sits on can be calculated as:

$$A = \frac{r_0^2}{2\sqrt{3}} \quad (11)$$

The average height of a surface made up of hemispheres can be calculated by measuring the average heights over the given area A , which is calculated using the following equation:

$$h = \frac{V_t}{A} = \frac{\sqrt{3}}{18} \pi r_0 = \frac{\pi}{3\sqrt{3}} r_0 = 0.605 r_0$$

(12)

The R_a value of a surface is the mean modulus of the derivation from the average height, the area where the heights have been measured can be divided into positive and negative deviations. For the area tested, the calculated heights can be split into three regions: Above the mean height on the sphere surface, below the mean height on the sphere and area between the beads. These three can be calculated and then brought together to calculate the R_a .

Derivations from the mean height are positive for a sector where $z > h$. This happens for $r < r_1 = \sqrt{1 - h^2} r_0$. The volume of this region is 1/12 of a spherical cap with the radius r_1 :

$$V = \frac{\pi h^2}{3} (3r_0 - h)$$

(13)

For the volume of the area of bead we are measuring, i.e. 1/12 of the spherical cap:

$$V_1 = \frac{\pi h^2}{36} (3r_0 - h)$$

(14)

The second volume is the region of the sphere outside of the spherical cap r_1 , and this can be determined via subtraction of the spherical cap and the volume directly beneath it:

$$V_2 = V_{ring} - (V_t - V_1 - V_1')$$

(15)

Where V_1' is the volume under h for $r < r_1$:

$$V_1' = \frac{\pi}{12} r_1^2 h$$

(16)

$$V_{ring} = \frac{\pi}{12} (r_0^2 - r_1^2) h$$

(17)

The final calculation is for the region outside of the sphere, but inside the triangle A :

$$V_3 = \left(\frac{1}{2\sqrt{3}} - \frac{\pi}{12} \right) r_0^2 h$$

(18)

Finally, to calculate the mean deviation (R_a), all of the volumes are added together and divided by the area of the triangle:

$$R_a = \frac{V_1 + V_2 + V_3}{A}$$

(19)

As you would expect with deviations from a mean, $V_1 - V_2 - V_3 = 0$.

References

- Aksak, B., P. Murphy and M. Sitti (2007). "Adhesion of Biologically Inspired Vertical and Angled Polymer Microfiber Arrays." Langmuir **23**(6): 3322-3332.
- Anyon, M. J., M. J. Orchard, D. M. A. Buzza, S. Humphries and M. M. Kohonen (2012). "Effect of particulate contamination on adhesive ability and repellence in two species of ant (Hymenoptera; Formicidae)." Journal of Experimental Biology **215**(4): 605-616.
- Arzt, E., S. Gorb and R. Spolenak (2003). "From micro to nano contacts in biological attachment devices." Proceedings of the National Academy of Sciences of the United States of America **100**(19): 10603-10606.
- Autumn, K. (2006). "How Geckos Toes Stick." American Scientist **94**: 124-134.
- Autumn, K., A. Dittmore, D. Santos, M. Spenko and M. Cutkosky (2006). "Frictional adhesion: a new angle on gecko attachment." Journal of Experimental Biology **209**: 3569-3579.
- Autumn, K. and N. Gravish (2008). "Gecko adhesion: evolutionary nanotechnology." Philosophical Transactions of the Royal Society A: Mathematical, Physical and Engineering Sciences **366**(1870): 1575-1590.
- Autumn, K., Y. Liang, S. T. Hsieh, W. Zesch, W.-P. Chan, T. W. Kenny, R. S. Fearing and R. J. Full (2000). "Adhesive force of a single gecko foot-hair." Nature **405**: 681-685.
- Autumn, K. and A. M. Peattie (2002). "Mechanisms of adhesion in geckos." Integrative and Comparative Biology **42**(6): 1081-1090.
- Autumn, K., M. Sitti, Y. A. Liang, A. M. Peattie, W. R. Hansen, S. Sponberg, T. W. Kenny, R. Fearing, J. N. Israelachvili and R. J. Full (2002). "Evidence for van der Waals adhesion in gecko setae." Proceedings of the National Academy of Sciences of the United States of America **99**(19): 12252-12256.
- Bargeman, D. and F. Van Voorst Vader (1973). "Effect of surfactants on contact angles at nonpolar solids." Journal of Colloid and Interface Science **42**(3): 467-472.
- Barnes, W. J. P. (2007). "Biomimetic solutions to sticky problems." Science **318**: 203-204.
- Barnes, W. J. P., M. Baum, H. Peisker and S. N. Gorb (2013). "Comparative Cryo-SEM and AFM studies of hylid and rhacophorid tree frog toe pads." Journal of Morphology **274**(12): 1384-1396.
- Barnes, W. J. P., P. P. Goodwyn, M. Nokhbatolfoghahai and S. Gorb (2011). "Elastic modulus of tree frog adhesive toe pads." Journal of Comparative Physiology A: Neuroethology, Sensory, Neural, and Behavioral Physiology **197**(10): 969-978.
- Barnes, W. J. P., C. Oines and J. M. Smith (2006). "Whole animal measurements of shear and adhesive forces in adult tree frogs: insights into underlying

mechanisms of adhesion obtained from studying the effects of size and scale." Journal of Comparative Physiology A: Neuroethology, Sensory, Neural, and Behavioral Physiology **192**(11): 1179-1191.

Barnes, W. J. P., J. Pearman and J. Platter (2008). "Application of peeling theory to tree frog adhesion, a biological system with biomimetic implications." European Academy Sciences E-Newsletter Science and Technology **1**(1): 1-2.

Barnes, W. J. P., J. Smith, C. Oines and R. Mundl (2002). "Bionics and wet grip." Tire Technology International **December**: 56-60.

Barthlott, W. and C. Neinhuis (1997). "Purity of the sacred lotus, or escape from contamination in biological surfaces." Planta **202**(1): 1-8.

Bauer, U., M. Scharmann, J. Skepper and W. Federle (2012). "Insect aquaplaning' on a superhydrophilic hairy surface: how *Heliophora nutans* Benth. pitcher plants capture prey." Proceedings of the Royal Society B: Biological Sciences **280**: 20122569.

Betz, O. (2002). "Performance and adaptive value of tarsal morphology in rove beetles of the genus *Stenus* (Coleoptera, Staphylinidae)." Journal of Experimental Biology **205**: 1097-1113.

Betz, O. (2003). "Structure of the tarsi in some *Stenus* species (Coleoptera, Staphylinidae): External morphology, ultrastructure, and tarsal secretion." Journal of Morphology **255**(1): 24-43.

Betz, O. and G. Kölsch (2004). "The role of adhesion in prey capture and predator defence in arthropods." Arthropod Structure & Development **33**(1): 3-30.

Beutel, R. G. and S. N. Gorb (2001). "Ultrastructure of attachment specializations of hexapods, (Arthropoda): evolutionary patterns inferred from a revised ordinal phylogeny." Journal of Zoological Systematics and Evolutionary Research **39**(4): 177-207.

Bhushan, B. (2007). "Adhesion of multi-level hierarchical attachment systems in gecko feet." Journal of Adhesion Science and Technology **21**(12-13): 1213-1258.

Bitar, L. A., D. Voigt, C. P. W. Zebitz and S. N. Gorb (2009). "Tarsal morphology and attachment ability of the codling moth *Cydia pomonella* L. (Lepidoptera, Tortricidae) to smooth surfaces." Journal of Insect Physiology **55**(11): 1029 - 1038.

Boesel, L. F., C. Greiner, E. Arzt and A. del Campo (2010). "Gecko-Inspired Surfaces: A Path to Strong and Reversible Dry Adhesives." Advanced Materials **22**(19): 2125-2137.

Bohn, H. F. and W. Federle (2004). "Insect aquaplaning: *Nepenthes* pitcher plants capture prey with the peristome, a fully wettable water-lubricated anisotropic surface." Proceedings of the National Academy of Science, USA **101**(39): 14138-14143.

- Bourges-Monnier, C. and M. E. R. Shanahan (1995). "Influence of Evaporation on Contact Angle." Langmuir **11**(7): 2820-2829.
- Bullock, J. M. R., P. Drechsler and W. Federle (2008). "Comparison of smooth and hairy attachment pads in insects: friction, adhesion and mechanisms for direction-dependence." Journal of Experimental Biology **211**(20): 3333-3343.
- Bullock, J. M. R. and W. Federle (2011). "The effect of surface roughness on claw and adhesive hair performance in the dock beetle *Gastrophysa viridula*." Insect Science **18**(3): 298-304.
- Burton, Z. and B. Bhushan (2006). "Surface characterization and adhesion and friction properties of hydrophobic leaf surfaces." Ultramicroscopy **106**(8-9): 709-719.
- Busshardt, P. and S. Gorb (2014). "Ground reaction forces in vertically ascending beetles and corresponding activity of the claw retractor muscle on smooth and rough substrates." Journal of Comparative Physiology A **200**(5): 385-398.
- Butt, H.-J. and M. Kappl (2009). "Normal capillary forces." Advances in Colloid and Interface Science **146**(12): 48 - 60.
- Cartmill, M. (1985). Functional Vertebrate Morphology. Functional Vertebrate Morphology
- M. Hidelbrand, D. M. Bramble, K. F. Liem and D. B. Wake. Cambridge, Belknap Press: 73-88.
- Casimir, H. B. G. and D. Polder (1946). "Influence of Retardation on the London-van der Waals Forces." Nature **158**: 787-788.
- Clarke, B. T. (1997). "The natural history of amphibian skin secretions, their normal functioning and potential medical applications." Biological Reviews **72**(03): 365-379.
- Clemente, C., J.-H. Dirks, D. Barbero, U. Steiner and W. Federle (2009). "Friction ridges in cockroach climbing pads: anisotropy of shear stress measured on transparent, microstructured substrates." Journal of Comparative Physiology A **195**: 805-814.
- Clemente, C. J., J. M. R. Bullock, A. Beale and W. Federle (2010). "Evidence for self-cleaning in fluid-based smooth and hairy adhesive systems of insects." Journal of Experimental Biology **213**: 635-642.
- Clemente, C. J. and W. Federle (2012). "Mechanisms of self-cleaning in fluid-based smooth adhesive pads of insects." Bioinspiration & Biomimetics **7**(4): 046001.
- Crawford, N., T. Endlein and W. J. P. Barnes (2012). "Self-cleaning in tree frog toe pads; a mechanism for recovering from contamination without the need for grooming." Journal of Experimental Biology **215**(22): 3965-3972.
- Cutkosky, M. R. (2015). "Climbing with adhesion: from bioinspiration to biounderstanding." Interface focus **5**(4): 20150015.

- Dai, Z., S. N. Gorb and U. Schwarz (2002). "Roughness-dependent friction force of the tarsal claw system in the beetle *Pachnoda marginata* (Coleoptera, Scarabaeidae)." Journal of Experimental Biology **205**(16): 2479-2488.
- Das, S., N. Cadirov, S. Chary, Y. Kaufman, J. Hogan, K. L. Turner and J. N. Israelachvili (2015). "Stick-slip friction of gecko-mimetic flaps on smooth and rough surfaces." Journal of The Royal Society Interface **12**(104): 20141346.
- Davies, M. S. and C. M. Case (1997). "Tenacity of attachment in two species of littorinid, *Littorina littorea* and *Littorina obtusata*." Journal of Molluscan Studies **63**(PT2): 235-244.
- del Campo, A., C. Greiner and E. Arzt (2007). "Contact Shape Controls Adhesion of Bioinspired Fibrillar Surfaces." Langmuir **23**(20): 10235-10243.
- Dirks, J.-H., C. J. Clemente and W. Federle (2010). "Insect tricks: two-phasic foot pad secretion prevents slipping." Journal of The Royal Society Interface **7**: 1-8.
- Dirks, J.-H. and W. Federle (2011). "Fluid-based adhesion in insects - principles and challenges." Soft Matter **7**: 11047-11053.
- Ditsche, P. and A. P. Summers (2014). "Aquatic versus terrestrial attachment: Water makes a difference." Beilstein Journal of Nanotechnology **5**: 2424-2439.
- Dixon, A. F. G., P. C. Croghan and R. P. Gowing (1990). "The mechanism by which aphids adhere to smooth surfaces." Journal of Experimental Biology **152**: 243-253.
- Drechsler, P. and W. Federle (2006). "Biomechanics of smooth adhesive pads in insects: influence of tarsal secretion on attachment performance." Journal of Comparative Physiology A: Neuroethology, Sensory, Neural, and Behavioral Physiology **192**(11): 1213-1222.
- Drotlef, D.-M., L. Stepien, M. Kappl, W. J. P. Barnes, H.-J. Butt and A. del Campo (2012). "Insights into the Adhesive Mechanisms of Tree Frogs using Artificial Mimics." Advanced Functional Materials **23**: 1137-1146.
- Drotlef, D. M., E. Appel, H. Peisker, K. Dening, A. del Campo, S. N. Gorb and W. J. P. Barnes (2015). "Morphological studies of the toe pads of the rock frog, *Staurois parvus* (family: Ranidae) and their relevance to the development of new biomimetically inspired reversible adhesives." Interface focus **5**(20140036).
- Duellman, W. E. and L. Trueb (1986). Biology of Amphibians. New York, McGraw-Hill.
- Eason, E. V., E. W. Hawkes, M. Windheim, D. L. Christensen, T. Libby and M. R. Cutkosky (2015). "Stress distribution and contact area measurements of a gecko toe using a high-resolution tactile sensor." Bioinspiration & Biomimetics **10**(1): 016013.
- Eisner, T. and D. J. Aneshansley (2000). "Defense by foot adhesion in a beetle (*Hemisphaerota cyanea*)." Proceedings of the National Academy of Sciences of the USA **97**(12): 6568-6573.

- Emerson, S. B. and D. Diehl (1980). "Toe pad morphology and mechanisms of sticking in frogs." Biological Journal of the Linnean Society **13**(3): 199-216.
- Endlein, T. and W. J. P. Barnes (2015). Wet Adhesion in Tree and Torrent Frogs. Encyclopedia of Nanotechnology. B. Bhushan. Netherlands, Springer: 1-20.
- Endlein, T., W. J. P. Barnes, D. S. Samuel, N. A. Crawford, A. B. Biaw and U. Grafe (2013). "Sticking under Wet Conditions: The Remarkable Attachment Abilities of the Torrent Frog, *Staurois guttatus*." PLoS ONE **8**(9): e73810.
- Endlein, T. and W. Federle (2008). "Walking on smooth or rough ground: passive control of pretarsal attachment in ants." Journal of Comparative Physiology A: Neuroethology, Sensory, Neural, and Behavioral Physiology **194**(1): 49-60.
- Endlein, T., A. Ji, D. Samuel, N. Yao, Z. Wang, W. J. P. Barnes, W. Federle, M. Kappl and Z. Dai (2013). "Sticking like sticky tape: tree frogs use friction forces to enhance attachment on overhanging surfaces." Journal of The Royal Society Interface **10**: 20120838.
- Ernst, V. V. (1973). "The digital pads of the tree frog *Hyla cinerea*. II. The mucous glands." Tissue and Cell **5**: 97-104.
- Federle, W. (2006). "Why are so many adhesive pads hairy?" Journal of Experimental Biology **209**(14): 2611-2621.
- Federle, W., W. Barnes, W. Baumgartner, P. Drechsler and J. Smith (2006). "Wet but not slippery: boundary friction in tree frog adhesive toe pads." Journal of The Royal Society Interface **3**(10): 689-697.
- Federle, W., E. L. Brainerd, T. A. McMahon and B. Holldobler (2001). "Biomechanics of the movable pretarsal adhesive organ in ants and bees." Proceedings of the National Academy of Science, USA **98**(11): 6215-6220.
- Federle, W. and T. Endlein (2004). "Locomotion and adhesion: dynamic control of adhesive surface contact in ants." Arthropod Structure & Development **33**: 67-75.
- Federle, W., U. Maschwitz, B. Fiala, M. Riederer and B. Holldobler (1997). "Slippery ant-plants and skilful climbers: Selection and protection of specific ant partners by epicuticular wax blooms in *Macaranga* (Euphorbiaceae)." Oecologia **112**: 217-224.
- Federle, W., M. Riehle, A. S. G. Curtis and R. J. Full (2002). "An integrative study of insect adhesion: mechanics and wet adhesion of pretarsal pads in ants." Integrative and Comparative Biology **42**: 1100-1106.
- Federle, W., K. Rohrseitz and B. Hoelldobler (2000). "Attachment forces of ants measured with a centrifuge: better "wax-runners" have a poorer attachment to a smooth surface." Journal of Experimental Biology **203**(3): 505-512.
- Flammang, P. (1996). Adhesion in echinoderms. Echinoderm Studies. Rotterdam, A.A. Balkema. **5**: 1-60.

- Flammang, P., J. Ribesse and M. Jangoux (2002). "Biomechanics of Adhesion in Sea Cucumber Cuvierian Tubules (Echinodermata, Holothuroidea)." Integrative and Comparative Biology **42**(6): 1107-1115.
- Frantsevich, L., A. Ji, Z. Dai, J. Wang, L. Frantsevich and S. N. Gorb (2008). "Adhesive properties of the arolium of a lantern-fly, *Lycorma delicatula* (Auchenorrhyncha, Fulgoridae)." Journal of Insect Physiology **54**(5): 818-827.
- Geim, A., S. Dubonos, I. Grigorieva, K. Novoselov, A. Zhukov and S. Shapoval (2003). "Microfabricated adhesive mimicking gecko foot-hair." Nature Materials **2**(7): 461-463.
- Gillies, A. G., H. Lin, A. Henry, A. Ren, K. Shiuan, R. S. Fearing and R. J. Full (2013). "Gecko toe and lamellar shear adhesion on macroscopic, engineered rough surfaces." Journal of Experimental Biology **217**: 283-289.
- Gorb, E. and S. Gorb (2009). "Effects of surface topography and chemistry of *Rumex obtusifolius* leaves on the attachment of the beetle *Gastrophysa viridula*." Entomologia Experimentalis et Applicata **130**(3): 222-228.
- Gorb, E., D. Voigt, S. Eigenbrode and S. Gorb (2008). "Attachment force of the beetle *Cryptolaemus montrouzieri* (Coleoptera, Coccinellidae) on leaflet surfaces of mutants of the pea *Pisum sativum* (Fabaceae) with regular and reduced wax coverage." Arthropod-Plant Interactions **2**: 247-259.
- Gorb, E. V., N. Hosoda, C. Miksch and S. N. Gorb (2010). "Slippery pores: anti-adhesive effect of nanoporous substrates on the beetle attachment system." Journal of The Royal Society Interface **7**(52): 1571-1579.
- Gorb, S., E. Gorb and V. Kastner (2001). "Scale effects on the attachment pads and friction forces in syrphid flies." Journal of Experimental Biology **204**(8): 1421-1431.
- Gorb, S., Y. Jiao and M. Scherge (2000). "Ultrastructural architecture and mechanical properties of attachment pads in *Tettigonia viridissima* (Orthoptera Tettigoniidae)." Journal of Comparative Physiology A: Neuroethology, Sensory, Neural, and Behavioral Physiology **186**(9): 821-831.
- Gorb, S., M. Varenberg, A. Peressadko and J. Tuma (2007). "Biomimetic mushroom-shaped fibrillar adhesive microstructure." Journal of The Royal Society Interface **4**(13): 271-275.
- Gorb, S. N. (2005). "Uncovering insect stickiness: Structure and properties of hairy attachment devices." American Entomologist **51**(1): 31-35.
- Gorb, S. N. (2007). "Smooth attachment devices in insects: functional morphology and biomechanics." Advances in Insect Physiology **34**: 81-115.
- Gorb, S. N. (2008). "Biological attachment devices: exploring nature's diversity for biomimetics." Philosophical Transactions of the Royal Society A: Mathematical, Physical and Engineering Sciences **366**(1870): 1557-1574.

- Grafe, T. U. and A. Keller (2009). "Bornean amphibian hotspot: the lowland mixed dipterocarp rainforest at Ulu Temburong National Park, Brunei Darussalam." Salamandra **45**: 16-25.
- Grafe, T. U. and T. C. Wanger (2007). "Multimodal Signaling in Male and Female Foot-Flagging Frogs *Staurois guttatus* (Ranidae): An Alerting Function of Calling." Ethology **113**(8): 772-781.
- Gravish, N., M. Wilkinson and K. Autumn (2008). "Frictional and elastic energy in gecko adhesive detachment." Journal of The Royal Society Interface **5**(20): 339-348.
- Gravish, N., M. Wilkinson, S. Sponberg, A. Parness, N. Esparza, D. Soto, T. Yamaguchi, M. Broide, M. Cutkosky, C. Creton and K. Autumn (2009). "Rate-dependent frictional adhesion in natural and synthetic gecko setae." Journal of The Royal Society Interface **7**: 259-269.
- Green, D. M. (1979). "Treefrog toe pads: comparative surface morphology using scanning electron microscopy." Canadian Journal of Zoology **57**: 2033-2046.
- Green, D. M. (1980). "Size differences in adhesive toe-pad cells of treefrogs of the diploid-polyploid *Hyla versicolor* complex." Journal of Herpetology **14**(1): 15-19.
- Green, D. M. (1981). "Adhesion and the Toe-Pads of Treefrogs." Copeia(4): 790-796.
- Grenon, J. F., J. Elias, J. Moorcroft and D. J. Crisp (1979). "A new apparatus for force measurement in marine bioadhesion." Marine Biology **53**(4): 381-388.
- Groot, E. P., E. J. Sweeney and T. L. Rost (2003). "Development of the adhesive pad on climbing fig (*Ficus pumila*) stems from clusters of adventitious roots." Plant and Soil **248**: 85-96.
- Guo, Z. and W. Liu (2007). "Biomimic from the superhydrophobic plant leaves in nature: Binary structure and unitary structure." Plant Science **172**(6): 1103-1112.
- Gupta, R. and J. Frchette (2012). "Measurement and Scaling of Hydrodynamic Interactions in the Presence of Draining Channels." Langmuir **28**(41): 14703-14712.
- Hanna, G. and W. J. P. Barnes (1991). "Adhesion and detachment of the toe pads of tree frogs." Journal of Experimental Biology **155**: 103-125.
- Hansen, W. R. and K. Autumn (2005). "Evidence for self-cleaning in gecko setae." Proceedings of the National Academy of Sciences of the USA **102**(2): 385-389.
- He, B., Z. Wang, M. Li, K. Wang, R. Shen and S. Hu (2014). "Wet Adhesion Inspired Bionic Climbing Robot." Mechatronics, IEEE/ASME Transactions on **19**(1): 312-320.
- Heepe, L. and S. Gorb (2014). "Biologically Inspired Mushroom-Shaped Adhesive Microstructures." Annual Review of Materials Research **44**(1): 1-31.

Herrel, A., M. Perrenoud, T. Decamps, V. Abdala, A. Manzano and E. Pouydebat (2013). "The effect of substrate diameter and incline on locomotion in an arboreal frog." Journal of Experimental Biology **216**(19): 3599-3605.

Hooke, R. (1665). Of the Feet of Flies, and several other Insects. Micrographia: 169-172.

Hosoda, N. and S. N. Gorb (2011). "Friction force reduction triggers feet grooming behaviour in beetles." Proceedings of the Royal Society B: Biological Sciences **278**(1712): 1748-1752.

Hosoda, N. and S. N. Gorb (2012). "Underwater locomotion in a terrestrial beetle: combination of surface de-wetting and capillary forces." **279**(1745).

Hsu, P. Y., L. Ge, X. Li, A. Y. Stark, C. Wesdemiotis, P. H. Niewiarowski and A. Dhinojwala (2012). "Direct evidence of phospholipids in gecko footprints and spatulae substrate contact interface detected using surface-sensitive spectroscopy." Journal of The Royal Society Interface **9**(69): 657-664.

Hu, S., S. Lopez, P. H. Niewiarowski and Z. Xia (2012). "Dynamic self-cleaning in gecko setae via digital hyperextension." Journal of The Royal Society Interface **9**(76): 2781-2790.

Huang, W. and X. Wang (2013). "Biomimetic design of elastomer surface pattern for friction control under wet conditions." Bioinspiration & Biomimetics **8**(4): 046001.

Huber, G., S. N. Gorb, N. Hosoda, R. Spolenak and E. Arzt (2007). "Influence of surface roughness on gecko adhesion." Acta Biomaterialia **3**(4): 607-610.

Huber, G., S. N. Gorb, R. Spolenak and E. Arzt (2005). "Resolving the nanoscale adhesion of individual gecko spatulae by atomic force microscopy." Biology Letters **1**(1): 2-4.

Irschick, D. J., C. C. Austin, K. Petren, R. Fisher, J. B. Losos and O. Ellers (1996). "A comparative analysis of clinging ability among pad-bearing lizards." Biological Journal of the Linnean Society **59**(1): 21-35.

Ishii, S. (1987). "Adhesion of a leaf feeding ladybird *Epilachna vigintioctomaculata* (Coleoptera: Coccinellidae) on a vertically smooth surface." Applied Entomology and Zoology **22**(2): 222-228.

Iturri, J., L. Xue, M. Kappl, L. García-Fernández, W. J. P. Barnes, H.-J. Butt and A. del Campo (2015). "Wet Adhesion: Torrent Frog-Inspired Adhesives: Attachment to Flooded Surfaces " Advanced Functional Materials **25**(10): 1498-1498.

Jagota, A. and S. J. Bennison (2002). "Mechanics of adhesion through a fibrillar microstructure." Integrative and Comparative Biology **42**(6): 1140-1145.

Johnson, K. L., K. Kendall and A. D. Roberts (1971). "Surface Energy and the Contact of Elastic Solids." Proceedings of the Royal Society of London. Series A, Mathematical and Physical Sciences **324**(1558): 301-313.

Keller, A., M.-O. Rodel, K. E. Linsenmair and U. Grafe (2009). "The importance of environmental heterogeneity for species diversity and assemblage structure in Bornean stream frogs." Journal of Animal Ecology **78**(2): 305-314.

Kendall, K. (1975). "Thin-film peeling-the elastic term." Journal of Physics D: Applied Physics **8**(13).

Kennedy, C. E. J. (1986). "Attachment may be a basis for specialization in oak aphids." Ecological Entomology **11**(3): 291-300.

Kerkut, G. A. (1953). "The forces exerted by the tube feet of the starfish during locomotion." Journal of Experimental Biology **30**(4): 575-583.

Kesel, A., A. Martin and T. Seidl (2003). "Adhesion measurements on the attachment devices of the jumping spider *Evarcha arcuata*." Journal of Experimental Biology **206**(Pt 16): 2733-2738.

Kesel, A., A. Martin and T. Seidl (2004). "Getting a grip on spider attachment: an AFM approach to microstructure adhesion in arthropods." Smart Materials and Structures **13**: 512-518.

Kier, W. M. and A. M. Smith (2002). "The Structure and Adhesive Mechanism of Octopus Suckers." Integrative and Comparative Biology **42**(6): 1146-1153.

Kinloch, A. J. (1987). Adhesion and adhesives: science and technology, Chapman & Hall, New York.

Koch, K., B. Bhushan and W. Barthlott (2008). "Diversity of structure, morphology and wetting of plant surfaces." Soft Matter **4**(10): 1943-1963.

Kovalev, A. E., A. E. Filippov and S. N. Gorb (2013). "Insect wet steps: loss of fluid from insect feet adhering to a substrate." Journal of The Royal Society Interface **10**(78): 20120639.

Labonte, D. and W. Federle (2013). "Functionally Different Pads on the Same Foot Allow Control of Attachment: Stick Insects Have Load-Sensitive "Heel" Pads for Friction and Shear-Sensitive "Toe" Pads for Adhesion." PLoS ONE **8**(12): e81943.

Labonte, D. and W. Federle (2015). "Scaling and biomechanics of surface attachment in climbing animals." Philosophical Transactions Royal Society B **370**(1661): 20140027.

Labonte, D., J. A. Williams and W. Federle (2014). "Surface contact and design of fibrillar 'friction pads' in stick insects (*Carausius morosus*): mechanisms for large friction coefficients and negligible adhesion." Journal of The Royal Society Interface **11**(94): 20140034.

Langer, M. G., J. P. Ruppertsberg and S. Gorb (2004). "Adhesion forces measured at the level of a terminal plate of the fly's seta." Proceedings of the Royal Society B: Biological Sciences **271**: 2209-2215.

Lee, J. and R. S. Fearing (2008). "Contact Self-Cleaning of Synthetic Gecko Adhesive from Polymer Microfibers." Langmuir **24**(19): 10587-10591.

- Lepore, E., P. Brambilla, A. Pero and N. Pugno (2013). "Observations of shear adhesive force and friction of *Blatta orientalis* on different surfaces." Meccanica **48**(8): 1863-1873.
- Liang, Y. A., K. Autumn, S. T. Hsieh, W. Zesch, W.-P. Chan, R. Fearing, R. J. Full and T. W. Kenny (2000). Adhesion force measurements on single gecko setae. Technical Digest of the 2000 Solid-State Sensor and Actuator Workshop. Hilton Head Island, SC.
- Megias-Alguacil, D., E. Tervoort, C. Cattin and L. J. Gauckler (2011). "Contact angle and adsorption behavior of carboxylic acids on α -Al₂O₃ surfaces." Journal of Colloid and Interface Science **353**(2): 512-518.
- Mizutani, K., K. Egashira, T. Toukai and J. Ogushi (2006). "Adhesive force of a spider mite, *Tetranychus urticae*, to a flat smooth surface." JSME International Journal Series C-Mechanical Systems Machine Elements and Manufacturing **49**(2): 539-544.
- Neinhuis, C. and W. Barthlott (1997). "Characterization and distribution of water-repellent, self-cleaning plant surfaces." Annals of Botany (London) **79**(6): 667-677.
- Niederegger, S. and S. Gorb (2003). "Tarsal movements in flies during leg attachment and detachment on a smooth substrate." Journal of Insect Physiology **49**(6): 611.
- Niederegger, S. and S. N. Gorb (2006). "Friction and adhesion in the tarsal and metatarsal scopulae of spiders." Journal of Comparative Physiology A: Neuroethology, Sensory, Neural, and Behavioral Physiology **192**(11): 1223-1232.
- Niewiarowski, P. H., S. Lopez, L. Ge, E. Hagan and A. Dhinojwala (2008). "Sticky gecko feet: The role of temperature and humidity." PLoS ONE **3**(5): e2192.
- Ohler, A. (1995). "Digital pad morphology in torrent-living ranid frogs." Asiatic Herpetological Research **6**: 85-96.
- Ong, Y., A. Razatos, G. Georgiou and M. M. Sharma (1999). "Adhesion forces between *E. coli* bacteria and biomaterial surfaces." Langmuir **15**: 2719-2725.
- Orchard, M. J., M. Kohonen and S. Humphries (2012). "The influence of surface energy on the self-cleaning of insect adhesive devices." Journal of Experimental Biology **215**(2): 279-286.
- Page, E. B. (1963). "Ordered hypotheses for multiple treatments: A significance test for linear ranks." Journal of the American Statistical Association **58**: 213-230.
- Peattie, A. M. (2009). "Functional demands of dynamic biological adhesion: an integrative approach." Journal of Comparative Physiology B **179**(3): 231-239.
- Peattie, A. M., J.-H. Dirks, S. Henriques and W. Federle (2011). "Arachnids Secrete a Fluid over Their Adhesive Pads." PLoS ONE **6**(5): e20485.

- Persson, B. N. J. (1998). "On the theory of rubber friction." Surface science reports **401**(3): 445-454.
- Persson, B. N. J. (1999). "Sliding friction." Surface science reports **33**: 83-119.
- Persson, B. N. J. (2007). "Biological adhesion for locomotion on rough surfaces: Basic principles and a theorist's view." Material Research Society Bulletin **32**: 486-490.
- Persson, B. N. J. (2007). "Wet adhesion with application to tree frog adhesive toe pads and tires." Journal of Physics: Condensed Matter **19**(37): 376110.
- Persson, B. N. J. and S. Zilberman (2002). "Adhesion between elastic bodies with randomly rough surfaces." Solid State Communications **123**(3-4): 173-177.
- Platter, J., J. Pearman and J. Barnes (2007). "How do tree frogs adhere well to smooth surfaces and yet detach easily when necessary?" Comparative Biochemistry and Physiology - Part A: Molecular & Integrative Physiology **146**(4, Supplement 1): S123.
- Prum, B., H. F. Bohn, R. Seidel, S. Rubach and T. Speck (2013). "Plant surfaces with cuticular folds and their replicas: Influence of microstructuring and surface chemistry on the attachment of a leaf beetle." Acta Biomaterialia **9**(5): 6360-6368.
- Prum, B., R. Seidel, H. F. Bohn and T. Speck (2011). "Plant surfaces with cuticular folds are slippery for beetles." Journal of The Royal Society Interface **9**: 127-135.
- Riskin, D. K. and M. B. Fenton (2001). "Sticking ability in Spix's disk-winged bat, *Thyroptera tricolor* (Microchiroptera : Thyropteridae)." Canadian Journal of Zoology-Revue Canadienne De Zoologie **79**(12): 2261-2267.
- Rizzo, N. W., Gardner K. H. Walls D. J. Keiper-Hrynko N. M. Ganzke T. S. and D. L. Hallahan (2006). "Characterization of the structure and composition of gecko adhesive setae." Journal of the Royal Society Interface **3**: 441-451.
- Ruffatto, D., A. Parness and M. Spenko (2014). "Improving controllable adhesion on both rough and smooth surfaces with a hybrid electrostatic/gecko-like adhesive." Journal of The Royal Society Interface **11**(93): 20131089.
- Scherge, M. and S. N. Gorb (2001). Biological micro- and nanotribology: nature's solutions. Berlin, Springer.
- Scholz, I., W. J. P. Barnes, J. M. Smith and W. Baumgartner (2009). "Ultrastructure and physical properties of an adhesive surface, the toe pad epithelium of the tree frog, *Litoria caerulea* White." Journal of Experimental Biology **212**(2): 155-162.
- Scholz, I., W. Baumgartner and W. Federle (2008). "Micromechanics of smooth adhesive organs in stick insects: pads are mechanically anisotropic and softer towards the adhesive surface." Journal of Comparative Physiology A **194**: 373-384.

- Schönherr, J. (1982). Resistance of Plant Surfaces to Water Loss: Transport Properties of Cutin, Suberin and Associated Lipids. Physiological Plant Ecology II. O. L. Lange, P. S. Nobel, C. B. Osmond and H. Ziegler, Springer Berlin Heidelberg. **12 / B**: 153-179.
- Shahsavani, H. and B. Zhao (2014). "Bioinspired Functionally Graded Adhesive Materials: Synergetic Interplay of Top Viscous-Elastic Layers with Base Micropillars." Macromolecules **47**(1): 353-364.
- Smith, A. M. (1991). "The role of suction in the adhesion of limpets." Journal of Experimental Biology **161**: 151-169.
- Smith, J., W. J. P. Barnes, R. Downie and G. Ruxton (2006). "Structural correlates of increased adhesive efficiency with adult size in the toe pads of hylid tree frogs." Journal of Comparative Physiology A: Neuroethology, Sensory, Neural, and Behavioral Physiology **192**(11): 1193-1204.
- Smith, J. M., W. J. P. Barnes, J. R. Downie and G. D. Ruxton (2006). "Adhesion and allometry from metamorphosis to maturation in hylid tree frogs: a sticky problem." Journal of Zoology **270**(2): 372-383.
- Stark, A. Y., I. Badge, N. A. Wucinich, T. W. Sullivan, P. H. Niewiarowski and A. Dhinojwala (2013). "Surface wettability plays a significant role in gecko adhesion underwater." Proceedings of the National Academy of Sciences (USA) **110**(16): 6340-6345.
- Stark, A. Y., T. W. Sullivan and P. H. Niewiarowski (2012). "The effect of surface water and wetting on gecko adhesion." Journal of Experimental Biology **215**(17): 3080-3086.
- Stark, A. Y., N. A. Wucinich, E. L. Paoloni, P. H. Niewiarowski and A. Dhinojwala (2014). "Self-Drying: A Gecko's Innate Ability to Remove Water from Wet Toe Pads." PLoS ONE **9**(7): 101885.
- Stork, N. E. (1980). "Experimental analysis of adhesion of *Chrysolina polita* (Chrysomelidae: Coleoptera) on a variety of surfaces." Journal of Experimental Biology **88**: 91-107.
- Tian, Y., N. Pesika, H. Zeng, K. Rosenberg, B. Zhao, P. McGuiggan, K. Autumn and J. Israelachvili (2006). "Adhesion and friction in gecko toe attachment and detachment." Proceedings of the National Academy of Sciences of the USA: 19320-19325.
- Tsipenyuk, A. and M. Varenberg (2014). "Use of biomimetic hexagonal surface texture in friction against lubricated skin." Journal of The Royal Society Interface **11**(94): 20140113.
- Voigt, D. and S. N. Gorb (2012). "Attachment ability of sawfly larvae to smooth surfaces." Arthropod Structure & Development **41**(0): 145-153.
- Voigt, D., J. M. Schuppert, S. Dattinger and S. N. Gorb (2008). "Sexual dimorphism in the attachment ability of the Colorado potato beetle *Leptinotarsa decemlineata* (Coleoptera: Chrysomelidae) to rough substrates." Journal of Insect Physiology.

Voigt, D., A. Schweikart, A. Fery and S. Gorb (2012). "Leaf beetle attachment on wrinkles: isotropic friction on anisotropic surfaces." Journal of Experimental Biology **215**(11): 1975-1982.

Vötsch, W., G. Nicholson, R. Müller, Y. D. Stierhof, S. Gorb and U. Schwarz (2002). "Chemical composition of the attachment pad secretion of the locust *Locusta migratoria*." Insect Biochemistry and Molecular Biology **32**(12): 1605-1613.

Waite, J. H., Andersen. N. H., Jewhurst, S., and C. Sun (2005). "Mussel adhesion: finding the tricks worth mimicking." Journal of Adhesion **81**: 297-317.

Walker, G. (1981). "The Adhesion of Barnacles." Journal of Adhesion **12**(1): 51-58.

Walker, G., A. B. Yule and J. Ratcliffe (1985). "The adhesive organ of the blowfly, *Calliphora vomitoria*: a functional approach (Diptera: Calliphoridae)." Journal of Zoology (London) **205**: 297-307.

Wang, K., B. He and R. J. Shen (2012). "Influence of surface roughness on wet adhesion of biomimetic adhesive pads with planar microstructures." Micro & Nano Letters **7**: 1274-1277.

Whitney, H. M. and W. Federle (2013). "Biomechanics of plant-insect interactions." Current Opinion in Plant Biology **16**: 105-111.

Wohlfart, E., J. O. Wolff, E. Arzt and S. N. Gorb (2014). "The whole is more than the sum of all its parts: collective effect of spider attachment organs." Journal of Experimental Biology **217**(2): 222-224.

Wolff, J. O. and S. N. Gorb (2012). "The influence of humidity on the attachment ability of the spider *Philodromus dispar* (Araneae, Philodromidae)." Proceedings of the Royal Society B: Biological Sciences **279**(1726): 139-143.

Wolff, J. O. and S. N. Gorb (2012). "Surface roughness effects on attachment ability of the spider *Philodromus dispar* (Araneae, Philodromidae)." Journal of Experimental Biology **215**(1): 179-184.

Wolff, J. O. and S. N. Gorb (2013). "Radial arrangement of Janus-like setae permits friction control in spiders." Scientific Reports **3**: 1101.

Wu, C. W., X. Q. Kong and D. Wu (2007). "Micronanostructures of the scales on a mosquito's legs and their role in weight support." Physical Review E (Statistical, Nonlinear, and Soft Matter Physics) **76**(1): 017301.

Yule, A. B. and G. Walker (1984). "The adhesion of the barnacle, *Balanus balanoides*, to slate surfaces." Journal of the marine biological association of the UK **64**: 147-156.

Zani, P. A. (2000). "The comparative evolution of lizard claw and toe morphology and clinging performance." Journal of Evolutionary Biology **13**(2): 316-325.

Zani, P. A. (2001). "Clinging performance of the western fence lizard, *Sceloporus occidentalis*." Herpetologica **57**(4): 423-432.

Zhou, Y., A. Robinson, U. Steiner and W. Federle (2014). "Insect adhesion on rough surfaces: analysis of adhesive contact of smooth and hairy pads on transparent microstructured substrates." Journal of The Royal Society Interface **11**(98): 20140499.

Zhu, L.-Y. (1999). "Strength and stability of a meniscus in a slider-disk interface." IEEE Transactions on Magnetics **35**(5): 2415-2417.